5-6-2024

Molecular Characterization of the Neisseria gonorrhoeae Zur Regulon in Response to Zinc Starvation

Sandhya Padmanabhan
Georgia State University

Molecular Characterization of the *Neisseria Gonorrhoeae* Zur Regulon in Response to Zinc Starvation

by

Sandhya Padmanabhan

Under the Direction of Cynthia Nau Cornelissen, Ph.D.

A Dissertation Submitted in Partial Fulfillment of the Requirements for the Degree of

Doctor of Philosophy in the Institute for Biomedical Sciences

Georgia State University

2024

ABSTRACT

Gonorrhea is a sexually transmitted infection, caused by the bacterial pathogen *Neisseria gonorrhea (Ngo)* and affects millions of individuals of all age groups across the globe every year. Infection with *Ngo* does not result in protection and no effective vaccine has been developed, leaving antibiotics as the only treatment option. With the emergence of strains showing high levels of antibiotic resistance, there is an urgent need for development of novel therapeutics for disease prevention. During pathogenesis the host employs nutritional immunity, to restrict important transition metals such as zinc away from *Ngo*. This process is counteracted in *Ngo* by the production of highly efficient zinc import TonB-dependent Transporters (TDTs) which are promising vaccine antigens and zinc shuttle ABC transporters found to be important for intracellular survival. In *Ngo* zinc homeostasis and transport proteins are regulated by the Zinc uptake regulator (Zur) which represses transcription in the presence of zinc and activates transcription in the absence of zinc. In this study, we performed RNA sequencing to identify the global profile of genes in *Ngo* under the control of Zur and found that it differentially regulates 26 genes in response to zinc levels. We report the activity of Zur activity as a global regulator, able to both repress and activate gene expression in the presence of zinc and identified a consensus region on their promoters. We went on to further characterize the promoter elements of the zinc import TDT, *tdfJ*, which results in dual regulation by zinc and iron. We characterize specificity and binding affinities for regulation of *tdfJ* by a second regulator, Ferric uptake regulator (Fur) in response to iron. The response of *tdfJ* to both iron and zinc and its potential to be an important invasin, makes it an attractive candidate to investigate female genital tract infections. The female genital tract is a

conglomerate of these conditions and infections here are often asymptomatic. Taken together, this research provides important knowledge on the regulation of virulence mechanisms in response to zinc, which will aid in the development of therapeutics and an efficacious vaccine against a gonococcal infection.

INDEX WORDS: *Neisseria gonorrhoeae*, Zur, *tdfJ*, Fur, nutritional immunity

Molecular Characterization of the *Neisseria Gonorrhoeae* Zur Regulon in Response to Zinc Starvation

by

Sandhya Padmanabhan

Committee Chair: Dr. Cynthia Nau Cornelissen

Committee: Cynthia Cornelissen, PhD

Timothy Denning, PhD

Zehava Eichenbaum, PhD

Electronic Version Approved:

Office of Academic Assistance – Graduate Programs

Institute for Biomedical Sciences

Georgia State University

March 2024

DEDICATION

This work is dedicated to my family and friends who have supported and inspired my academic journey.

To my parents, Latha and Padmanabhan, who have both worked very hard to give me every opportunity that has led me to where I am today, thank you. Amma and Appa thank you for inspiring me and instilling in me the desire to pursue my goals. Thank you for not only believing in my potential but also providing me with unceasing emotional support. Being awarded the title of Dr. Padmanabhan is a small token of appreciation of the sacrifices my father made of his own dream to pursue a doctoral education. To my husband Ajay, who has been my pillar of support, thank you for your unwavering love, and immense patience. You inspire me every day to be a better person and my success would not be eminent if not for your encouragement. Thank you for being by my side always, I love you. To my grandmother Bhanu paati, who has been my cheerleader, supporting my endeavors and blessing me with well wishes, thank you. To my brother, Bharadwaj, you have inspired me with your wisdom and your determination to achieve what you put your mind to. Thank you for always being there for me, and I have no doubts that you will reach great heights in your career. To Aarthi chithi, who is with me in spirit and blessing me from heaven, thank you for wishing the very best for me. I miss you dearly. To my close friends Olivia, Pooneh and Nivi, who have looked out for my well-being and were instrumental for my success, thank you for being by my side through thick and thin.

As an ode to my upbringing and vedic heritage here is a verse that is meaningful to me-

"अथो खल्वाहुः काममय एवायं पुरुष इति; स यथाकामो भवति तत्क्रतुर्भवति, यत्क्रतुर्भवति तत्कर्म कुरुते, यत्कर्म कुरुते तदभिसंपद्यते"- Brihadaranyaka Upanishad (4.5.5)

"You are what your deep, driving desire is. As you desire, so is your deed. As your deed is, so is your destiny."

ACKNOWLEDGEMENTS

First, I would like to thank my mentor, Dr. Cynthia Nau Cornelissen, whose guidance, and support have been invaluable throughout this journey. She has been a source of great inspiration to me as a leading scientist in the field, encouraging me to explore new ideas and grow as an independent researcher while believing in myself. Her expertise, insightful feedback, patience, and encouragement have all played a pivotal role in shaping my scientific career and honing my analytical skills. I will forever look up to her as my role model for the rest of my professional career. I would like to express my heartfelt gratitude and appreciation to her for providing me with the best resources and opportunities necessary for successfully completing my thesis and achieving future milestones.

I am also highly indebted to the members of my dissertation committee, Dr. Timothy Luke Denning and Dr. Zehava Eichenbaum for their expertise, encouragement and valuable feedback that have been instrumental in enhancing not only my dissertation research but also expanding my scientific knowledge and professional network.

Next, I would like to thank Dr. Julie Stoudenmire for her unconditional support with both technical expertise and helping me navigate the ups and downs of this academic journey. Her contributions to my success have been indispensable, and I am forever grateful to her for her patience, encouragement, and unwavering belief in my capabilities.

I would also like to extend my gratitude to Dr. Alisson Criss from the University of Virginia, who has provided me with both resources as a collaborator and on professional career

advice. I am also grateful to Dr. Nicholas Noinaj from Purdue University for his expertise on protein stability and purification.

I would also like to thank T'Keyah Johnson from the Institute for Biomedical Science at Georgia State University for her constant support on all matters of the graduate school and for also helping me make the seamless transition from Virginia Commonwealth University to Georgia State University.

Finally, I would not be here if not for the support of former and current lab members of the Cornelissen Lab, with special mentions of Dr. Michael Kammerman, Dr. Ashley Greenawalt, Dr. Stavros Maurakis, Dr. Olivia Awate, Pooneh Tavakoley, Alexis Branch and Reeham Victor for their camaraderie, support and stimulating discussions, which have enriched my academic experience and given me a sense of community.

TABLE OF CONTENTS

ACKNOWLEDGEMENTS ..... **V**

LIST OF TABLES ..... **XII**

LIST OF FIGURES ..... **XIII**

LIST OF ABBREVIATIONS ..... **XIV**

CHAPTER 1. INTRODUCTION **1**

I. Family Neisseriaceae **1**

II. Pathogenic *Neisseria* **2**

III. Meningococcal Disease **2**

A. Epidemiology ***2***

B. Disease ***3***

C. Treatment and Prevention ***4***

IV. Gonococcal Disease **6**

A. Epidemiology and Incidence ***6***

B. Disease ***7***

C. Immune Responses to Gonorrhea ***8***

D. Treatment and Prevention ***9***

V. Virulence Factors of *Neisseria gonorrhoeae* **11**

A. Type IV Pilus ***11***

B. Opacity Proteins 12

C. Porin 14

D. Lipooligosaccharides (LOS) 14

E. IgA1 Protease 15

VI. Host Metal Restriction and Homeostasis 16

A. Iron 16

B. Zinc 20

VII. Metal Acquisition by Pathogenic *Neisseria* 22

A. Two Component TDTs- 22

B. Single Component TDTs- 24

C. The Ton Motor Complex 25

D. ABC Transporters 26

VIII. Regulation of Gene Expression 27

IX. Research Objectives 28

CHAPTER 2 MATERIALS AND METHODS 28

I. Bacterial Strains and Routine Maintenance 28

II. *Ngo* Growth Conditions for Zur Regulation and RNA Sequencing Experiments 32

III. RNA Isolation and Processing for Gene Regulation and Promoter Analysis 32

IV. Quality Control for RNA and cDNA 37

V. Primer Design and Efficiency Testing 38

VI. RT-qPCR for Measuring Target Gene Expression 38

VII. 5' Rapid Amplification of cDNA Ends (5' RACE) for Identification of the Transcriptional Start Site 39

VIII. SDS PAGE and Western Blotting Analysis 39

IX. Coomassie Stain 41

X. Expression and Purification of Recombinant His-NgFur 41

XI. DNA-Protein Interaction (DPI) ELISA 42

XII. Fur Scrambled Promoter ELISA 44

XIII. *In Silico* Promoter Analysis and Prediction 45

XIV. Statistical Analysis 45

CHAPTER 3. CHARACTERIZING THE DUAL REGULATION OF *NEISSERIA GONORRHOEAE TDFJ*, IN RESPONSE TO ZINC AND IRON 46

I. INTRODUCTION 46

II. RESULTS 48

A. tdfJ and znuA Show Significant Changes in Gene Expression by RT-qPCR 48

B. Zur Binds a Consensus Region on the tdfJ Promoter and Tightly Regulates its Expression 52

C. Two Fur-binding Sites on the tdfJ Promoter Result in Iron-dependent Induction of tdfJ 56

D. Fur Binds the Specific Fur-box Consensus Sequence Regions 1 and 2 on PtdfJ 59

III. DISCUSSION 62

CHAPTER 4- RNA SEQUENCING ANALYSIS FOR THE ZINC AND ZUR-DEPENDENT TRANSCRIPTOME OF *NEISSERIA GONORRHOEAE* FA1090 68

I. INTRODUCTION 68

II. RESULTS 71

A. Zinc- and Zur-dependent Genes in FA1090 are Repressed in Response to Zinc Excess 71

B. adhP and norB are Zn::Zur-activated Genes 74

C. Comparison of Ngo Zur Regulon Genes with Other Transcriptomic Studies in Neisseria Sp 82

D. Ribosomal Genes rpmE2/J2 Show the Highest Fold Change for Expression by RT-qPCR. 87

E. Zur Binds to the Zur Box Sequence on the Promoters of the Differentially Regulated Genes to Either Repress or Induce Expression 90

F. Enrichment Analysis of Differentially Zinc Regulated Genes in the WT 92

III. DISCUSSION 94

CHAPTER 5 THE ROLE OF THE GLOBAL REGULATOR ZUR AS AN ACTIVATOR AND REPRESSOR OF GENE EXPRESSION IN *NEISSERIA* 98

I. INTRODUCTION 98

II. RESULTS..... 100

A. Structural and Mechanistic Insights into Neisseria Zur and its Conservation Among Gram Negative Pathogens. 100

B. Zur Box Consensus is Evolutionarily Conserved Across Pathogenic Bacteria..... 104

C. Beyond the Role of Zur as a Repressor of Gene Expression- Mechanisms of Activation 106

D. Neisseria Zur is Not Self-regulated and is Transiently Expressed Under Zinc Restriction 109

E. Apo-Zur Regulation and Biochemical Properties of Metal Selectivity of Neisseria Zur 110

F. Physiological Significance of Zinc Availability and Zur in Pathogenesis..... 111

III. CONCLUSION 113

CHAPTER 6 SUMMARY AND PERSPECTIVES 115

REFERENCES 125

VITAE 172

LIST OF TABLES

Table 1. Strains and Plasmids 30

Table 2. Primers and Gene Blocks used in this study. 33

Table 3. List of differentially expressed genes by Zur in FA1090 77

Table 4. Comparision of Zur regulon studies in Ngo 84

LIST OF FIGURES

Figure 1 tdfH, tdfJ, ngo1049 and znuA are zinc-regulated by Zur 51

Figure 2 tdfJ and ngo1049 harbor an exact match to the predicted Zur-box consensus sequence in their promoters. 54

Figure 3. The tdfJ promoter elements from 5'RACE analysis. 55

Figure 4. The tdfJ promoter contains two upstream Fur binding regions for iron regulation .. 57

Figure 5. Fur binds specifically to the Fur box hexameric repeat regions on tdfJ 60

Figure 6. List of differentially expressed genes by Zur in Ngo FA1090 in response to zinc..... 74

Figure 7. rpmE2/J2 and adhP show high-fold change for expression among Zur repressed and induced genes in Ngo 89

Figure 8. A Zur box consensus sequence for Ngo Zur 91

Figure 9. GO and KEGG enrichment analysis for Zur regulated genes in WT Ngo..... 93

Figure 10. Predicted secondary structure and model of Ngo Zur 103

Figure 11. Evolutionary relationship among different Zur and their conserved Zur boxes 105

LIST OF ABBREVIATIONS

βME	beta mercaptoethanol
%	percent
°C	degrees Celsius
<	less than
>	greater than
~	approximately
5'RACE	5' Rapid Amplification of cDNA Ends
A_{450}	Absorbance at 450 nanometers
ABC	ATP-binding cassette
AP	Alkaline Phosphatase
apo-	empty/no metal bound
ATP	adenosine triphosphate
BCIP	5-bromo-4-chloro-3-indolyl-phosphate
bp	base pairs
BSA	Bovine Serum Albumin
CDC	Centers for Disease Control and Prevention
CDM	Chelex-treated Chemically Defined Medium
cDNA	Complementary DNA
CFU	Colony Forming Units

CO_2	Carbon Dioxide
cv	column volume
DNA	Deoxyribonucleic acid
dNTP	Deoxynucleoside triphosphate
DPI	DNA-Protein Interaction
DTT	dithiothreitol
ECL	Enhanced Chemiluminescence substrate
EDTA	ethylenediaminetetraacetic acid
ELISA	Enzyme Linked Immunosorbent Assay
Fur	Ferric uptake regulator
GCB	Gonococcal Broth
GO	Gene Ontology
GSP	Gene Specific Primer
H_2SO_4	Sulphuric acid
HCl	Hydrochloric acid
HEPES	N-2-hydroxyethylpiperazine-N'-2-ethanesulfonic acid
His	Histidine tag
HRP	Horseradish peroxidase
IPTG	isopropyl ß-D-1-thiogalactopyranoside
K_D	dissociation constant

kDa	Kilo Dalton units
KEGG	Kyoto Encylopedia of Genes and Genomes
KU	Klet Unit
L2FC	Log_2 fold-change
LB	Luria Bertani Broth
LOS	lipooligosaccharide
M	Molar
mg	milligram
mL	milliliter
mM	milli molar
Mn^{2+}	$MnCl_2$
NaOH	Sodium hydroxide
NBT	Nitro blue tetrazolium
NET	Neutrophil extracellular trap
Ngo	*Neisseria gonorrhoeae*
Ni^{2+}- NTA	Nickle activated nitrilotriacetic acid
nt	nucleotide
OD_{600}	Optical Density at 600nm
OMV	Outermembrane vesicle
PBS	Phosphate Buffer Saline

PBS-T	Phosphate Buffer Saline +Tween 20
PCR	Polymerase Chain reaction
PMSF	phenylmethylsulfonyl fluoride
RNA	Ribonucleic acid
RNA Seq	RNA Sequencing
rpm	Revolutions per minute
RT	Reverse Transcriptase
RT-qPCR	Real Time -quantitative PCR
SDS-PAGE	Sodium Dodecyl Sulfate- Polyacrylamide Gel Electrophoresis
STI	Sexually transmitted infection
TB	Terrific Broth
TBS	Tris Buffer Saline
TBS-T	Tris Buffer Saline+ Tween 20
TDT	TonB- dependent transporters
TMB	Tetramethyl benzidine substrate
TOPO	Topoisomerase based cloning
TPEN	N,N,N’,N’-tetrakis(2-pyridinylmethyl)-1,2-ethanediamine
WCL	whole cell lystae
WHO	World Health Organization
WT	Wild type

Zn	$Zn_2(SO_4)_2$
Zur	Zinc uptake regulator
α	alpha
β	beta
µg	microgram
µL	microliter
µM	micromolar

CHAPTER 1. INTRODUCTION

I. Family Neisseriaceae

The family *Neisseriaceae* comprises of the genus *Neisseria* and several heterogeneous genera *Moraxella*, *Kingella*, *Eikenella*, *Alysiella*, *Simonsiella*, *Acinetobacter* among others constituting a branch under the umbrella of β-proteobacteria (1). Upon repeated revision of this taxonomy over the decades, *Moraxella* and *Acinetobacter* have now been classified as part of the *Moraxellaceae* family based on 16SrRNA gene sequence analysis and whole genome sequencing (2, 3). Members of *Neisseriaceae* are non-spore forming, gram-negative, aerobes or facultative anaerobes rod-shaped or coccidal, oxidase positive and catalase positive organisms.

The members of *Kingella* and *Eikenalla* are predominately human commensals that colonize the bowel and oral cavities, occasionally causing opportunistic infections of the joints and bones (4). The genus *Neisseria* is named after Albert Neisser who discovered *Neisseria gonorrhoeae* as diplococci within neutrophils in urethral exudates from patients in 1879. This genus is comprised of several commensal species and two pathogenic members, *N. gonorrhoeae* and *N. meningitidis* (5). Members of *Neisseria* are non-motile diplococci with flattened sides, that have optimum growth temperatures in the range of 35-37°C, in the presence of sufficient CO_2 (6). Characteristic features of majority of these human-associated *Neisseria* include utilization of carbohydrates sugars glucose or maltose resulting in acid production, nitrite reduction to produce nitric oxide except for the commensal *N. mucosa* which reduces nitrate to nitrite and breakdown of sucrose to polysaccharides (7).

II. Pathogenic *Neisseria*

N. meningitidis an agent of acute bacterial meningitis and *N. gonorrhoeae* the agent of gonorrhea, are both human-specific pathogens. *N. meningitidis* can be carried asymptomatically by healthy individuals where they colonize the nasopharynx (8). Severe cases of meningitis can cause dissemination to the brain and meninges resulting serious complications and even death. By contrast *N. gonorrhoeae* is always pathogenic and is never human associated commensally like *N. meningitidis*. *N. gonorrhoeae* can colonize host urogenital mucosa, oropharynx, and nasopharynx however dissemination to distal sites can occur (5). Although both *N. gonorrhoeae* and *N. meningitidis* are similar at the genomic level they cause markedly difference diseases. Though rare, the rest of the commensal *Neisseria* can occasionally cause opportunistic infections in immunocompromised individuals resulting in endocarditis, septicemia, otitis and meningitis (5, 9).

III. Meningococcal Disease

A. Epidemiology

N. meningitidis frequently inhabit the human nasopharynx as colonization carriers resulting in asymptomatic infections which constitutes 10% of individuals. Of this population, 25% can be colonized over several months, and about 40% are transiently colonized with a third being intermediately colonized (10-12). Carriage rates are dependent on age with maximum carriage in early adulthood (13). High rates of meningococcal carriage up to a 100% have been reported in epidemic outbreaks and among university students and some military recruits in several countries. As a result of this close contact, transmission is person to person through

exposure to upper respiratory tract secretions (14). Besides age and direct contact, several risk factors such as tobacco use, respiratory tract infections of viral or bacterial origin and socioeconomic backgrounds influence carriage rates and risk of disease (15). Meningococcal disease is also eminent and detrimental in individuals with defects in complement regulation and are at an elevated risk for recurrent serious infections. Meningococcal disease incidence varies from very rare at 1 to as high as 1000 cases per 100000 per year, with the highest rates occurring the meningitis belt of sub-Saharan Africa (16). This is primarily believed to be from seasonal variations with the "dry season" resulting in the highest number of cases ranging from Ethiopia in the east to Senegal in the west (17, 18). The polarity between asymptomatic carriage and occasional devastating disease is attributable to the variable capsular polysaccharide composition, resulting in the different serogroups A, B, C, W-135, X and Y responsible for more than 90% of the meningococcal cases worldwide (16). Currently in Europe, United States, Australia and New Zealand, serogroups B, Y and C dominate, while serogroup A has emerged as the primary source in Africa, causing epidemic outbreaks every 5- 10 years (19).

B. Disease

During pathogenesis initial attachment and invasion of *N. meningitidis* to the nasopharyngeal mucosa, is facilitated by the type IV pilus and opa protein respectively (20). Twitching motility of meningococci further aids in the penetration of mucsoa and attachment to epithelial cells, which is required for colonization (20). After attachment, the meningococcal adhesins further stimulate the epithelial cells of the nasopharynx to engulf the meningococci into phagocytic vacuoles, enabling parasite induced endocytosis into the subepithelial membranes (21).This can lead on to entry of meningococci into the bloodstream, causing disseminated

infection and sepsis, which although more frequent is less clinically recognized (20, 22). The dissemination can lead to meningococcal colonization and seeding of the meninges, pericardium, and synovial joints, resulting in meningitis. Meningococcal meningitis progresses quickly with the presentation of typical symptoms of fever, nausea, photophobia, stiffness of neck and sudden onset of severe headache, which if not treated in a timely manner can result in life-threatening disease progression (18) (23). Sepsis from meningococcal colonization, known as meningococcemia, can lead to hypotension and a purplish rash which can then develop further to a renal hemorrhage and organ failure. This form of sepsis is however rare, occurring in <20% of the patients, of the 75% showing meningococcal bloodstream colonization (23). Pneumonia can occur in up to 15% of the patients with invasive meningococcal meningitis, although detection is minimal due the high number of asymptomatic carriers (23).

C. Treatment and Prevention

Early detection of meningococcal disease has proved to be a problem due to asymptomatic carriage and overlap of symptoms with less life-threatening infections such as the common cold. Typically, blood and cerebrospinal fluids are collected from patients for rapid detection using nucleic acid amplification tests such as quantitative Polymerase Chain Reaction (qPCR) for detection of *N. meningitidis* DNA (24). Following detection patients are treated with antibiotic therapy based on information of antimicrobial resistance among *N. meningitidis* subtypes (25, 26). During the early 1930s sulfonamides were prescribed for treatment of meningococcal disease, however with the emergence of drug resistant strains and capsular subtypes, penicillin became the preferred antimicrobial for treatment which continues to be in use till date (27). Before antimicrobial therapy was available, meningococcal infection had a

mortality rate of around 70%. Since the use of antibiotics and advanced medical technology, these rates have significantly decreased to approximately 9-12% per infection, and up to 40% for those with meningococcemia (28). Despite these improvements, convalescent patients still face serious complications such as hearing loss, limb loss, and neurological disabilities in 11-19% of cases (29, 30). Owing to how severe infections can be and easily spread with 5-10 days of direct contact, containment and prevention strategies are crucial for meningococcal infection, especially for caretakers and medical staff. To minimize the risk and spread of infection the medical staff are often required to receive prophylactic antibiotics (27, 31, 32). Although antibiotic resistance appears to be rare in meningococci, penicillin resistant strains have emerged in the recent past. Due to this reason vaccinations has become the primary method for preventing meningococcal infection globally. The MPSV4 vaccine, produced by Sanofi Pasteur, targeting serogroups A, C, Y, and W-135 has been in use since 1981. However, its efficacy is limited as it does not stimulate T-cells or provide long-term immunity for immunological memory being a polysaccharide only vaccine (33-35). The recent advent of protein conjugate vaccines like MenACWY or Menactra have addressed these limitations and are now recommended for routine vaccination (36, 37). This protein conjugate vaccine however, omits the N. meningitidis serogroup B, which is responsible for 32% of the cases in the United States and 64% of the cases in Europe, Australia and New Zealand (38). In serogroup B the capsule polysaccharide is made up of sialic acid with the specific α2-8 linkage, that is found in several human tissues especially in the developing central nervous systems of fetuses and children (39-41). This results in molecular mimicry, reducing immunogenicity towards such a vaccine and the threat of autoimmune activity against self-antigens. Therefore, serogroup B polysaccharide was removed from the conjugate

vaccine Menactra. To overcome this issue with serogroup B immunotolerance, other outer membrane components were targeted, resulting the 4-component vaccine containing factor H binding protein (fHbp), *Neisseria* adhesion A (NadA), and *Neisseria* heparin-binding antigen (NHBA) (42). These three protein components along with detoxified outer membrane vesicles from the New Zealand outbreak strain NZ98/254 make up the 4-component vaccine, 4CMenB/ Bexero, licensed for use in the United States (43). Efficacy studies have found that 4CMenB is 80-96% effective against target strains, if they express wither fHbp, NadA or NHBA or if they express the P1.4 subtype of PorA (44, 45). Expression of more than one of these antigens directly affects the efficacy of this vaccine (45). Another serogroup b vaccine Trumenba is also licensed in the United States and consists of two distinct fHbp variants Both 4CMenB/Bexsero and Trumenba have shown effectiveness against serogroup B with minimal safety concerns (46). Within the United States 4CMenB is recommended at the age of 16, while MenACWY is recommended to adolescents aged 11 to 12 years, with a booster at the age of 16 (47).

IV. Gonococcal Disease

A. Epidemiology and Incidence

Gonorrhea is an STI and is the second most commonly reported infectious disease in the United States caused by the human pathogen *Neisseria gonorrhoeae* (*Ngo*). It is a huge strain on medical costs with cases soaring at 82.4 million globally each year, with the Center for Disease Control and Prevention (CDC) estimating of over 700,000 cases here in the United States alone as of 2022 (48, 49). Medical costs in the United States as of 2018 were estimated at about $271 million which is huge medical burden (50). The lack of protective immunity from a gonorrhea

infection and spread due to lack of awareness and treatment options leads to these high incidence numbers (51). Spread of gonorrhea is through direct sexual contact and is prevalent among young adults in the age group of 15 to 24 years and factors such as socioeconomic background, race and sexual orientation also influence the incidence groups (49, 50) For example infections are higher in the category of men who have sex with men (MSM) due to co infections with HIV which is higher incidence in individuals with gonorrhea (52-54). Other coinfections are possible such as Chlamydia further increasing the risk of serious disease outcomes in these individuals (55). About 50% of women present with asymptomatic gonorrhea, thereby making them silent carries and also at risk of long term and rather severe consequences from the lack of treatment (56, 57).

B. Disease

Gonorrhea is caused by the pathogenic *Neisseria gonorrhoeae* that primarily infects the genital organs. They affect the mucosal and glandular epithelial surface of the genitourinary tract, but can also colonize in the rectum, pharynges and conjunctiva (58). Using surface structures, the infecting gonococci adhere to the mucosal epithelium thereby colonizing and replicating within the cells (59). A small percent of this colonized *Ngo* are able to invade and transcytose into the epithelial layer leading localized or disseminated infections (60). Localized inflammatory response is a characteristic of gonococcal infections marked by the presentation of purulent discharge, due to the recruitment of neutrophils and macrophages to the site. In men, *Ngo* primarily causes symptomatic urethritis, which can ascend from lack of treatment to cause prostatitis and epididymitis (61, 62). In women, *Ngo* primarily causes cervicitis, however, pose a greater risk of ascension due to the prevalence of asymptomatic presentations as compared to

men. Ascending infections in women lead to serious sequalae such as pelvic inflammatory disease, salpingitis and infertility to name a few (56, 63). In symptomatic infections as seen in 90% of the cases for men, symptoms present within 2 to 5 days after exposure (62). However, women don't see symptoms 5 to 10 days post exposure and can go undetected for longer periods of time in more than 50% of the cases in women (62). Dissemination is a prospect for infections in both men and women, which results in endocarditis, meningitis, and septic arthritis (64-67). Gonococcal infections can also be transmitted from mother to neonates during childbirth, resulting in conjunctivitis that may even lead to blindness (68, 69).

C. Immune Responses to Gonorrhea

It is evident by now that there is no protective immunity or immunological memory from a gonococcal infection and *Ngo* skew the immune response towards an innate Th17 response by inducing tissue production of the transforming growth factor β (TGF-β) and interleukin 10 (IL-10). These cytokine mediators limit the Th1 and Th2 mediated adaptive immune response that would have developed protective immunity (70). The Th17 response induces neutrophil recruitment mediated by the production of pro inflammatory cytokines IL-17 and IL-22 (71). Studies on lower genital tract infection models in mice have recently shown evidence that mice immunizations with gonococcal antigens in the presence of IL-12, which is a Th1 activating cytokine, allows faster clearance and protection from re-infection in female mice (72). Another study showed promise on administration of TGF-β blocking antibodies, that allowed for a Th1 and Th2 mediated adaptive response leading to long term protection in mice (73). However, there are several limitations as *Ngo* is a human specific pathogen and mouse models do not mimic a human infection, leaving treatment options not being straightforward.

Despite the presence of profuse neutrophilic responses to symptomatic natural gonococcal infections, revealed that cytokine and antibody responses to these uncomplicated cervical and urethral infections were weak and short-lived (74). An experimental urethral infection model limited to men, showed elevated levels of IL-8, IL-6, IL-1β and TNF inflammatory cytokines in the plasma and urine samples (75). However, no evidence of enhanced protection to re-infection was observed upon after 2 weeks of treatment to the first experimental infection. Examination of antibody levels in male and female gonorrhea patients showed a local increase in cervical and vaginal IgA1 and IgG levels in female patients, however only a modest increase in serum IgA1 in women alone (76). All these suggest that gonococci subvert the induction of humoral immune response to uncomplicated infections through an unknown mechanism and vaccine efforts should strategize mucosal and systemic immunizations using novel concepts.

Efforts focused on effective vaccine development have garnered some interest towards Transferrin binding proteins (Tbps) due to promising immune response to meningococcal infections (77). However, antibodies below limit of detection were observed against recombinant Tbps, showcasing a lack of both systemic and local antibody response to these proteins during a natural gonococcal infection (78). This study established the starting point and baseline response, over which a robust antibody response needs to be induced to create an effective gonococcal vaccine.

D. Treatment and Prevention

Unlike meningococcal disease, several challenges lie in successfully treating and implementing prevention strategies for gonococcal disease. The virulence determinant of *Ngo* which are ideal targets for a gonorrhea vaccine, undergo high frequency phase and antigenic

variations, thereby making the target redundant and ineffective antibody responses to these evolving antigens (79). Current treatment options are limited to antibiotic therapy in the absence of a successful vaccine and the lack of protective immunity (51). Antibiotics have been used for treatment of a gonorrhea infection for several decades. However, they have a penchant to develop resistance to these antibiotics while maintaining these resistant determinants through the years (80-85). The antibiotic rollout has been from sulfonamides to penicillin in the early 1900s, however since then Ngo strains have emerged that show resistance to all known antibiotic classes (86-88). The most recent WHO and CDC updated recommendation for antimicrobial therapy as of 2020 is a single intramuscular dose of 250mg of ceftriaxone for treatment of uncomplicated gonorrhea (89). Alternative combinations of antibiotics of 2 g azithromycin and either 240 mg gentamycin or 320 mg Gemifloxacin, have been recommended for treating individuals with β lactam sensitivity (90, 91). With dwindling antibiotic therapies, the emergence of an untreatable *Ngo* is on the horizon and there is an urgent need for research and development for the design and implementation of novel therapeutics and vaccines. Recently there was evidence to show that the meningococcal OMV vaccine Bexsero, elicited cross protective antibodies against gonorrhea and this may be considered with follow up research (92). For detection of a gonococcal infection, specimens from urogenital mucosa are collected through swabs and are examined either visually under a microscope for the presence of intracellular gonococci within neutrophils or nucleic acid amplification testing (NAATs) which is a more sensitive option for detection (86, 93). Today practicing safe sex and efficient screening among populations at increased risk are recommended for contact tracing and limiting outbreaks among groups.

V. Virulence Factors of *Neisseria gonorrhoeae*

Ngo being a human host-adapted pathogen, has evolved along with the human host over several centuries, displaying an impressive array of *Ngo* being a human host-adapted pathogen, has emerged from and evolved along with commensals, retaining common features whilst also developing unique characteristics that are critical for their pathogenicity. *Ngo* display an array of impressive virulence factors that enable adhesion, invasion, nutrient acquisition, and immune evasion. These virulence factors are typically surface structures that aid in colonization and transmission. The genes that encode these virulence factors are subject to high frequency phase and antigenic variation, contributing to the mechanism of immune evasion by the gonococcus.

A. Type IV Pilus

Type IV pili are outer membrane filamentous structures that are present universally in gram-negative bacteria including *N. gonorrhoeae* (94). This filamentous pilin can extend several microns from the bacteria cell surface and is about 6 nm in diameter (95). This filamentous structure is made up of 15 proteins which play a role in biogenesis, assembly and disassembly (96). Four steps are involved in pilin synthesis: assembly, functional maturation, counter retraction and emergence on the cell surface which are completed by regulation of 23 genes (97). Assembly of the pilus structure is complicated and involves the major pilus subunit called the PilE with is a 20KDa protein. During pilus biogenesis several minor pilus subunits are involved aiding in the maturation and these include PilD peptidase, PilQ pore-forming complex, PilC tip-associated protein, PilF, PilG, PilT and PilP (98-100). In gonococcal pathogenesis the Type IV pilus play primary roles as an adhesin enabling attachment to epithelial surfaces, microcolony

formation, allowing bacterial twitching motility and DNA uptake for natural transformation (95, 101). During twitching motility, the PilT ATPase and PilC work together to rapidly assemble and disassemble the pilus resulting in the twitching motions of *N. gonorrhoeae* (102, 103). The natural competency of Type IV pilus allows uptake of naked DNA, allowing lateral transfer of genes, which is a major contributor to the antigenic diversity among gonococcal strains and gain of antimicrobial resistance determinants (104, 105). The gonococcal pilus is subject to high frequency phase and antigenic variation. During antigenic variation, the promoter-less, silent *pilS* gene is exchanged for the *pilE* gene by a non-reciprocal Rec-A dependent mechanism, resulting in antigenically distinct gene chimeras, occurring at a frequency of once per 100 cells (106, 107). The *pilC* gene expression is RecA-independent phase variation due to frameshift mutations occurring within a homo-guanine tract occurring within the signal peptide region, turning the gene on/off (108). A similar phase variated is noted in pile that contains a poly-C tract within the coding region, allowing it to slip out of frame during DNA replication and causing decreased pilus production (108).

B. Opacity Proteins

The gonococcal opacity proteins, also known as Opas are integral outer membrane proteins that were originally named so as they cause gonococcal colonies to appear opaque, when viewed by phase contrast microscopy (109, 110). A single gonococcal cell can possess up to 11 *opa* genes which are constitutively expressed (111, 112). Each Opa contains conserved, semi and hyper variable regions with the hyper variable regions of the protein located on the outside of the outer membrane (111). The Opa protein structure constitutes an 8-stranded β barrel, generating 4 surface-exposed loops (95). Opa protein expression like the Type IV pilus

undergoes high frequency phase and antigenic variation, by changing the number of pentameric repeat units -CTCTT- located within its leader peptide region. This results in an on/off switching of expression from slip-strand mispairing, allowing a single to express either none or several different Opa proteins (113-115). Opa proteins play a major role in gonococcal infections which is supported by the observation of recovery of *opa* expressing *Ngo* from patient exudates and male urethral experimental infections (116, 117). They play a critical role in invasion of epithelial cells and recognize two different human cell receptors to initiate invasion (118). They are the OpaHS which recognize heparin sulphate proteoglycans and the OpaCEA which recognize the carcinoembryonic antigen cell adhesion molecule (CEACAM) comprised of the various CD66 (119). They are the OpaHS which recognize heparin sulphate proteoglycans and the OpaCEA which recognize the carcinoembryonic antigen cell adhesion molecule (CEACAM) comprised of the various CD66 molecules (120-124). These specific interactions of Opas with host proteins affects the disease outcome and invasive capacity. During vaginal colonization Opa association with CEACAM 5, has been shown to enhance colonization for a longer period of time in the lower genital tract, while association with CEACAM 1 was found to enable transcytosis through epithelium and ultimately aid in dissemination (125). Binding of Opas to CEACAM 3 on neutrophils initiates voluntary phagocytosis, however, more recent studies have suggested that this interaction occurs minimally to alleviate the pressure on *Ngo* to survive the toxic oxidative stresses of neutrophils (126, 127). CEACAM 1 interactions with Opa have been shown to have effects on immune responses to infection by arresting activation of CD4+ T cells and death of B-cells, thereby evading immune response with the loss of immunological memory (128, 129). A second arm of immune evasion by Opas is in their ability to skew the immune response away

from innate Th-1 and Th-2 responses, mediated by TGF-β and IL-10 towards an adaptive Th-17 response which is favorable for *Ngo* survival (70, 130).

C. Porin

The outer membrane porin protein, Por is the most abundant protein in the gonococcus, constituting approximately 60% of the total protein. Serological classification of gonococci are based on Por, with 9 distinct serovars identified for *Ngo* (131). There are two different classes of Por in *Neisseria* being PorA and PorB, with PorA being associated with disease complications while PorB being associated with uncomplicated mucosal infections (132, 133). In *Ngo* however, *porA* is a pseudogene which is not expressed (134). Only PorB is produced in gonococci and they further produce two subtypes PorB1A and PorB1B (135). Within these subclasses PorB1A is associated with dissemination phenotype and PorB1B is present in localized infections (136). Porins aid in the survival of gonococci by allowing the transport of ions and nutrients across the outer membrane (137). They can translocate into host cell membranes, disrupting cell signaling and phagosome maturation to escape killing, thereby promoting the intracellular survival of gonococci (138-140). Resistance to serum and classical and alternate complement pathway mediated killing has been observed upon PorB1A binding to host Factor H and C4b binding protein (141-143).

D. Lipooligosaccharides (LOS)

Like most other gram-negative bacteria, the gonococci also possess Lipopolysaccharides (LPS) on their outer membrane, however unlike most LPS the gonococci lack the O antigens in their polysaccharide core, and are designated as Lipooligosaccharide (LOS) (131). There is much

variation in the type of LOS produced by gonococcal cells and this is due to the highly variable composition of the oligosaccharide carbohydrate content and length, with specific compositions being essential for pathogenesis (144). In addition to its role as an endotoxin, the gonococcal LPS can mimic human glycosphingolipids and bind receptors such as asialoglycoprotein enhancing invasion of urethral epithelia (145-147). During an infection, gonococcal sialyltransferase work to deposit sialic acid from the host cytidine-5'-monophospho-N-acetylneuraminic acid (CMP-NANA) onto certain variants of LOS, contributing to serum resistance (148-150). Resistance to complement-mediated killing and bacteria antimicrobial peptides is attributed to the gonococcal LOS masked by deposition of phosphoethanolamine (PEA) in addition to sialylation. Deposition of PEA has a significant effect with strains lacking this phenotype showing lower colonization rates in mouse infection models (151-154). As indicated previously, LOS is subject to phase variation of the glycosyltransferase genes *lgtA*, *lgtC* and *lgtD* that contain a poly-G tract within the coding region causing them to slip and vary in terminal sugars of the LOS polymer thereby also resulting in antigenic variability (155, 156). Research shows that LOS allows the gonococcus to fluctuate between being invasive and serum resistance, interfering with the invasion of certain cell types (157).

E. IgA1 Protease

The human mucosa is the site for most infections including gonococcal colonization and is enriched in the immunoglobulin IgA to combat infections. *Ngo* produce an IgA protease, which upon release from the cell, undergoes endo and proteolytic cleavage, to produce the mature form of IgA1 protease (158). This mature form of IgA1 protease targets proline-rich hinge region of the IgA1 heavy chain. This cleavage site is determined by the type of the IgA1 protease

expressed by gonococci and there are two classes of IgA1 protease. The class 1 protease recognized proline/serine bond at residue 237 and class 2 targets a proline/threonine bond at residue 235 (159-161). The IgA1 protease cannot cleave IgA2, however can cleave the glycoprotein lysosome-associated membrane protein 1 (LAMP1) found within lysosomes and late endosomes. Cleavage of LAMP1 accelerates lysosomal degradation thereby increasing the intracellular survival rates of *Ngo* (162-165).

VI. Host Metal Restriction and Homeostasis

Neisseria like most bacteria require trace metals such as iron and zinc for survival and pathogenesis. These transition metals are used by bacteria for important cellular and metabolic functions. The host engages in protecting against infection by withholding free zinc or iron away from *Ngo* by the process termed as nutritional immunity and this is effective against most pathogens.

A. Iron

Iron is an essential micronutrient for all living organisms including humans and it plays key roles in biochemical and physiological process such as energy metabolism, oxygen transportation and DNA replication (166). It is critical for facilitating redox reactions and as a cofactor for the functioning of several key enzymatic reactions, due to its redox oxidation states as ferrous (Fe^{2+}) and ferric (Fe^{3+}) iron. Despite its advantageous roles, this redox potential of iron can have adverse effects on biological molecules and cells due to the destructive nature of Fenton chemistry. This reaction which involves Fe^{2+} and hydrogen peroxide, generates reactive oxygen species (ROS) capable of harming biomolecules such as lipids, proteins and DNA (167). To

minimize the toxicity from this Fenton chemistry, majority of the iron in mammals is held within intracellular compartments, complexed with hemoproteins and iron-storage proteins (166). Therefore, the bioavailability of free iron is low in humans, which is further decreased during an infection by the process of nutritional immunity (168).

1. Transferrin

Transferrin is a pivotal human iron transport protein that is an 80kDa glycoprotein. It is abundant in human serum and facilitates iron transport to various tissues in the body (169). Structurally, transferrin has a bi-lobed configuration comprising of N-terminal and C-terminal domains with high-affinity iron-binding regions that coordinates a single Fe^{3+} ion, with a dissociation constant of approximately 10^{-7} to 10^{-9} M (170, 171). Within the spectrum of human serum, transferrin concentrations accounts for approximately 25 to 50µM, with 30% of total iron binding sites available harboring an iron atom at any given time, with a slight preference for the N-lobe pocket (172-174). All cells with a metabolic requirement for iron, express transferrin, with a preference for binding ferrated transferrin. Although diferric transferrin binds more tightly, both monoferric forms establish stable complexes with the host cell receptor. Following binding the transferrin-host receptor complex is engulfed and internalized into an endosome, where iron-liberation occurs through acidification, leaving an apo-transferrin-receptor complex to be recycled to the cell surface (169, 175, 176). Upon reaching the cell surface, a new ferrated-transferrin molecule displaces the apo-transferrin, binding the receptor with higher affinity than the apo form under neutral pH conditions (175, 176).

2. Lactoferrin

Lactoferrin belonging to the transferrin family of the host iron binding and transport proteins, is less abundant in serum as compared to transferrin, however, is it found in various secretions including the saliva, semen, vaginal fluids, urine, bile, amniotic fluids, blood plasma and specific leukocytes (177, 178). Within milk it ranks as the second most abundant protein after casein (175, 179-181). Like transferrin, lactoferrin also has a bi-lobed structure and is an 80 kDa glycoprotein, demonstrating a high affinity for iron binding (182, 183). However, unlike transferrin lactoferrin has shown to bind metal ions other than iron, including, copper, manganese, and zinc (184). It is also able to maintain its iron bound state over a broader range of pH unlike transferrin which requires a neutral pH. This property along with lactoferrin's widespread presence across various anatomical sites makes it particularly effective in not only maintaining iron homeostasis but also in restricting bacterial growth. This dual function is achieved via two mechanisms, one through iron sequestration and second through autoproteolysis of its N-terminus, which generates small antimicrobial compounds known as lactoferricins (185-188). These compounds interact with bacterial surface receptors, disrupting membrane integrity and ultimately leading to bacterial cell lysis (185-188).

3. Heme and Hemoproteins

Heme is a small porphyrin ring coordinating ferrous iron, stores about 70% of human iron (189). Heme is essential for oxidative stress responses, oxygen storage and electron transport, coordinating catalytic functions within the cell (190). However, this catalytic potential can also lead to potential toxicity of the cell when heme is present in excess, much like most transition

metal ions, leading to the production of reactive oxygen species. To prevent this toxicity 95% of the heme is kept bound within hemoproteins of which hemoglobin makes up 67% (191). Hemoglobin is present as a tetramer made up of two α and two β subunits together binding four heme molecules (191). Hemoglobin is abundant in erythrocytes, however, are subject to hemolysis, releasing $\alpha\beta$ dimers in the blood (192). To overcome toxicity Haptoglobin then binds the dimers released and shuttling them to the liver to clear them (193-195). Albumin and hemopexin also play a role in mitigating heme toxicity if heme is released from hemoglobin or hemopexin during damage (193).

4. Ferritin

Ferritin is an iron storage and binding protein that binds to intracellular iron unlike transferrin, lactoferrin and hemoproteins which bind extracellular iron (196, 197). Ferritin is composed of a heteropolymer of 24 subunits, composed of heavy and light chains. The mature protein at 450 kDa form a nearly spherical structure capable of accommodating 4500 iron atoms (198-200). Ferritin is upregulated in macrophages during an infection, which is followed by an inflammatory response. This causes the serum iron levels to drop and thereby increasing the cellular iron concentrations and leading to holding of iron within ferritin (196, 197). This iron from ferritin is released during iron-deplete conditions by the process of proteasomal degradation (201, 202). The importance of this ferritin regulation has been shown to crucial for survival of cells, with ferritin knockout mice showing a survival defect (203).

B. Zinc

Zinc has gained focus on its role in cellular processes and is crucial for enzymatic, catalytic functions, signaling and as a structural component of proteins much like iron has. Metalloproteins and enzymes utilize zinc as structural or catalytic components (184, 204). Within eukaryotic cells, the cytoplasm contains 50% of zinc, the nucleus contains 40% of total zinc and the remaining 10% is present with membranes and cell walls (205). In prokaryotes, 80% of the zinc is utilized in enzymatic components and only 6% is within bacterial proteins (205). Zinc due to its catalytic propensity can be toxic to the cell in abundance and are tightly regulated and stored within proteins much like iron storage and neutralization. Free zinc within the body is at picomolar ranges because majority of the intracellular zinc which in total is at about hundreds of micromolar in concentration is present in proteins functioning as zinc stores and within nutritional immunity proteins (206). An example of excess zinc mediated toxicity is exhibited by inhibition of clathrin-mediated insulin endocytosis, disrupting insulin clearance (207). This highlights the need for a tight control of zinc within the cell.

1. S100 Proteins

The S100 family of proteins play a central role in calcium signaling and homeostasis in mammals. They are EF-hand containing proteins that exist as obligate dimers, with each four-helix monomers combining to form a stable form of antiparallel dimer with 8 helices (208). With more than 20 identified members of the S100 protein family, each of the S100 protein share a common structural unit consisting of a helix-Ca^{2+} binding loop-helix motif, forming in pairs to make a stable helix bundle (209). Although homodimerization is mostly preferred,

heterodimerization is possible as seen in S100A8/S100A9 heterodimer which is an important nutritional immunity zinc sequestration protein calprotectin (210). Beyond its involvement in calcium regulation, they are integral to various intracellular processes including cell cycle regulation, transcription, motility, cell growth and differentiation. S100 proteins are also important biomarkers for disease, inflammation, and immune modulation. Anti- inflammatory response regulation by S100 proteins involve scavenging of reactive oxygen species (ROS), leading to apoptosis of tumor cells and endothelial cells (211). S100 proteins exhibit characteristics akin to cytokines and chemokines due to their interaction with pattern recognition receptors such as receptor for advanced glycation end products (RAGE) and Toll-like receptor 4 (TLR4) (211-213). Thereby triggering a range of responses, such as recruitment of inflammatory cells neutrophils, macrophages, as well as the activation of proinflammatory cytokines via the NF-κB and MAPK pathways (214, 215). Several S100 proteins are associated with inflammatory disease such as S100A7's immune modulatory effect in association with atopic dermatitis and psoriasis and S100A8/A9 calprotectin in inflammatory bowel disease, cystic fibrosis, and rheumatoid arthritis (216-219).

Owing to their zinc sequestration abilities, S100 protein function as nutritional immunity protein preventing bacteria growth and pathogenesis. This has been demonstrated in various pathogens such as *Staphylococcus aureus*, *Helicobacter pylori*, *Candida albicans*, *Acinetobacter baumannii*, *Escherichia coli*, *Pseudomonas aeruginosa*, and *Salmonella enterica serovar typhimurium* by using S100A7, S100A12 or calprotectin for antimicrobial effects by nutrient limitation (220-224).

2. Metallothioneins

Metallothioneins are small cysteine-rich proteins that aid in zinc homeostasis by sensing intracellular zinc levels. A single metallothionein is able to coordinate up to 7 zinc ions (225, 226). Between 5 and 15% of cytosolic zinc is bound by metallothioneins, while other zinc ions are shuttled in and out of endosomes (227, 228).

VII. Metal Acquisition by Pathogenic *Neisseria*

Nme and *Ngo* have evolved sophisticated mechanisms to flourish within their obligate human host environment, notable by hijacking critical trace metals for survival. Their primary strategy involves synthesis of high affinity TonB-dependent outer membrane transporters (TDTs). TDTs works alongside the Ton motor complex and specific high affinity ABC transporters for the transport of metal ion from the outer membrane, through the periplasm and into the cytoplasm (229). There are 8 known TDTs in *Neisseria*, majority of which have been characterized as iron importers and 2 are known zinc import TDTs (229).

A. Two Component TDTs-

All known TDTs have 22-strands to make up the β-barrel spanning the outer membrane, along with 11 flexible extracellular loops positioned between the barrel's antiparallel strands (230-232). Additionally, there's a folded plug domain at the N-terminus, obstructing the barrel's pore (230-232). To enhance transporter function, three gonococcal TdT systems employ a second component: a lipid-modified accessory protein anchored to the outer membrane. The most well-characterized of these is the transferrin-iron uptake system, which binds to the C-lobe of human transferrin, extracting its iron (233, 234). The key component, transferrin binding protein A

(TbpA), that binds apo- and Fe-transferrin, facilitating iron transfer through the outer membrane. The second motif, found in all TdTs, is a short N-terminal amino acid sequence called the TonB-box, interacting with the TonB protein from the Ton motor complex to power the transporter (235). Mutations in this region abolished nutrient transport while having no effect on transferrin binding (236). The third motif, situated in the plug domain, comprises the residues EIEYE. This negatively charged motif is thought to transiently chelate the iron atom after from transferrin, playing a crucial role in iron utilization (237).

The second component, TbpB, is a bi-lobed lipoprotein with specificity for Fe-transferrin, binding exclusively to the N-lobe of TbpB. TbpB significantly enhances the efficiency of iron import by TbpA although it is not necessary for transferrin binding (233, 238-242). *tbpAB* is present in all gonococcal and meningococcal strains, organized into an iron-regulated bicistron with *tbpB* preceding *tbpA* (243, 244). TbpA exhibits high degree of conservation among gonococcal isolates, with over 95% sequence identity, while TbpB displays antigenic variability, suggesting a potential role to protect TbpA (245, 246). The importance of iron piracy is evident from an experimental urethral infection study in human males, where a gonococcal strain unable to utilize transferrin failed to establish infection (247).

The lactoferrin-iron acquisition system, composed of the transporter lactoferrin binding protein A (LbpA) and the lipoprotein LbpB, scavenges iron from human lactoferrin and shares significant similarities with the transferrin system (248). *lbpA* and *lbpB* are organized in a bicistronic operon with the B gene preceding the A gene (249, 250). Beyond iron acquisition, LbpB also protects *Neisseria* from the lactoferrin-derived lactoferricin (251). Unlike the transferrin

system, approximately half of gonococcal isolates express the lactoferrin system, and LbpB expression is phase-off most times, through slipped-strand mispairing (250, 252).

The third system in *Neisseria* is the hemoglobin/haptoglobin (Hb/Hp) uptake system, which comes in two forms: HmbR and HpuAB (253). While *N. meningitidis* can potentially express both systems, all known *N. gonorrhoeae* strains are limited to HpuAB due to the absence of functional *hmbR* (253-256). The *hpuAB* locus encodes two proteins: the lipoprotein HpuA and the TonB-dependent transporter HpuB, essential for acquiring heme-iron from human hemoglobin and hemoglobin-haptoglobin complexes. Unlike the transferrin and lactoferrin systems, both HpuA and HpuB are indispensable for ligand binding and utilization (254, 255, 257). The HpuAB system undergoes high-frequency phase variation due to a poly-G tract in *hpuA*, and its significance during infection varies based on whether the host is male or female (258, 259). Gonococcal isolates from women with localized infections generally harbor isolates lacking HpuAB expression, however phase-on isolates have been recovered from women infected early in their menstrual cycle (260). These findings imply that while HpuAB expression is not essential for gonococcal colonization, the Hb/Hp system is favored during menstruation when hemoglobin is abundant, likely due to increased ligand availability (260).

B. Single Component TDTs-

The remaining five TdTs function independently, and do not require an additional lipoprotein. FetA (FrpB) binds to siderophores—small, non-ribosomal compounds produced by other bacteria to obtain iron (261). Although *Neisseria* themselves don't produce siderophores, they've developed a strategy to utilize those produced by other species, such as ferric enterobactin, ferric salmochelin, and dihydroxybenzoic acid (262, 263). Like other receptors for

hemoglobin and lactoferrin, *Neisseria* FetA undergoes phase variation through slipped-strand mispairing, though in the promoter region rather than in the coding sequence (264).

The remaining four TdTs, collectively referred to as TonB-dependent function (Tdf) F, G, H, and J, share similar names. Among them, TdfH and TdfJ are more extensively studied. TdfH (CbpA) is found in both pathogenic *Neisseria* species but is less common in commensals. It binds human calprotectin and extracts zinc from it with high affinity, possibly aiding in manganese acquisition as well (265). TdfJ (ZnuD) is present in all *Neisseria* species and is crucial for zinc uptake. Upon binding zinc, it undergoes structural changes facilitating zinc transport to the periplasm (266). While TdfF and TdfG are less explored, their transcriptional regulation suggests involvement in iron uptake, with TdfF potentially contributing to gonococcal survival in human cervical epithelial cell culture (267). TdfF is found in both pathogenic *Neisseria* species, whereas TdfG is specific to the gonococcus (268).

C. The Ton Motor Complex

The Ton motor complex energizes the transport of iron, iron chelates, heme and zinc and consists of three proteins in the cytoplasmic membrane: TonB, ExbB and ExbD. TonB forms a dimer in vivo, yet its exact role in physiological processes remains unclear (269). The interaction dynamics between TonB and TdTs, from association and dissociation, are still not fully understood (270, 271).

In terms of function, when a ligand binds a TdT, it triggers a structural change that exposes the TonB-box, a short N-terminal amino acid sequence at the periplasm side. The C-terminal end of TonB, located in the periplasm and extending from the cytoplasmic membrane, then binds to the TonB-box, creating a stable complex that physically connects the TdT to the cytoplasmic

membrane (272). However, the precise mechanism by which TonB facilitates transport after forming this complex remains not fully understood. Several models have been proposed, all suggesting that the complex utilizes the proton motive force to alter the conformation of the TdT plug domain, possibly through pulling, rotation, or denaturation (230, 273, 274). For example according to one model, the C-terminal end of TonB, bound to the TdT plug, drawing the plug towards the periplasm and partially unfolds it, creating a channel in the TdT β-barrel for nutrient traversal (230). Molecular dynamics simulations support the feasibility of such a model within the constraints of the TonB/TdT binding interaction and proton motive force energy.

D. ABC Transporters

Iron or zinc atoms from the outer membrane, move across the periplasmic space, through the cytoplasmic membrane, and into the cell's cytoplasm. This is facilitated by a dedicated ATP-binding cassette (ABC) transporter. These transporters comprise of three components, which include a periplasmic binding protein, which captures metal ions; a cytoplasmic permease, forming a conduit for entry into the cell; and an ATPase, providing energy through ATP hydrolysis (275, 276). The *Neisseria* genome harbors multiple genes that encode ABC transporters, with three systems collectively serving the TdTs. Specifically, the FbpABC transporter supports the transferrin and lactoferrin systems, FetA relies on the FetBCD system, and ZnuABC assists TdfH and TdfJ (237, 262, 277, 278) (229, 279, 280). Despite the existence of diverse ABC transporters, *Neisseria* lacks a dedicated transporter for heme. Additionally, while potential interactions between TdfF and TdfG with ABC transporters are conceivable, they remain incompletely understood.

VIII. Regulation of Gene Expression

Maintaining metal homeostasis is essential for Ngo's survival and pathogenicity, so as to overcome both metal ion sequestration and toxicity imposed by the host. To this end *Ngo* tightly controls the regulation of its iron and zinc uptake systems depending on the availability of these metal ions using two FUR family regulators, Ferric uptake regulator (Fur) that regulates iron homeostasis and the Inc uptake regulator (Zur) that maintains zinc homeostasis (281, 282). The FUR family regulators are abundant in prokaryotes and share a common winged-helix DNA binding domain on their N-terminus and a dimerization metal binding domain at the C-terminus. This dimerization domain is composed of histidine rich residues, $HHHXHX_2CX_2X$ which are characteristic for DNA-binding (283). Both Fur and Zur coordinate their cognate metal ions Fe2+ and Zn2+ respectively to bind promoter DNA during excess iron or zinc (228). In the absence of metal during nutritional immunity, these regulators cannot bind DNA and therefore the genes are transcribed, including expression of the above-mentioned *Ngo* TDTs, TonB motor complex and ABC transporters (284, 285). Fur and Zur recognize conserved DNA sequences on the promoter of genes known as Fur and Zur box to bind and regulate expression (283). These consensuses are mostly conserved across families with both pathogenic *Neisseria* showing conservation of the Fur and Zur box they recognize (282, 283, 285). The Fur family of regulators control virulence, defense against ROS and transport of metal ions. In several pathogens such as *E. coli*, *Vibrio cholerae*, a *fur* mutant results partial or complete loss of fitness in animal models of infection, with a loss of critical metabolic and catabolic functions (286, 287). This further signifies the critical contributions of these regulators in virulence and disease.

IX. Research Objectives

The goal of the research study described in this dissertation is to understand the multifactorial role the Zinc uptake regulator (Zur) plays in *Ngo*. We aimed to demonstrate a comprehensive and experimentally validated analysis of transcriptomic responses to variation in zinc availability by *Ngo* Zur. We pursued three objectives to address our overall goal. 1. We performed transcriptomic RNA Seq analysis to get the big picture on all the genes Zur controls in *Ngo* when faced with zinc starvation versus zinc excess and consolidated genes that were paramount for virulence and homeostasis functions. 2. We then narrowed down our analysis of Zur's function as a global regulator able to both activate and repress gene expression and evaluate genes and their promoter characteristics that allow activation in the presence of zinc. We determined a conserved Zur-box that *Ngo* Zur recognizes to activate and repress gene expression. 3. Next we explored the characteristic of the promoter of *tdfJ*, coding for the zinc uptake TDT TdfJ, an important vaccine antigen. We identified a key characteristic in the control of *tdfJ* for its maximal expression owing to its dual control by iron and zinc. We determine conserved regions and propose a mechanism that allows for the dual control of this virulence gene.

CHAPTER 2 MATERIALS AND METHODS

I. Bacterial Strains and Routine Maintenance

Strains and plasmids used in this study are listed in Table 1. Plasmids were propagated in *Escherichia coli* strains TOP10, DH5alpha or BL21 DE3 pLysE. *E. coli* strains were cultured in Luria-Betrani (LB) broth media supplemented with antibiotics carbenicillin (100 µg/mL), kanamycin (50

μg/mL) or erythromycin (34 μg/mL). *Neisseria gonorrhoeae* (*Ngo*) WT and mutant strains were routinely maintained on GC medium (Difco) base agar plates with Kellogg's supplement and 12 μM $Fe(NO_3)_3$ (GCB Plates) at 36°C and 5% CO_2 atmospheric conditions . For long-term storage, strains were stored in either *E. coli* or GC freezing media at -80C. *Ngo* growth conditions for specific regulation experiments are described below.

Table 1. Strains and Plasmids

Strain/ Plasmid	Genotype/ relevant characteristics	Reference
E.coli		
DH5-α	F + endA1 glnV44 thi-1 recA1 relA1 gyrA96 deoR nupG purB20 ϕ80dlacZΔM15 Δ(lacZYAargF)U169, hsdR17(rK– mK+), λ–	NEB
TOP10	F – mcrA Δ(mrr-hsdRMS-mcrBC) ϕ80lacZΔM15 ΔlacX74 recA1 araD139 Δ(ara-leu)7697galU galK rpsL (Strr) endA1 nupG	Invitrogen
BL21 (DE3) pLysE	F^-*ompT hsd*SB (r_B–, m_B–) *gal dcm* (DE3) pLysE(Cam^r)	Invitrogen
N.gonorrhoeae		
FA1090	Wildtype (Δ*lbpA*, HpuAB off)	(288)
MCV964	FA1090 *zur*::*kan* (Kan^r)	(289)
MCV404	FA1090 *fur*-1(Erm^r)	Dr. Aminat T. Oki, (289)
Plasmids		
pET-19b	His-tag expression vector	Novagen
pCR4-TOPO	TOPO TA cloning vector	Invitrogen
pCR2.1-TOPO	TOPO TA cloning vector	Invitrogen
pGSU606	pET19b + FA1090 *fur*	This study
pGSU605	pCR4.TOPO+5'RACE *tdfJ* insert (from FA1090 *zur*+Zn RNA)	This study
pGSU611	pCR2.1 TOPO TA+5'RACE *tdfJ* insert (from FA1090 WT+TPEN 2 RNA)	This study
pGSU612	pCR2.1 TOPO TA+5'RACE *tdfJ* insert (from FA1090 WT+TPEN 3 RNA)	This study

pGSU613	pCR2.1 TOPO TA+5'RACE *tdfJ* insert (from FA1090 WT+TPEN 5 RNA)	This study
pGSU622	pCR4.TOPO+gbGSU014 gene block for scrambled Fur box P_{tbpB}	This study
pGSU623	pCR4.TOPO+gbGSU015 gene block for scrambled Fur/Zur box-1 P_{tdfJ}	This study
pGSU624	pCR4.TOPO+gbGSU016 gene block for scrambled Fur/Zur box-2 P_{tdfJ}	This study
pGSU625	pCR4.TOPO+gbGSU017 gene block for scrambled Fur/Zur box-3 P_{tdfJ}	This study
pGSU626	pCR4.TOPO+gbGSU018 gene block for scrambled Fur/Zur box-4 P_{tdfJ}	This study
pGSU627	pCR4.TOPO+gbGSU019 gene block for scrambled Fur/Zur box-5 P_{tdfJ}	This study
pGSU628	pCR4.TOPO+gbGSU020 gene block for scrambled Fur box- all P_{tbpB}	This study
pGSU629	pCR4.TOPO+gbGSU021 gene block for scrambled Fur/Zur box- all P_{tdfJ}	This study

II. *Ngo* Growth Conditions for Zur Regulation and RNA Sequencing Experiments

Ngo strains FA1090 WT and MCV964 (FA1090 *zur::kan*) (Table 1) (289), were grown under zinc-restricted conditions as previously described (290). Briefly, non-piliated colonies were selected and passaged onto GCB plates containing 5 µM *N,N,N′ N′* -tetrakis-(2- pyridylmethyl)-ethylenediamine (TPEN) (Sigma), a zinc-specific, to deplete any internal zinc stores of *Ngo*. Single non-piliated gonococcal cells from GCB TPEN plates, were used inoculated into 50 mL chelex-treated chemically defined media (CDM) at an initial OD_{600} of ≅ 0.9. The strains were grown at 36°C and 5% CO_2 with vigorous shaking at 225 RPM in acid-washed baffled flasks and allowed to grow exponentially. After doubling of OD_{600} (approx. 1.5 to 2 hours), the CDM was supplemented with either 20µM Zn(SO4)2 for excess zinc condition or 7 µM TPEN for zinc-deplete condition. Both strains were allowed to grow to mid or late log phase (about 2.5 to 3 hours), with the OD_{600} being measured every 30 min to 1 hour, to track the growth curve. Whole cell lysates were collected by normalizing the OD to 100,00KU (Klett units) at 600nm. The remaining sample was used for RNA isolation, for subsequent RNA Sequencing, RT-qPCR or 5'RACE.

III. RNA Isolation and Processing for Gene Regulation and Promoter Analysis

RNA was harvested from the 50 mL zinc-restricted growth cultures, at mid- to late- log phase. The cultures were pelleted and resuspended in Nucleoprotect RNA (Macherey-Nagel) according to manufacturer's protocol (291). After complete permeation, samples were centrifuged at 10,000 rpm for 2 minutes to remove RNA protect and pellets were stored at -80C until RNA extraction. The stored pellets were thawed on ice on the day of RNA isolation under a laminar flow hood. The hood was cleaned with 10% bleach, 70% ethanol, DNA ZAP (Invitrogen

Cat: AM9890) reagent and water prior to use. The unit was sterilized under UV for at least 30 mins before RNA isolation. RNA isolation was performed using the NucleoMag RNA isolation Kit (Macherey Nagel) in a semi-automated system using the Eppendorf EpMotion 5073 liquid handler, according to manufacturer's instructions (292). User intervention was added at the clear lysate step to allow for external centrifugation of the samples to generate a lysate. The bench spaces were cleaned thoroughly with DNA Zap, RNase Zap (Invitrogen Cat:AM9780) and 5% bleach. Samples pellets were thawed on ice and placed in the EpMotion benchtop along with the RNA isolation kit reagents, DNA and RNAse-free tips, and reservoirs, at their respective designated positions, programmed in the EpMotion software. After isolation, RNA samples were further treated with TURBO DNase (Invitrogen Cat: AM2238) according to manufacturer's protocol (293). cDNA was generated using the Superscript IV First-Strand Synthesis System (Invitrogen Cat: 18091050), and quality of samples were validated through + and – reverse transcriptase controls and bleach agarose gel electrophoresis (294).

Table 2. Primers and Gene Blocks used in this study.

Primer	**Sequence**	**Purpose/Target**
Zur regulation *tdfJ* project		
oGSU102	AGATACCGCCTTGTCGCAAC	*tdfJ* forward RT-qPCR
oGSU103	TTGATGCCTGCGGATGTCAG	*tdfJ* reverse RT-qPCR
oGSU104	ATCGACCCGTCAGGATGTGT	*tdfH* forward RT-qPCR

oGSU105	TGCCGTCCACCATCGTATTG	*tdfH* reverse RT-qPCR
oGSU108	TCCGCAGTGCAAAACTCGTC	*znuA* forward RT-qPCR
oGSU109	TGGTGGTGTCCTTCGTGGTC	*znuA* reverse RT-qPCR
oGSU309	CAAAGACCGCCTGCACATCT	*ngo1049* forward RT-qPCR
oGSU310	GCCTGTTTCCAGCCTGCTTT	*ngo1049* revrse RT-qPCR
***tdfJ* promoter analysis**		
oGSU112	TGGTTCAATACTTTAAT	*tdfJ* gene specific primer (GSP1) -5'RACE -R
oGSU210	TGACCGCGAATAACGGGAGC	*tdfJ* gene specific primer 2 (GSP2) -5'RACE -R
oGSU211	ATTGCGAAGCGTGGATGCCC	*tdfJ* gene specific primer 3 (GSP3) -5'RACE -R
oGSU229	GGCCACGCGTCGACTAGTACGGGIIGGGIIGGGIIG	Abridged Anchor Primer (AAP) -5'RACE- F, provided in kit
oGSU230	GGCCACGCGTCGACTAGTAC	Abridged Universal Amplification Primers (AUAP) -5'RACE-F, provided in kit
Fur DPI-ELISA		
oGSU261	CATGCCATATGATGGAAAAATTCAGCAACAT	FA1090 *fur* forward-cloning into pET19b
oGSU262	CATGCGGATCCTTAACGTTTGCCCTTGGCCT	FA1090 *fur* reverse cloning into pET19b
oGSU299	CGATAGCTAACATATAGCGGCGTTCG	P_{tdfJ} forward
oGSU300	/5BiotinTEG/AGTTTCATGCGCTTGGGCGA	5'BIOTIN-TEG P_{tdfJ} reverse
oGSU303	TTGCCGCAACTTGGAAAGTGC	P_{tbpB} forward
oGSU304	/5BiotinTEG/CAAGATCGAAACTGCCGCCT	5'BIOTIN-TEG P_{tbpB} reverse
oGSU385	CAACGGCAATCGTGCGATATGG	P_{rmpM} forward

oGSU386	/5BiotinTEG/GAAGCGAGCAATGCAACGAA	5'BIOTIN-TEG P_{rmpM} reverse
RNA Seq Project		
oGSU397	TGGAATACGGCGAGGCATTG	*adhP* forward RT-qPCR
oGSU398	TCACACCGTCGGCAACTTCT	*adhP* reverse RT-qPCR
oGSU399	CGCTTGGCCGATGAATACCG	*norB* forward RT-qPCR
oGSU400	GCGCTTCTTGGCTTGGCAAT	*norB* reverse RT-qPCR
oGSU403	CAGGTTCTGTCTTCGCTCAA	*rpmJ2* forward RT-qPCR, provided by Criss AK, UVA
oGSU404	CAGCGTTGGCGCGAT	*rpmJ2* reverse RT-qPCR, provided by Criss AK, UVA
oGSU405	AATGAAGGCTGGCTGATTCG	*rpmE2* forward RT-qPCR, provided by Criss AK, UVA
oGSU406	ATAGACGGGATGTGAGGAAGAG	*rpmE2* reverse RT-qPCR, provided by Criss AK, UVA
Gene Blocks	**Sequence**	**Purpose/Target**
gbGSU014	CTAAGGGAGTTTGGGAAAGATTGCCGCAACTTGGAAAGTGCCC TCTCCCCAGCCCTCCGCCGCGCAGGGGAGGGAGCGGATTGCAG CAGGTTTGGCGGTTGCAGGCGGTTTTAAAAGCAGCGCGGGAAT GACGGTATTTTGGTTTATTTACGGGCCCGGGCCCAAAGCATTTG CAAATTTTTTAAAAACGAAGGGCCCGGGCCCCCTTATCATTCTTT AATTGAATCGGGTTTGTTATGAACAATCCATTGGTGAATCAGGC TGCTATGGTGTTGCCTGTGTTTTTGTTGAGCGCTTGTCTGGGCG GAGGCGGCAGTTTCGATCTTG	Scrambled Fur box P_{tbpB}-1
gbGSU015	CGATAGCTAACATATAGCGGCGTTCGTGTTCACATCATTAACTT CCCGGGAACTAGGGTTAATACAAATTAACGCCATTAAATATCAC AACCGTGTCATTTGAAAAACTTTTGCCTATGCCCTCTGAGTATTC TCAAAATCTTATGATA**GGGCCCGG**GCAATGTTAGGGAACGACA AAATTTTGAAATGCGACGAGAAGCCAAAATGGCACAAATCACA CTCAAACCCATTGTTTTATCAATTCTTTTAATCAACACACCCCTCC TCGCCCAAGCGCATGAAACT	Least Scrambled Fur and Zur box P_{tdfJ}-1
gbGSU016	CGATAGCTAACATATAGCGGCGTTCGTGTTCACATCATTAACTT CCCTAAAATTAGGGTGGGCCAAAGCCCACGCCATTAAATATCAC AACCGTGTCATTTGAAAAACTTTTGCCTATGCCCTCTGAGTATTC TCAAAATCTTATGATAGGGCCCGGGCAATGTTAGGGAACGACA AAATTTTGAAATGCGACGAGAAGCCAAAATGGCACAAATCACA	Scrambled Fur and Zur box P_{tdfJ}-2

	CTCAAACCCATTGTTTTATCAATTCTTTTAATCAACACACCCCTCC TCGCCCAAGCGCATGAAACT	
gbGSU017	CGATAGCTAACATATAGCGGCGTTCGTGTTCACATCATTAACTT CCCTAAAATTAGGGTTAATACAAATTAACGCCATTCCCGGGCAC AACCGTGTCATTTGAAAAACTTTTGCCTATGCCCTCTGAGTATTC TCAAAATCTTATGATAGGGCCCGGGCAATGTTAGGGAACGACA AAATTTTGAAATGCGACGAGAAGCCAAAATGGCACAAATCACA CTCAAACCCATTGTTTTATCAATTCTTTTAATCAACACACCCCTCC TCGCCCAAGCGCATGAAACT	Scrambled Fur and Zur box P_{tdfJ}-3
gbGSU018	CGATAGCTAACATATAGCGGCGTTCGTGTTCACATCATTAACTT CCCTAAAATTAGGGTTAATACAAATTAACGCCATTAAATATCAC AACCGTGTCATTTGAAAAACTTTTGCCTATGCCCTCTGAGTATTC CCGGGCCCGGGTGATAGGGCCCGGGCAATGTTAGGGAACGAC AAAATTTTGAAATGCGACGAGAAGCCAAAATGGCACAAATCAC ACTCAAACCCATTGTTTTATCAATTCTTTTAATCAACACACCCCTC CTCGCCCAAGCGCATGAAACT	Scrambled Fur and Zur box P_{tdfJ}-4
gbGSU019	CGATAGCTAACATATAGCGGCGTTCGTGTTCACATCATTAACTT CCCGGGAACTAGGGTGGGCCAAAGCCCACGCCATTCCCGGGCA CAACCGTGTCATTTGAAAAACTTTTGCCTATGCCCTCTGAGTATT CCCGGGCCCGGGTGATAGGGCCCGGGCAATGTTAGGGAACGA CAAAATTTTGAAATGCGACGAGAAGCCAAAATGGCACAAATCA CACTCAAACCCATTGTTTTATCAATTCTTTTAATCAACACACCCCT CCTCGCCCAAGCGCATGAAACT	Scrambled Fur and Zur box P_{tdfJ}-5
gbGSU020	CTAAGGGAGTTTGGGAAAGCTTGCCGCAACTTGGAAAGTGCAC TCTCCCAAGCCCTTCGCAGCGCAGGAGAGGGAGCGGACTGCAG CAGGTTTGGCGGTTGCAGGCGGTTGGGAAAGCAGCGCGGGAA GGACGGGGCCTTGGTTGCGTCACCCCAAAGGGCCGGAAGCAC CCGCAAGCCCTTCAGGACCAAGCGAAACCCCAACCCTTCCCAGT CTTGGCCTGAACCGGGTTTGTGGGGAACAACCCCTTGGTGAAC CAGGCTGCTCGGGTGTTGCCTGTGTCGGTGTTGAGCGCTTGTCT GGGCGGAGGCGGCAGTTTCGATCTTG	100% Scrambled Fur box P_{tbpB}
gbGSU021	CGATAGCTAACATATAGCGGCGTTCGCGTCCACAGCCCCAACTT CCAACCAAGGAGAGTGCGGACAAGGTCACGCCACCCAAGACCA CAACCGTGTCAGGTGAACCACTTGGGCCCAGGCCCTCTGAGGA GTCTCACAACCTTGGGACAGGGAAACTGCAAGGTCACCCAAGG ACAACGTTCTGAACTGCGACGAGAAGCCAAAGCGGCACAAAGC ACACTCAAACCCAGGGTTTGCTCAACTCTGGTCAGCAACACACC CCTCCTCGCCCAAGCGCATGAAACT	100% Scrambled Fur and Zur box P_{tdfJ}

IV. Quality Control for RNA and cDNA

RNA isolated by EpMotion was treated with TURBO DNase (as mentioned in the previous step) after a first round of concentration measurement. Approximately 2 µg of total RNA (200 ng/µL) isolated from each condition and each replicate was treated with TURBO DNase according to manufacturer's protocol (293). A small portion of the DNase-treated RNA diluted to a final concentration of 25 ng/µL was used to examine the quality of the RNA via a PCR. PCR reactions with 5 ng RNA per reaction was setup using the GoTaq 2x mastermix and RNAse- DNA-free water for *rmpM* expression. The PCR reaction was run for 35 cycles in a BioRad thermocycler and the products were analyzed using a 2% agarose gel electrophoresis in 1XTris-acetate EDTA (TAE) buffer. The gel was run at constant voltage of 135V and imaged on a Chemidoc under UV trans illumination. Presence of bands on the gel from the PCR products indicated contamination with DNA resulting in further cleanup of RNA. Clear gel with no PCR products were desired results and positive control FA1090 genomic DNA and negative no template controls were used to make decisions on quality. Similarly, cDNA products of clean RNA + and – reverse transcriptase (RT) were subject to quality control PCR with *rmpM* primers oGUS195 and oGSU196. These products were analyzed on a Chemidoc after agarose gel electrophoresis and absence of products in – RT samples were expected for clean RNA.

DNase-treated RNA samples were further controlled for their quality using a bleach gel electrophoresis method for RNA Seq sample preparation (295). Total DNase-treated RNA at a concentration of 500 ng to 1 µg was diluted with 6x DNA loading dye and loaded onto a 5% bleach 1% agarose gel and run in 1xTAE at 135 V. The gel was imaged using a Chemidoc under a UV transilluminator to visualize 5S, 16S and 23SrRNAs at 120bp, 14kb and 30 Kb respectively.

V. Primer Design and Efficiency Testing

Prior to RT-qPCR, primers (Table 2) were carefully designed to be less than 25 bp in length, amplify regions no greater than 200 bp and tested to have primer efficiencies between 90% and 95%. The primer sequence stability, hairpins and ΔG values were analyzed on the IDT website prior to placing primer orders for testing (296). Primer efficiencies were tested in gradient concentrations of primer ranging from 10 µM to 40 µM concentrations and gradient concentrations of genomic FA1090 DNA from 1 µg serially diluted by a factor of 10. PCR was set up for each primer set and each primer concentration with the SYBR Hi-ROX Sensimix (Bioline Cat: QT60505) along with melt curve data to check for primer specificity. PCR program was setup in the CFX96 BioRad thermocycler and standard curves for the range of DNA concentrations were analyzed for primer efficiency. Primers with annealing temperatures at 60°C were chosen for each gene, to match the annealing temperature of the *rmpM* reference gene primer set that was determined after primer efficiency tests. Primers and concentrations that yielded efficiencies between 90 and 95% were chosen for RT-qPCR analysis of target genes. Standard curve for these efficiency tests were plotted using the BioRad CFX96 software.

VI. RT-qPCR for Measuring Target Gene Expression

RT-qPCR was performed with the SYBR Hi-ROX SensiMix (Bioline Cat: QT60505) polymerase on a Bio-Rad CFX96 thermocycler. RT-qPCR was set up for 35 cycles and normalized expression of each target gene was calculated in biological and technical triplicates. The specificity of the primers was checked by a melt curve (95°C for 1 min, 55°C for 1 min and an increment in temperature to 95°C at 0.5°C/s rate for 10 s). Gene expression was normalized to

the expression of the housekeeping reference gene *rmpM*. Expression was calculated using ΔCq values with the $E = 2^{\Delta Cq}$ formula where E is the expression and ΔCq is the normalized threshold cycle value for each gene (297).

VII. 5' Rapid Amplification of cDNA Ends (5' RACE) for Identification of the Transcriptional Start Site

The *tdfJ* transcript 5' end was identified using the 5' RACE Version 2.0 Kit according to manufacturer's protocol (298). Two individually isolated RNA samples from either the FA1090 WT+ TPEN or FA1090 *zur*+ TPEN sample, were used to determine the transcriptional start site. *tdfJ* gene specific primer 1 oGSU112 was used for making gene specific cDNA (Table 2). Gene-specific primers oGSU210 and oGSU211 (Table 2) were used for the amplification of 5' RACE gene-specific PCR products with AAP provided in the kit (Table 2). Gene specific PCR was performed on a Bio-Rad thermocycler using the Platinum Taq DNA polymerase (Invitrogen Cat: 15966005) and 10 mM dNTPs (299). The PCR products were cleaned and concentrated before cloning into the pCR2.1-TOPO TA vector (Invitrogen Cat: K457502) and sequenced at Genewiz (300). Sequence analysis was performed by aligning sequences from at least three different plasmids, after cloning the RACE amplification products from each RNA sample in biological replicates. Sequence aligning and comparison was done using ApE and SnapGene Viewer (301, 302).

VIII. SDS PAGE and Western Blotting Analysis

Whole-cell lysates of gonococci were harvested by pelleting cultures at a standardized optical density and resuspending cells in 2x Laemmli solubilizing buffer (BioRad, cat number) before storage at −20°C. Lysates were thawed and mixed with βME to a final concentration of

5%. Samples were then briefly centrifuged and boiled for 2 min at 100°C. Protein samples were separated on a precast 4-to-20% gradient polyacrylamide gel (BioRad, cat number) before transfer to nitrocellulose. Prior to transfer, the SDS PAGE electrophoresis gel was analyzed by stain-free method to ensure equivalent protein loading and separation. The blots were further stained with Ponceau S after transfer, to verify equal protein sample loading. To detect TdfJ, TbpB and Ngo1049, the blots were blocked in 5% (wt/vol) Bovine Serum Albumin (BSA) dissolved in 1x High Salt-Tris Buffer Saline with 0.1% Tween 20 (HS-TBST). The blots were probed with peptide- or protein-specific polyclonal antisera diluted in blocker or for 1 h at room temperature. Polyclonal Rabbit anti-TdfH and -TbpB were diluted at 1:2500, Guinea Pig anti-TdfJ was diluted at 1:200, Guinea Pig anti-Ngo1049 was diluted at 1:500 and Guinea Pig anti ZnuA was diluted at 1:1000 in a 5% BSA blocker. The blots were washed three times with 1x HS-TBST and then probed with AP-conjugated anti-host (guinea pig or rabbit) IgG secondary antibodies at 1:5000 in BSA blocker for 1 h at room temperature. The blots were washed again after secondary antibody incubation and developed using either nitroblue tetrazolium (NBT)–5-bromo-4-chloro-3-indolylphosphate (BCIP) for AP-conjugated secondary antibodies or the ECL substrate (BioRad) for the HRP labelled secondary antibody after incubating for about 10 to 15 mins at room temperature with gentle shaking. To detect recombinant His-NgFur, the blots were blocked in 5% (wt/vol) skim milk in 1x HS-TBST and probed with anti-His HRP antibody diluted at 1:1000 in blocker for 1 hour at room temperature. The NgFur blots were developed using ECL substrate from BioRad. Blots were imaged on a Bio-Rad ChemiDoc gel imaging system using the Colorimetric or auto-ECL detection.

IX. Coomassie Stain

To detect purified protein His-NgFur, which does not contain tryptophan residues, SDS-PAGE gels of purification products of NgFur, were stained with Coomassie blue (0.25% Coomassie R-250, 50% methanol, 10% glacial acetic acid). The stain free gel imaging system on the Chemidoc gel imager only works for proteins that are rich in tryptophan and since NgFur has no tryptophan we resorted to using the Coomassie staining of purified His- NgFur (303). The gel was stained for 1 hour at room temperature and de-stained in 20% methanol and 5% acetic acid overnight at 4°C to minimize background. The stained gels were then imaged under the colorimetric setting in a Chemidoc gel analyzer to look for purified Fur.

X. Expression and Purification of Recombinant His-NgFur

The coding sequence for FA1090 *fur* was PCR amplified with primers oGSU261 and oGSU262 (Table 2). The resulting PCR product was digested with EcoR1 and BamH1 and cloned into the pET19b vector that contains a 10X polyhistidine tag at the N-terminus, to result in the plasmid pGSU606 (Table 1). This plasmid after sequence confirmation was purified and transformed into BL21(DE3 pLysE) competent cells. The His-NgFur protein was expressed in a starter culture of the BL21 (pGSU606) plasmid in 5 mL Luria Bertani broth supplemented with 100 µg/mL of carbenicillin; this starter culture was sub-cultured into Terrific Broth (TB) supplemented with 100 µg/mL carbenicillin. Expression culture was grown with 1 mM inducer-isopropyl β- d-1 thiogalactopyranoside (IPTG) at 37°C for 4 hours. Cell pellets were harvested by centrifugation and stored at -80°C before lysis. Cell pellets were re-suspended in lysis buffer (20 mM HEPES, 250 mM NaCl, pH 8.0, 1 mM phenylmethylsulfonyl fluoride (PMSF), 1 U/µL Pierce

Universal Nuclease for Cell lysis) and lysed using a Dounce homogenizer, with 10 mL of buffer used per gram of cell pellet (304). The resulting cell suspension was mechanically lysed by sonication at 50% amplitude at Pulse-time mode, with sonication at 30 second intervals for 10 minutes. Insoluble fraction was removed by centrifugation at 12,500xg for 1 hour at 4°C and the resulting clear supernatant was mixed with pre-equilibrated nickel-nitrilotriacetic acid (Ni^{2+}- NTA) resin, 10 mM 2-Mercaptoethanol (βME) and 1 mM PMSF at 4°C overnight. The Ni^{2+}-NTA resin was collected in a chromatography column and washed with 30 column volumes (cv) and eluted with 10 cv total with wash buffer (20 mM HEPES, 150 mM NaCl, pH 8.0, 10 mM βME, 1 mM PMSF) containing 50 to 500 mM imidazole. Clean His-tagged NgFur eluted with buffer containing 200-, 300- and 400-mM imidazole. These fractions were pooled together and dialyzed against 1x Phosphate Buffer Saline (pH 8.0), overnight at 4°C to remove the imidazole. The purity of purified His-NgFur was determined by SDS-PAGE electrophoresis followed by staining with Coomassie blue. No reducers such as, Dithiothreitol (DTT) and βME were added to the dialyzed His-NgFur as they would interfere with downstream assays. Protein concentration was measured and His-NgFur was aliquoted, and flash-frozen at 80°C.

XI. DNA-Protein Interaction (DPI) ELISA

A biotinylated DNA probe was produced by PCR amplification of the promoter regions of *tbpB*, *ngo1049*, *tdfJ* and *rmpM*, using 5' BIOTIN-TEG tagged reverse primers, oGSU300 (P_{tdfJ}), oGSU302 ($P_{ngo1049}$), oGSU304 (P_{tbpB}) and oGSU386 (P_{rmpM}). These primers were designed and validated on IDT with HPLC purification prior to ordering. PCR amplified biotinylated DNA probes were bound to a streptavidin-coated 96-well plate (Pierce High-Capacity Plates, Cat: 15500) and

ELISA was carried out according to the protocol by Brand, L. H., *et al* (305) with the following modifications. Biotinylated PCR DNA, diluted to 12.5 pmols in 1x Low- Salt Tris Buffer Saline (LS-TBS) was bound (100 µL per well) to a pre-washed streptavidin-coated high-capacity plate (~125 pmol BIOTIN binding capacity) and incubated for 2 hours at room temperature with gentle shaking. After 2 hours the plate was washed in a programmed plate washer 5 times at 300 µl each with 1x phosphate buffer saline (PBS) pH 7.2. A 5 % milk in 1x LS-TBS with 0.05 % Tween 20 blocker was added at 200 µL per well and incubated at 4°C overnight. His-NgFur at the highest required concentration (20µM) was loaded with Mn^{2+} from $MnCl_2$ in the molar ratio of 1:2 Fur:Mn2+ (40µM MnCl2) and left in a nutator at 4°C for 1 hour. Mn^{2+} loaded His-NgFur was then serially diluted in Fur dialysis buffer, 1xPBS at pH=8.0 to the desired gradient concentrations ranging from 20µM to 10µM Fur and added to the DNA bound plate for 1 hour at room temperature with gentle shaking. The plate was washed five times with 1X PBS supplemented with 0.05% Tween 20 (PBS-T) in the plate washer. An anti-His HRP labelled antibody (BioLegend Cat: J099B12) was diluted in blocker at 1:1000 and used to detect the DNA bound His-NgFur, by incubating for 1 hour at room temperature with gentle shaking. The plate was washed after the anti-His antibody step in 1x PBS-T and photometric detection was performed with the Slow TMB substrate (Thermo Fischer Cat: 34024). The reaction was stopped with 0.18 M sulfuric acid and the resulting absorbance was read at 450 nm in a plate reader. The binding affinity K_D was determined through competition of biotinylated P_{tbpB}, $P_{ngo1049}$, P_{tdfJ} and P_{rmpM} with their respective unlabeled 10x excess PCR promoter DNA counterparts. The binding curves were plotted and His-NgFur K_D to P_{tdfJ} was determined by a Linear regression model curve fitting with the Hill equation plot in GraphPad PRISM (306). The specificity of His-NgFur to the promoters

were determined through binding to biotinylated scrambled sequence of P_{tdfJ} Fur and Zur boxes and P_{tbpB} Fur box. The binding curves were generated by determining the µg of protein bound to an ELISA plate through a standard curve plot for His-NgFur in biological triplicates and technical quadruplets. The K_D for the promoters were also done in biological triplicates and technical duplicates to obtain statistical significance.

XII. Fur Scrambled Promoter ELISA

For creating scrambled versions of P_{tdfJ} and P_{tbpB} promoter Fur and or Zur binding regions, we synthesized gene blocks through IDT. Gene blocks gbGSU015 to gbGSU019 and gbGSU021 containing modified Fur and Zur box regions on P_{tdfJ} to varying capacity with sequence scarmbling on gbGSU015 being the least. gbGSU021 was made where 100% scrambling of Fur and Zur box regions of P_{tdfJ} were achieved. Scrambling was done by modifying the consensus repeat regions for Fur or Zur box, that is AT strings to G's and C's. A similar approach was taken to synthesize gene blocks gbGSU014 and gbGSU020 for scrambled Fur box of P_{tbpB}, where gbGSU020 is the most scrambled P_{tbpB} Fur box. These gene blocks were prepared according to manufacturer's protocol (IDT) and then TOPO cloned using the Invitrogen Zero BLUNT TOPO cloning vector (Cat: 450245). Top 10 or DH5-α *E. coli* were transformed with the TOPO cloned DNA and selected on LB plates with Kanamycin at 50µg/mL overnight at 37°C. The transformed colonies were confirmed through sequencing and resulted in plasmids pGSU623 to pGSU629 described in Table 1. pGSU623 and pGSU628 contain plasmid DNA with scrambled P_{tbpB} and plasmids pGSU624 to pGSU67 and pGSU629 contain plasmid DNA with versions of scrambled P_{tdfJ}. Plasmid DNA from these plasmids were isolated by growing them overnight in liquid LB media at 37°C and using the Zymoresearch Plasmid Mini Prep Kit. Plasmid DNA were them amplified by PCR using labelled

Biotinylated primers for DPI-ELISA (oGSU299-oGSU300 for P_{tdfJ} and oGSU303 -0gUS304 for P_{tbpB}) using the NEB Phusion Polymerase (Cat: M0530S) and 10mM dNTP. This resulted in biotinylated scrambled versions of P_{tbpB} and P_{tdfJ} ready to be bound on the streptavidin ELISA Plates for a Fur DPI-ELISA as described in the previous section (Section- 11). DPI ELISA was used to measure the absorbance values for Fur binding and resulting values were plotted using Excel as bar graphs.

XIII. *In Silico* Promoter Analysis and Prediction

Online promoter prediction software such as BPROM (307) and PRODORIC- Virtual Footprint (308) were used to identify the putative promoter elements and DNA Fur- and Zur-binding sites, along with consensus sequences, through pattern recognition. In addition to online prediction tools, predicted promoters from RNA Sequencing were analyzed using Geneious Prime, WebLogo 3 and MEME Suite (309-312), to generate a consensus logo for *Ngo* FA1090 Fur and Zur box using alignment to known sequences of consensus.

XIV. Statistical Analysis

Mean with standard deviation (SD) was calculated for all data, wherever appropriate and statistical significance was analyzed by Student's *t* tests or one-way ANOVA. Significance was set at $p < 0.05$. For RNA sequencing differential gene expression *p*- adjusted values <0.05 were considered as significant. Enrichment analysis for GO and KEGG were analyzed as significantly enriched for pathways with *p* values <0.05. *p*-adjusted values were not considered here as pathways and not individual genes were compared for enrichment. Prism software version 3.0 was used for graphing gene expression bar graphs and protein binding affinity K_D calculations (306).

CHAPTER 3. CHARACTERIZING THE DUAL REGULATION OF *NEISSERIA GONORRHOEAE TDFJ*, IN RESPONSE TO ZINC AND IRON

I. INTRODUCTION

Neisseria gonorrhoeae (*Ngo*) causes the sexually transmitted infection gonorrhea, that affects predominately younger adults, both men and women, worldwide. *Ngo* is a major public health concern and the World Health Organization (WHO) estimates that there were 82.4 million new cases as of the year 2020, a 118% increase since 2007 (313). There is no protective immunity, no effective vaccine, and historically only antibiotics have been used to treat infection. The current recommended treatment is a third-generation cephalosporin, ceftriaxone, due to the increasing numbers of resistant strains to all the other classes of antibiotics used over the decades (314). However, with the threat of untreatable *Ngo*, the Center for Disease Control and Prevention (CDC) specified *Ngo* a superbug and an urgent threat pathogen (315). This is alarming and there is an urgent need for vaccine and therapeutics to treat gonorrhea. Gonococcal infection in men, primarily results in an inflammatory response that is accompanied by a purulent discharge with polymorphonuclear leukocytes (PMNs), which leads to urethritis (316, 317). In women, gonococcal infection primarily results in cervicitis, but is often asymptomatic or accompanied by nonspecific symptoms (76). As a result of asymptomatic infection, untreated infection can cause serious irreversible sequelae such as pelvic inflammatory disease (PID), ectopic pregnancies, and even infertility (317, 318). This molecular difference in pathogenesis and immune response to infection in men and women is not well understood and emphasizes a gap in knowledge on the mechanisms by which *Ngo* adapt to these two distinct environments.

The human host employs strategies for immune clearance of *Ngo* including a robust inflammatory response with an influx of neutrophils or PMNs that entrap pathogens in neutrophil NETs (317, 319). The gonococcus has, however, been shown to be escape the harsh neutrophil NETs and in turn evade capture and phagocytosis. In fact, intact *Ngo* have been noted in these purulent urethral or cervical exudates from patients presenting with gonorrhea. These host immune cells also produce antimicrobial agents and proteins to limit essential nutrients for bacterial survival by a process termed nutritional immunity (320). *Ngo* has developed highly efficient transport systems, called TonB-dependent transporters (TDTs), to overcome this nutrient limitation and scavenge for metals by metal piracy from host proteins, wreaking havoc in the host. There are 8 known TDTs in *Ngo* of which 2 are characterized as zinc importers. Zinc import and homeostasis is a key feature in maintaining virulence and pathogenesis in several pathogens, including the gonococcus. The two, zinc import TDTs are TdfH and TdfJ, which function with an inner membrane ZnuABC transporter to cooperatively import zinc. TdfH binds S100A8/A9 (calprotectin), which is enriched inside human neutrophils to hijack zinc, while TdfJ binds S100A7 (psoriasin) secreted by mucosal epithelia, found inside the female cervical and vaginal mucosa (229, 289, 321, 322). These TDTs are conserved across all strains of *Ngo* and have been implicated as important vaccine antigens (323). ZnuA has also been demonstrated to be essential for gonococcal survival in an epithelial infection model (321), suggesting zinc import is crucial for survival. At the molecular level these zinc import proteins are regulated by the Zinc uptake regulator (Zur) which senses internal and external cellular zinc levels in order to maintain zinc homeostasis and overcome zinc starvation or toxicity imposed by the host (324). When faced with zinc toxicity, Zur binds the excess Zn^{2+} ions and blocks transcription of Zur regulated genes

including *tdfH*, *tdfJ* and *znuABC* (282, 325). During zinc-starvation, Zur does not repress these promoters and transcription and protein production is enhanced to combat the zinc stress. Zur carefully modulates the expression of these genes by binding to specific regions on their promoters, which is the subject of this study.

During pathogenesis, *Ngo* face different levels of metal environments, including zinc-dependent toxicity and starvation depending on the host sex and tissue type (268, 317, 326). The female genital tract is more zinc starved than the male genital tract (327). Given the fact that women tend to have a higher percentage of asymptomatic infections, coupled with the variation in zinc levels between the male and female host, it is important to ask the question if *Ngo* utilize one TDT over the other, and if this impacts disease progression between different hosts. In this study, we sought to characterize the extent to which these virulence genes respond to zinc and are regulated by Zur along with the promoter elements that modulate their expression levels. We identify a candidate gene that has a dual regulatory mechanism and speculate its possible role in gonococcal infections in women.

II. RESULTS

A. tdfJ and znuA Show Significant Changes in Gene Expression by RT-qPCR

We previously demonstrated that the gonococcal zinc import TDTs, TdfH and TdfJ and their cognate ABC transporter, ZnuABC, are all regulated at the translational level by Zur, in a zinc-dependent manner (289). However, the extent of transcriptional regulation by Zur on these genes under excess and low zinc conditions has not been studied. Here we sought to quantify the level of regulation by Zur on these *tdfJ* and *tdfH* by RT-qPCR. We grew the FA1090 (WT) and an

isogenic *zur* mutant (*zur)* in chelex-treated defined medium (CDM), under excess zinc (20 µM Zn_2SO_4) or low zinc (7 µM TPEN) conditions. TPEN was added as a zinc-specific chelator to induce zinc- starvation. Cells were collected during exponential phase and mRNA and whole cell lysates were processed for gene expression and protein analysis. RT-qPCR was performed to measure the log_2-fold-change for gene expression for *tdfH*, *tdfJ*, and *znuA.* Gene expression levels for *ngo1049* and *tbpB* were also measured as a positive and negative control, respectively. RT-qPCR expression for these genes were normalized to *rmpM* expression levels, a house keeping gene not regulated by zinc or Zur. *tdfJ* expression was 24-fold higher in the absence of zinc in WT cells as compared to the *zur* mutant (Figure 1b). *tdfJ* expression in the *zur* mutant under excess zinc is comparable to the expression in the absence of zinc, indicating a Zur-dependent mechanism of regulation. *tdfH* expression is increased 3-fold in the absence of zinc in WT cells, and periplasmic zinc binding protein, *znuA*, was increased 38-fold, with no significant difference in the *zur* mutant (Figure 1a and 1d, respectively). *znuA* is necessary for zinc assimilation during attachment of *Ngo* (321), making its tight regulation by Zur important during infection. In WT cells, *ngo1049* expression was increased 46-fold in the absence of zinc, which was not seen in the *zur* mutant (Figure 1c). *tbpB*, however, showed no significant difference in the WT or *zur* mutant (Figure 1e). Western blotting for whole cell lysates showed complementary protein expression levels to RT-qPCR. TdfJ was only produced in the absence of zinc in the wildtype while having no qualitative difference in protein levels in the *zur* mutant in the presence or absence of zinc (Figure 1a). TdfH did not appear to be fully repressed in the presence of zinc in the wildtype, which was shown in a previous study to be a result of strain-specific difference between FA1090 and FA19 *Ngo* (Figure 1b) (289). There was no difference in TdfH protein levels in the *zur* mutant in the presence or

absence of zinc (Figure 1b). ZnuA protein levels were similarly expressed to complement the RT-qPCR expression data. ZnuA was produces in the absence of zinc in the wildtype with no difference in the *zur* mutant in protein levels for zinc abundance or zinc depletion (Figure 1c). One thing to note is the small yet-significant difference in *tdfJ* and *znuA* expression in the *zur* mutant between high and low zinc levels (Figure 1). This difference is however not visible in their protein expression levels in the *zur* mutant, suggesting another layer to their transcriptional regulation. This difference in the *zur* mutant was also seen in the positive control *ngo1049* expression in the *zur* mutant which was further recapitulated in the western data with a visible difference in the *zur* mutant Ngo1049 production between zinc-excess and low zinc conditions (Figure 1d). The transcriptional and translational regulation by Zur, overall are complementary, however suggesting a stricter transcriptional layer in regulation by Zur in response to zinc.

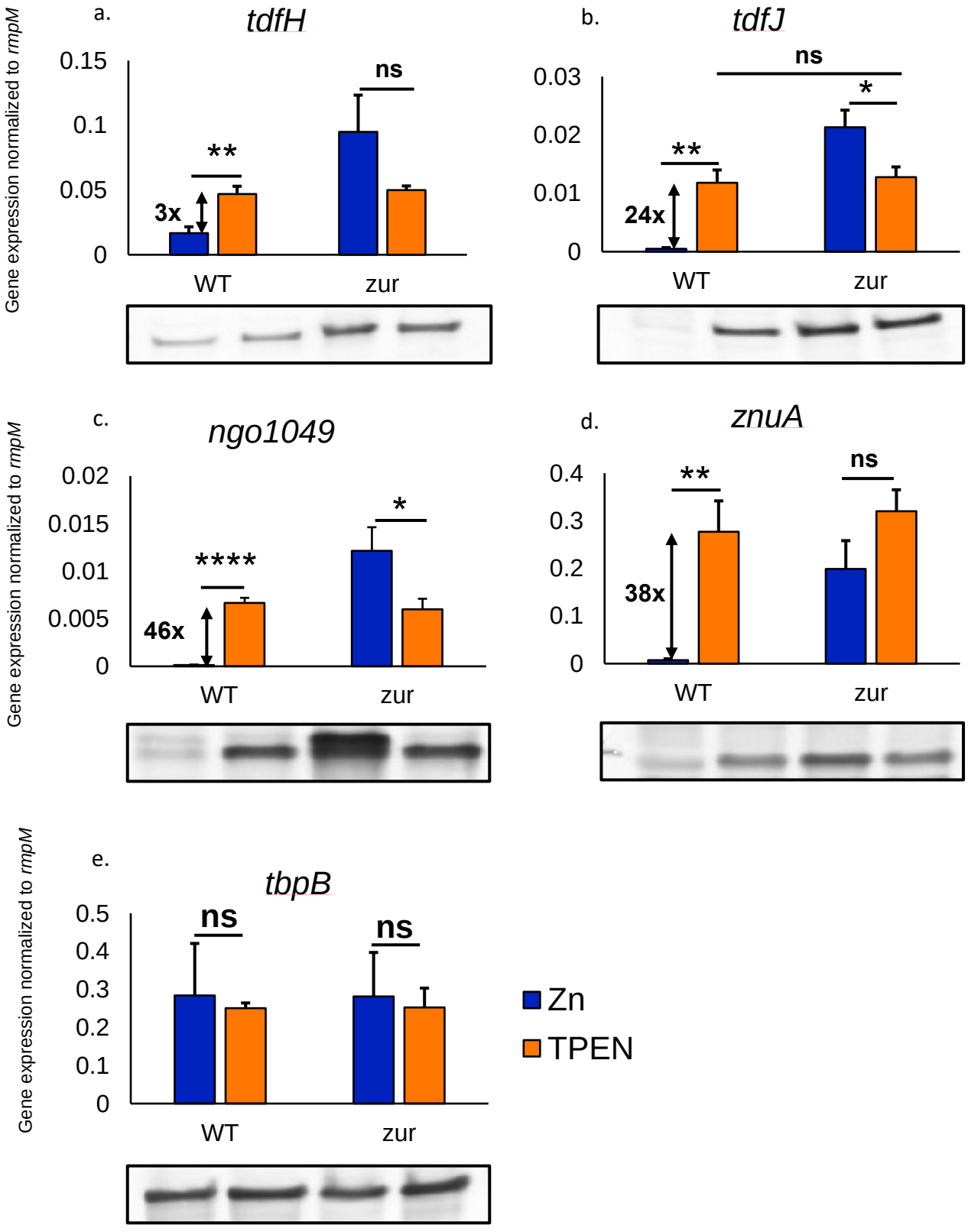

Figure 1 *tdfH*, *tdfJ*, *ngo1049* and *znuA* are zinc-regulated by Zur

Figure 1. *tdfH (a), tdfJ (b), ngo1049 (c)* and *znuA* (d) are all zinc-regulated by Zur. Gene expression was normalized to *rmpM* before plotting bar graphs. *tbpB (e)* expression was also computed as a negative control for zinc-regulated expression. Excess zinc condition is depicted in blue while the zinc-restricted condition in the presence of TPEN is shown in orange. 2^{Δ}Cq values from three individual biological replicates were averaged. Student's *t* test was used to calculate statistical significance. The corresponding western blots for protein expression of TdfH, TdfJ, NGO1049, ZnuA and TbpB are shown below the respective RT-qPCR plots. * $p<0.05$,** $p<0.005$, **** $p<0.00005$, ns- not significant, $p>0.05$.

B. Zur Binds a Consensus Region on the tdfJ Promoter and Tightly Regulates its Expression

Previously, a putative consensus sequence for Zur binding in *Neisseria meningitidis* (*Nme*) was generated (282). Using the *Nme* predicted sequence in combination with RNA Seq promoter prediction for zinc- and Zur-regulated genes an *Ngo* Zur consensus logo was generated using WebLogo software (312) (Figure 2a). *In silico* promoter analysis of the putative promoters of *tdfH*, *tdfJ*, *znuA,* and *ngo1049*, identified a perfect consensus *Ngo* Zur box in the *tdfJ* and *ngo1049* promoters (Figure 2b). The predicted Zur-box upstream of *tdfH* has a 16 % match to the *Ngo* consensus sequence and demonstrated less difference in expression between the zinc replete and zinc deplete conditions. *znuA* showed a 92 % match for the consensus Zur-box sequence and a much higher difference between zinc replete and zinc deplete conditions. Since *tdfJ* exhibited both a bigger difference in expression between the zinc replete and zinc depleted condition and a 100 % match to the Zur box consensus we further characterized its promoter elements using BPROM and PRODORIC online webtools (307, 308) (Figure 3). Interestingly, the prediction

software identified two potential translational starts with an ATG encoding for a methionine within 15 base pairs of each other. There was no canonical Shine Delgarno-Ribosome Binding Site (RBS)-like sequence (AGGAGG) in front of the first ATG, however, six nucleotides upstream of the second ATG was a predicted RBS (GAGAAG) (Figure 3). To potentially identify which translational start codon is being used, we determined the transcriptional start site (+1) for the *tdfJ* promoter. We used 5' Rapid Amplification of cDNA Ends (5' RACE) (298) to identify the transcriptional start site for *tdfJ* using mRNA isolated from the WT + TPEN cells or the *zur* mutant + Zn cells, to maximize the *tdfJ* transcripts. Using gene specific *tdfJ* primers dC- tailed *tdfJ* cDNA was amplified and TOPO cloned into DH5α competent cells. The location of the +1 was determined as the first nucleotide preceding which the dC tailed ends from sequencing of transformed colonies. Multiple sequences from three different biological replicates (either FA1090 WT +TPEN or FA1090 *zur* + Zn 5' RACE products) were aligned using ApE (301) and the +1 was identified as the adenosine, 25 base pairs upstream of the second ATG and 7 base pairs downstream from the predicted -10 region (Figure 3). The identified +1 is only 7 base pairs upstream of the first potential ATG (without room for an RBS upstream), therefore, the second ATG was designated as the translational start for TdfJ.

a.

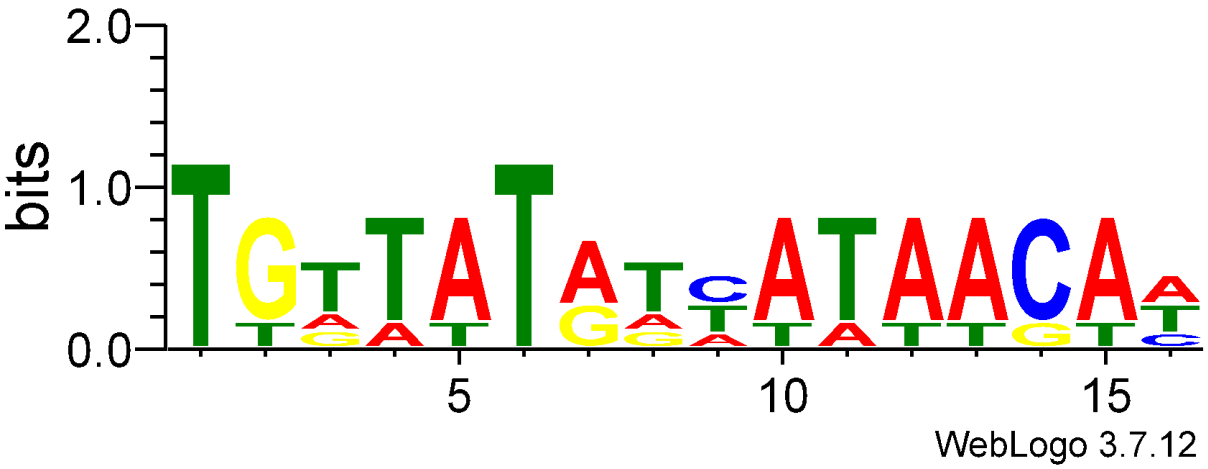

b.

ORF ID	Gene name	Zur box sequence	% Similarity
	Consensus	**TGTTATDNHATAACA**	
NGO0952	***tdfH***	TTGATTGTTTATTGT	**16**
NGO1205	***tdfJ***	**TGTTATATAATAACA**	**100**
NGO0168	***znuA***	**TGATATAACATAACA**	**92**
NGO1049	***ngo1049***	**TGTTATAGCATAACA**	**100**

Figure 2 *tdfJ* and *ngo1049* harbor an exact match to the predicted Zur-box consensus sequence in their promoters.

Figure 2. *tdfJ* and *ngo1049* harbor an exact match to the predicted Zur-box consensus sequence in their promoters. a) Graphical representation of the Ngo Zur-box was generated from predicted Zur binding locations on zinc-regulated promoters using WebLogo 3. b) A nucleotide sequence alignment of the predicted Zur-boxes in the promoters of the zinc-regulated genes in *Ngo*. The conserved palindromic repeats separated by three nucleotides in the middle are bolded and shown in red to signify complementarity to the Zur box consensus sequence.

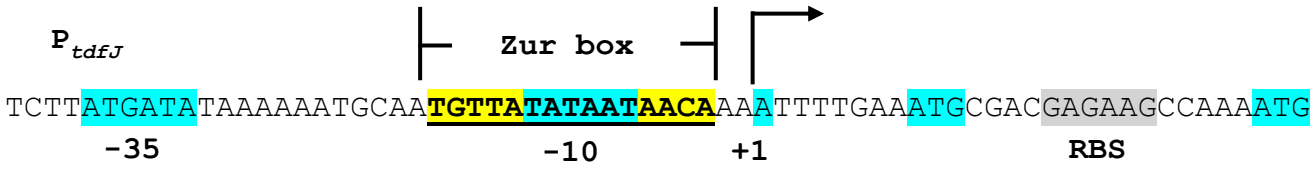

Figure 3. The *tdfJ* promoter elements from 5'RACE analysis.

Figure 3. The *tdfJ* promoter elements based on 5'RACE analysis. The *tdfJ* promoter map shows the identified +1, predicted -10 and -35 regions and a Zur-box overlapping the -10 region. The two predicted initiator codon ATG, -10 and -35 and the +1 regions are highlighted in blue, and the Zur box palindrome is underlined and bolded in yellow. The canonical ribosome binding site (RBS) sequence is highlighted in grey.

C. Two Fur-binding Sites on the tdfJ Promoter Result in Iron-dependent Induction of tdfJ

Along with the repression of TdfJ by zinc, *tdfJ* expression is induced in the presence of iron (229, 328). Yu. C, *et al.*, showed that *tdfJ* expression was induced in wildtype cells in the presence of iron, but not in the *fur* mutant (328). We showed that this iron induction of TdfJ is further enhanced when zinc is absent (329). Additionally, our *in silico* promoter analysis of *tdfJ* revealed two putative Fur-binding sites upstream of the -10 and -35 (Figure 4a). This site prediction was based on a compilation of known *Neisseria* Fur-box consensus sequences and our RNA sequencing data for iron regulation in FA1090 (328, 330, 331). This Fur-box consensus region was identified as a hexameric repeat of GATAAT-ATAATAATTATC-TTT (Figure 4b). On the *tdfJ* promoter (P_{tdfJ}), the first predicted Fur-box site (Fur Box-1) lies about 58 base pairs upstream of the -35 region (Figure 4a). This region was included in the approximately 300 base pairs potential Fur-box location established by Yu et al., however a Fur binding affinity to P_{tdfJ} was not established from an EMSA (328). The second putative Fur-box site (Fur Box-2) was located overlapping the -35, -10 regions and the Zur-box (Figure 4a). We hypothesized that the iron-induction of *tdfJ* is mediated through Fur and that Fur occupies both site-1 and 2 of P_{tdfJ}, to activate gene expression when the promoter is de-repressed. To test this, we used the DNA-Protein Interaction ELISA approach (305). Briefly, biotinylated P_{tdfJ} was bound to streptavidin coated ELISA plates along with positive control P_{tbpB} and negative control P_{rmpM} DNA. Manganese loaded, purified recombinant His-tagged *Ng*Fur was added to the ELISA plate, for detection of DNA bound Fur using an anti-His antibody. The absorbance at 450nm (A_{450}) was measured and binding affinity K_D was calculated with respect to the µg of Fur bound to the bound DNA. 10x excess unlabeled P_{tdfJ} competed with bound biotinylated P_{tdfJ} on the ELISA plate, resulting in

reduced signal. Specific binding of Fur was calculated as: Specific Binding = µg of Fur bound to BIOTIN-tagged P_{tdfJ} - µg of Fur bound to 10x excess unlabeled P_{tdfJ}. Fur was calculated to have a K_D of 2 for the positive control promoter, P_{tbpB}, and a K_D of 6 for P_{tdfJ}. A K_D was not able to be established for the negative control P_{rmpM} as the binding curve never achieved saturation at the concentrations tested (Figure 4c).

Figure 4. The *tdfJ* promoter contains two upstream Fur binding regions for iron regulation

a.

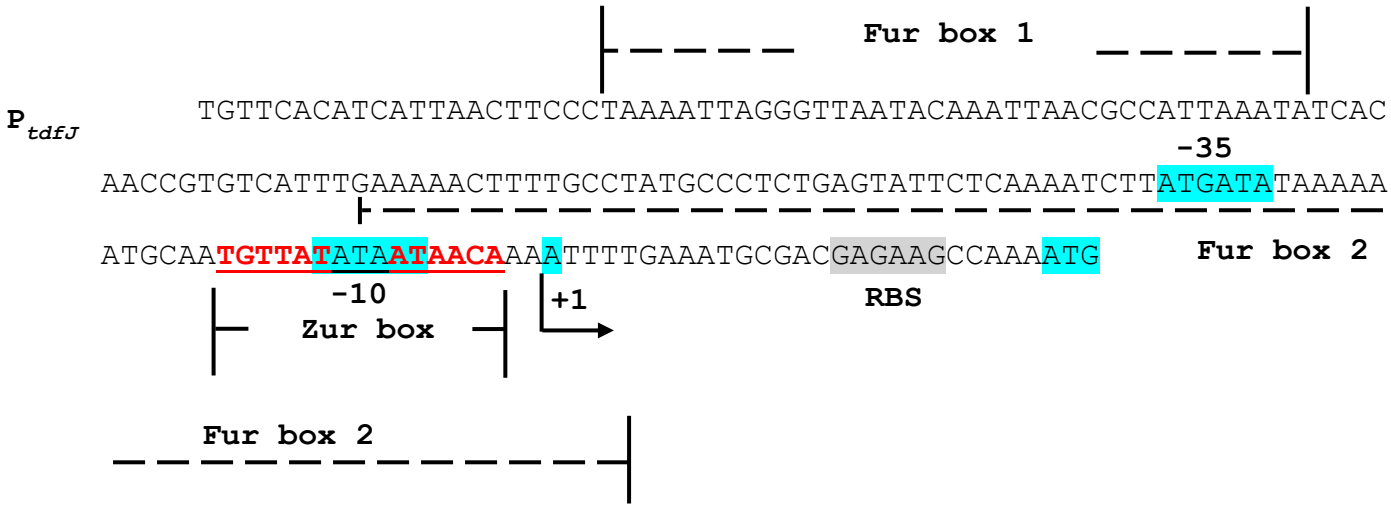

b.

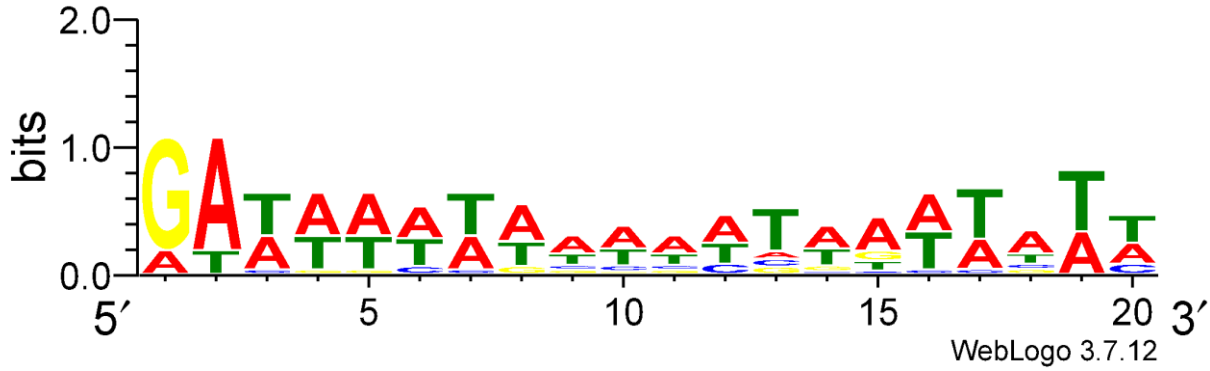

ORF ID	Gene name	Fur box sequence
	Consensus	**GATAAT-ATAATAATCATC-TTT**
NGO1496	*tbpB*	AAAATAAATAAAATAATAATCCTTATCATT
Fur box-1	*tdfJ*	GTTAATACAAATTAACGCCATTAAATATC
NGO1205		
Fur box-2	*tdfJ*	GAAAACTTTTGCCTATGCCCTCTGAGTATTCTCAAA
NGO1205		
Fur box-2	*tdfJ*	GATATAAAAAATGCAATGTTATATAATAACAAA
NGO1205		
NGO1779	*fur*	GAAATTGCGTATTATAGCGTCTATTATTTT

c.

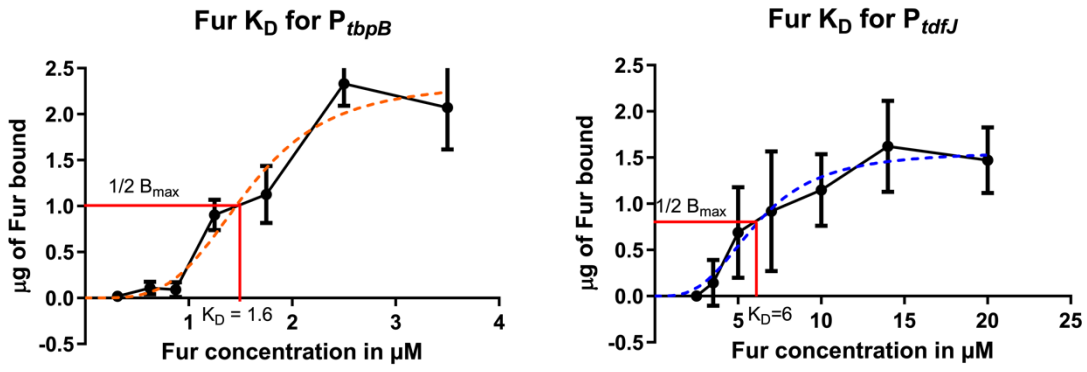

Figure 4. The *tdfJ* promoter contains two upstream Fur binding regions for iron regulation. a) The two locations of predicted Fur boxes upstream of *tdfJ* are labelled along with the identified *tdfJ* promoter elements. b) Graphical representation of the Fur-box of *Ngo* from predicted Fur binding locations was generated using WebLogo 3. The *Ngo* Fur box consensus sequence was determined from RNA Sequencing analysis of iron regulated promoters and consists of hexameric repeat regions. An alignment of the Fur box of Fur regulated promoters *tbpB* and *fur* are depicted along with the *tdfJ* promoter predicted Fur box. c) Fur binding affinity (K_D) for positive control promoter P_{tbpB} and P_{tdfJ} promoter were calculated based on a linear regression model on Graphpad PRISM 5.0. The respective Kds are depicted as the slope intercept on the x-axis. The K_Ds are based on an average from three biological replicate ELISAs for Fur binding to P_{tbpB} and P_{tdfJ}. P_{rmpM} was used as a negative control, not depicted here.

D. Fur Binds the Specific Fur-box Consensus Sequence Regions 1 and 2 on PtdfJ

To establish the specificity of Fur for the two Fur-box sites on P_{tdfJ}, we scrambled the predicted Fur-box sequences by changing the ATAAT-ATAATAATTAT-TTT repeats to a string of G's and Cs (Figure 5a). We sequentially scrambled different portions of the 2 Fur-boxes and made 6 sets of scrambled P_{tdfJ}, shown in Figure 5a from most to least scrambled. Biotinylated scrambled promoter sequences were bound to streptavidin ELISA plates along with biotinylated wildtype P_{tdfJ} and the level of 10 µM Fur binding measured. An increase in P_{tdfJ} scrambling correlated with a decrease in Fur binding absorbance values (A_{450}), with the most scrambled P_{tdfJ} (both Fur-box 1 and 2) showing a significant loss in Fur binding (Figure 5b).

a.

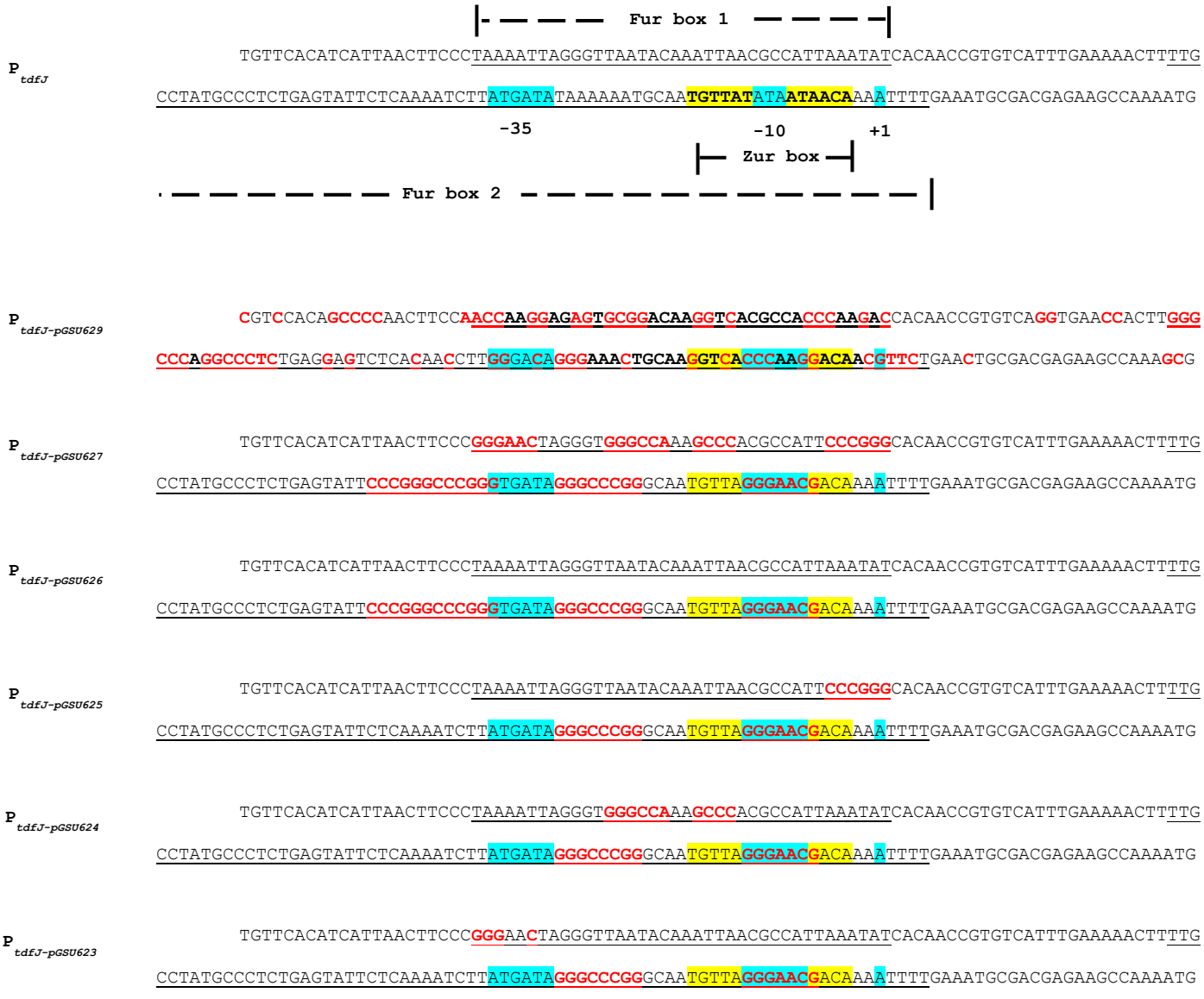

Figure 5. Fur binds specifically to the Fur box hexameric repeat regions on *tdfJ*

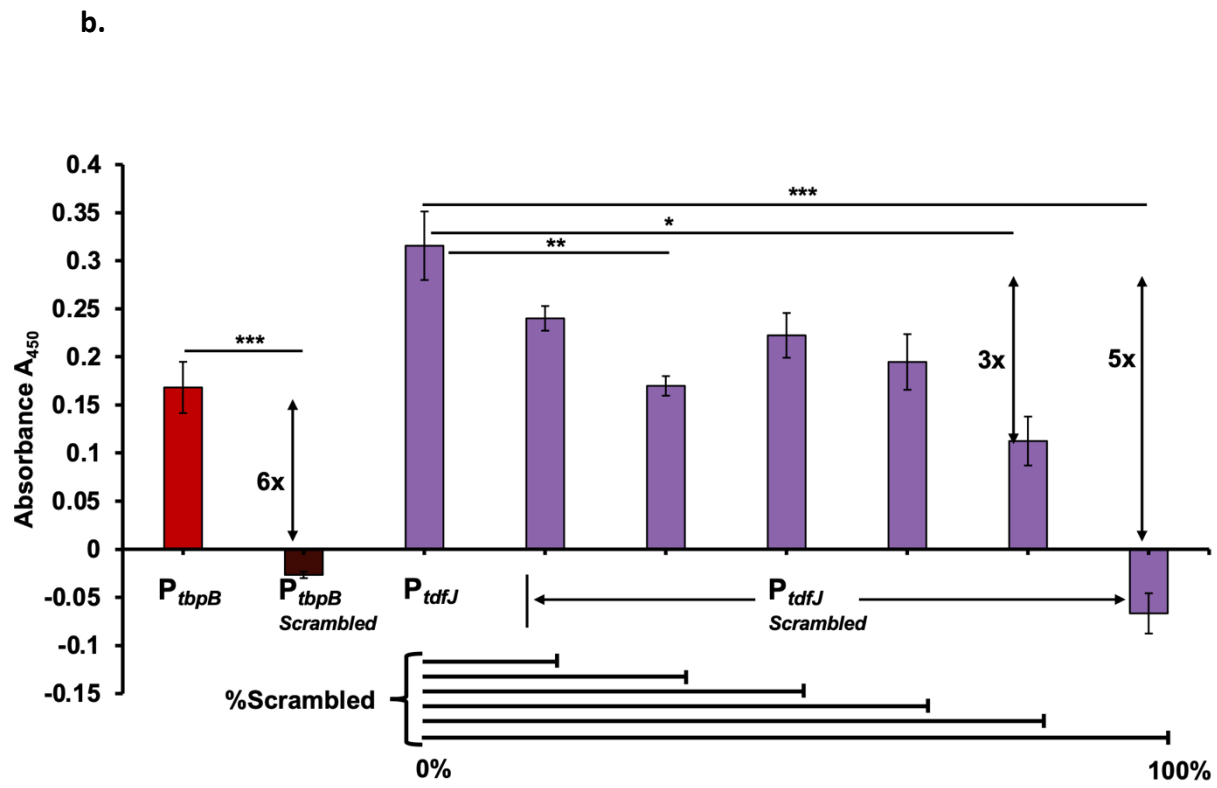

Figure 5. Fur binds specifically to the Fur-box hexameric repeat regions on P_{tdfJ}. a) A series of scrambled sequences of the Fur-box locations 1 and 2 in *tdfJ* aligned to the wildtype *tdfJ* promoter. The scrambled nucleotides are denoted in red and the percentage of nucelotides scrambled is listed to the left of each TdfJ promoter. b) Fur-binding ELISA of wildtype and scrambled P_{tbpB} and P_{tdfJ} promoters. The A_{450} of Fur binding to promoters is on the x-axis, while promoter sequences are across the y-axis. Wild-type P_{tbpB} (light red) and scrambled P_{tbpB} (dark red) were used as positive and negative controls, respectively. Wild-type P_{tdfJ} promoter is in light green and scrambled P_{tdfJ} promoter sequences are denoted in dark green. Fold difference with respect to wildtype promoters is denoted by arrows. A student's *t* test was performed for statistical analysis from three biological replicates. *, $p<0.05$; **, $p<0.005$; ***, $p<0.0005$.

III. DISCUSSION

In this study, we show that *tdfJ*, *tdfH* and *znuA* are zinc-regulated by Zur at the transcriptional level, with *tdfJ* and *znuA* showing high fold-changes for gene expression. The gene expression results complement protein production. The gene expression levels in response to TPEN are similar in the wildtype and *zur* mutant, however for *tdfJ*, *znuA* and *ngo1049* the expression in the *zur* mutant in response to excess zinc appeared to be further de-repressed than from addition of TPEN alone. This was although not complementary in protein expression except for in Ngo1049. This suggests a tight control by Zur at the transcriptional level which is not fully derepressed upon addition of TPEN in this study. In theory we would have expected the zinc excess levels in the *zur* mutant to look like the TPEN treated condition. We should consider the effects of TPEN, as it not only restricts zinc but is able to chelate iron, and can disrupt cell membrane integrity, which could add to the lack of full de-repression by TPEN.

This study is the first to indicate the correct translational start for TdfJ, based on *in silico* and promoter characterization experiments, ending the long-standing debate on which ATG is utilized by *Ngo*. *tdfJ* promoter analysis established the presence of both Fur and Zur boxes helping explain a mechanism for dual regulation by iron and zinc. Through a novel DNA binding ELISA approach, we were able to show that Fur binds the *tdfJ* promoter with a specific affinity. We also show that Fur recognizes and binds more flexibly than possibly Zur. While Zur recognizes a much smaller Zur-box region, the Fur box is a much larger sequence of at least 30 bp and is spread across the *tdfJ* promoter (Figure 5a). TdfJ is unique among the TDTs for its ability to be dually regulated by both zinc and iron metal ions. The *Nme* homologue of *tdfJ*, *znuD* has also been shown to be induced by iron and repressed by zinc, with a speculation of being Fur- and Zur-

mediated respectively (332). Analysis of the *znuD* putative promoter elements implicates a striking match to the *tdfJ* promoter characterized in this study. The mechanism that Fur utilizes to activate gene expression here has not been characterized, however, based on existing evidence Fur can activate *tdfJ* expression through a direct mechanism involving Fur binding to P_{tdfJ} (328). The direct mechanism may involve competition between Fur and a repressor, for the same site on the promoter. This has been previously demonstrated in the activation of *Ngo norB*, by Fur, where Fur competes with a repressor, ArsR for binding the Fur-box, thereby resulting in de-repression and increase in expression of *norB (333)*. However, this mechanism in the context of P_{tdfJ} has not been considered because Fur, the activator, and Zur, the repressor, are not competing for the same site on the promoter (Figure 5a). Based on the location of the Fur-box, and evidence from other studies, the Fur-box is at a position optimal for RNA polymerase recruitment (281, 328, 334). Zur as a repressor is not bound when zinc is absent, which is a condition necessary for *tdfJ* expression (282, 289). TdfJ is unique among the TDTs for its ability to be dually regulated by both zinc and iron metal ions. The *Nme* homologue of *tdfJ*, *znuD* has also been shown to be induced by iron and repressed by zinc, with a speculation of being Fur- and Zur-mediated respectively (332). Analysis of the *znuD* putative promoter elements implicates a striking match to the *tdfJ* promoter characterized in this study. The mechanism that Fur utilizes to activate gene expression here has not been characterized, however, based on existing evidence Fur can activate *tdfJ* expression through a direct mechanism involving Fur binding to P_{tdfJ} (328). The direct mechanism may involve competition between Fur and a repressor, for the same site on the promoter. This has been previously demonstrated in the activation of *Ngo norB*, by Fur, where Fur competes with a repressor, ArsR for binding the Fur-box, thereby resulting in

de-repression and increase in expression of *norB (333)*. However, this mechanism in the context of P_{tdfJ} has not been considered because Fur, the activator, and Zur, the repressor, are not competing for the same site on the promoter (Figure 5a). Based on the location of the Fur-box, and evidence from other studies, the Fur-box is at a position optimal for RNA polymerase recruitment (281, 328, 334). From the context of both Fur and Zur regulating *tdfJ*, we need to understand if they would act at the same time and which regulator has a greater affinity for the promoter. This would depend on the signal, which is the presence or absence of their cognate metal ions Fe^{2+} and Zn^{2+} respectively. Since Fur recognizes a larger area spanning from the upstream of the -35 region to the -10 region (denoted Fur box 1 and 2) (Figure 5a), sterically it would not be possible for Zur also to be bound at the same moment. We hypothesize that when Zur is bound in the presence of Zn^{2+}, the interaction between Zur and the *tdfJ* Zur box is of greater affinity, preventing Fur-Fe^{2+} from displacing Zur to act on *tdfJ*. However, the absence of Zn^{2+} and therefore Zur would allow room for Fur to bind in the presence of Fe^{2+} to induce *tdfJ* expression by recruiting RNA Polymerase. This hypothesis needs to be tested experimentally to determine: 1) the specificity and affinity of Zur to the *tdfJ* promoter and 2) competition between Fur and Zur for the *tdfJ* promoter which acting at the same time at various Mn^{2+} and Zn^{2+} concentrations. Preliminary efforts have been taken to address the binding affinity and specificity of Zur to P_{tdfJ}, however, several obstacles were faced with obtaining a stable form of purified recombinant *Ng*Zur for binding assays. Protein sequence analysis for Ngo Zur showed strain specific difference in the length of Zur between FA1090 and FA19 with the latter from attaining stability during crystallization efforts. Protein crystallization efforts are currently being carried out at Purdue University's Department of Biological Sciences by Dr. Nicholas Noinaj and Swati Mundre, to

obtain a recombinant form of FA1090 *Ng*Zur that is stable when purified to use in our DNA binding ELISAs. Zur as a repressor is not bound when zinc is absent, which is a condition necessary for *tdfJ* expression (282, 289).

In a recent study characterizing the Zur regulon in *Neisseria meningitidis* (*Nme*), *Nme* Zur differentially regulated genes of the Zur regulon, by binding to a Zur-box that was identical to the *Ngo* Zur-box identified here (Figure 2) (282). *Nme* homologues of *tdfJ* (*nmb0964*) and *ngo1049* (*nmb1475*) also showed perfect matches to their predicted Nme Zur-box and showed high fold-changes for gene expression in the presence of TPEN. This conservation of Zur-boxes among the pathogenic *Neisseria* species, is interesting and illustrates the importance of evolutionary conservation to maintain zinc homeostasis. However, whether this is specific to pathogenic *Neisseria* has not been probed into. Since several of the host adaptations have been conserved across both commensals and pathogenic species, it would not be surprising if Zur boxes were also conserved among the *Neisseria* commensals. This conservation of Zur-boxes has been investigated across several β-proteobacteria, including *Bacillus subtillis, Yersinia pestis, Pseudomonas aeruginosa, Escherichia coli*, *Acinetobacter baumanii* and *Salmonella typhimurium* and the conserved sequence was identified to be **GAAATGTTATA-N-TATAACATTTC** (324). All these studies have showed the potential of Zur in pathogensis due to its importance in maintanence of zinc homeostasis of several virulence genes, in Ngo these important zinc homeostasis virulence genes are *tdfH*, *tdfJ* and *znuA*. Chapter 5 of this dissertation describes the paradigm of virulence genes under the control of Zur and is discussed there in further detail.

Zur maintains zinc homeostasis by tightly controlling the level of expression of the genes it regulates. Zinc-bound Zur dimerizes and represses transcription of genes by binding to a

consensus Zur-box on the promoter of the gene, thereby blocking RNA polymerase transcription initiation (325). In this study, we demonstrate a possible correlation between a consensus Zur-box and higher a higher fold-change for gene expression. *tdfJ*, *znuA* and *ngo1049* with a 90-100% match to the Zur box also show a 24, 38 and 46-fold-change for expression respectively in the absence of zinc, however *tdfH* with a 16% match to the Zur-box consensus shows only a fold-change of 3. (Figures 1 and 2). Therefore, the strength of gene regulation by *Ngo* Zur is dependent on the accuracy and length of the palindromic consensus sequence. Further, TdfJ has been identified as an ideal vaccine antigen for the prevention of gonorrhea (229, 304). Its, tight transcriptional regulation by Zur in response to zinc, demonstrate its potential to be a molecular tool that will allow further investigation of its role during infection and enhance the understanding behind creating an efficacious vaccine. This requires further characterization of the *tdfJ* promoter elements that allow it to be regulated by Zur and zinc.

It is also important to consider the physiological relevance of the existence of an environment that will allow for TdfJ expression particularly, that is iron enriched, and zinc deprived. To answer this question, we would need to scope the availability of zinc and iron, or their lack thereof, for the expression of *tdfJ*. Zinc is primarily secreted by the prostate and is abundant in the male reproductive organs and human semen as compared to other body tissues and secretions (335). In contrast, much less is known about the bioavailability of zinc in the female reproductive tract, but is known to be more zinc starved with vaginal fluid comprising of no zinc in daily secretions (336). S100A7 and calprotectin zinc-sequestering proteins, are also enriched in the ectocervix of the female reproductive tract, causing low levels of zinc (337). Overall, the female reproductive tract is more zinc-starved compared to the male reproductive

tract, making the female reproductive tract an ideal environment for the expression of *tdfJ* and other Zur-repressed genes. In addition to low levels of zinc, iron enrichment occurs in the female vaginal canal during the menstrual cycle when tissue and red blood cells lyse to release heme and hemoglobin that are sources of iron. This provides a conducive zinc-starved iron-rich surrounding for enhanced *tdfJ* expression. It is, however, unknown if TdfJ plays a role in the asymptomatic nature of infections predominately seen in women. Preliminary studies on the involvement of TDTs in invasion of ME180 cervical epithelial cells showed promising results for TdfJ as a potential invasion, although the study concluded that only TdfF was important during invasion. There is scope for further analysis of these results and can be revisited to explain TdfJ s role during infection of cervical versus urogenital epithelium (267). There is much to be understood on the nutrient metal bioavailability during gonococcal pathogenesis and the combined effect of multifactorial players. Using the *tdfJ* promoter as a molecular tool to access the environmental differences between the male and female genital tracts in terms of iron and zinc, will expand the scope and knowledge on these multifactorial players and help parse out the mechanisms of gene regulation that take place during gonococcal pathogenesis.

Collectively, our study is the first to lay out a dual mechanism of regulation of TdfJ, by two distinct metal ions and regulators Fur and Zur. Future studies testing the *tdfJ* promoter as a zinc and iron sensitive reporter in different pathological environments including neutrophils, where *Ngo* survive phagocytosis, epithelial cells, and transgenic mice infection models, will be valuable to the field and aid in deciphering targeted treatment options and outcomes.

CHAPTER 4- RNA SEQUENCING ANALYSIS FOR THE ZINC AND ZUR-DEPENDENT TRANSCRIPTOME OF *NEISSERIA GONORRHOEAE* FA1090

I. INTRODUCTION

Zinc is an important transition metal and plays several structural, catalytic, and regulatory functions in prokaryotes. The role of zinc has especially gained some interest among pathogens for its importance in virulence and pathogenicity (338). For example, under zinc-starved environments, bacterial cells use high affinity zinc transporters to increase their internal pool of zinc, which is a critical response during severe host-induced nutritional immunity (221, 320). On the other hand, high zinc concentrations can lead to highly toxic environments, increasing oxidative stress and ultimately killing bacterial cells, a mechanism used by innate immune cells such as PMNs and macrophages (339). Therefore, zinc homeostasis is extremely crucial to bacterial pathogens in keeping internal levels of zinc in check while regulating the import and export of metal ions for maintaining pathogenicity and survival in the host. This tight regulation of import and export of zinc in the bacterial cell is maintained at the molecular level by the Zinc uptake regulator (Zur) (325, 340, 341). The regulatory and mechanistic basis of regulation by Zur on zinc regulated genes has been well characterized in many bacterial pathogens such as *Escherichia coli*, *Bacillus subtilis*, *Corynebacterium diphtheriae*, *Neisseria meningitidis* (*Nme*), *Streptomyces coelicolor* and *Yersinia pestis* (282, 341-344). The principal concept involves Zur acting as a repressor; upon zinc binding the affinity of Zur to the cognate DNA sequence, the Zur box, on gene promoters is enhanced. The increase in affinity, and therefore binding of Zur, blocks RNA polymerase transcriptional initiation of the Zur responsive genes, carefully controlling the internal level of zinc with respect to the environment.

Neisseria gonorrhoeae (*Ngo*), a closely related pathogen to *Nme*, is responsible for causing the sexually transmitted infection, gonorrhea in humans (345). A classical clinical presentation of a gonococcal infection is a sustained inflammatory response accompanied by purulent urethral or cervical exudates, consisting of human neutrophils and intact *Ngo* within (346, 347). These neutrophils are enriched with the nutritional immunity protein calprotectin, that has antimicrobial activity and chelates and restricts zinc away from pathogens (289, 320). During mucosal colonization of the vaginal tissues, other strategies to restrict zinc are employed as part of the innate immune response to gonorrhea. Psoriasin or S100A7, another innate immune protein, is secreted by these mucosal surfaces to limit zinc availability to *Ngo* (321). *Ngo* however does not succumb to these strategies and regulates genes to produce zinc import proteins on their outer surface called TonB-Dependent Transports (TDT). Zinc import TDTs TdfH and TdfJ bind to calprotectin and psoriasin, respectively, and allow for the import of the zinc being withheld (229, 289). This zinc is then released into the periplasm where a zinc shuttle protein, ZnuA, carries the zinc to a cytoplasmic ABC transporter to be internalized for utilization. This coordinated effort of zinc acquisition by TDTs is mediated by the control of the zinc uptake regulator Zur (289). In *Nme* a study focusing on the zinc-dependent transcriptome revealed 17 genes that were differentially regulated by Zur (282). Interestingly, 2 genes were induced by Zur in the presence of zinc, shifting the focus of Zur as a repressor alone and towards its potential activity as an activator (282). The homologue of several *Nme* Zur regulon genes in *Ngo* have pathological significance, including the TDT genes, which are implicated in survival and virulence of *Ngo* during host colonization and infection (282, 321).

The Zur transcriptome of Ngo has not been characterized and in this work, we describe the genes that are controlled by *Ngo* Zur by comparing zinc stress and zinc excess conditions between wildtype FA1090 and an isogenic *zur* mutant strain. We use RNA sequencing to predict the transcriptome of differentially regulated genes and describe 26 genes that fall under the *Ngo* Zur regulon. Using promoter prediction analysis, we were able to validate and compare the Zur binding sequence on the promoters and compare the extent of regulation by RT-qPCR fold changes for expression. Much like the global regulator Fur, Zur, which is a FUR family regulator, is also able to act as an activator to enhance gene expression by binding to Zur-boxes further upstream on the promoter (281, 328). We also show an overlap of genes differentially regulated by oxidative stress response and zinc starvation under the control of *Ngo* Zur. This is relevant from the context of mimicking a host response to infection and will make key contributions in evaluating essential virulence genes and zinc homeostasis in *Ngo*.

Importance: With no effective vaccine available to prevent gonorrhea and the high number of multidrug resistant *Ngo* strains, effective use of antibiotics for treatment is a waining option (348). This dictates an urgent need for effective therapeutic strategies to treat a gonococcal infection which includes *Ngo* strategies to overcome nutritional immunity such as zinc starvation. Our results provide the basis for understanding the Zur regulatory pathways and molecular mechanisms used by *Ngo* to adapt to host zinc environments.

II. RESULTS

A. Zinc- and Zur-dependent Genes in FA1090 are Repressed in Response to Zinc Excess

Gene expression profiles of the wildtype strain FA1090 and the FA1090 *zur* mutant were compared under excess and low zinc conditions by RNA Sequencing. 26 genes were differentially regulated of which 18 genes were down regulated and 8 genes were up regulated when zinc was present (Figure 6). This suggests that *Ngo* Zur predominately acts as a repressor in the presence of zinc much like the *Nme* Zur (282). Of the 18 repressed genes, *ngo0952* (*tdfH*), *ngo1205* (*tdfJ*), *ngo1049*, *ngo0168* (*znuA*) and *ngo0170* (*znuC*) are zinc homeostasis genes, that are involved in active zinc uptake from the outer membrane to the cytoplasm during zinc-limitation (229, 266, 289). In *Ngo*, the outer membrane transporters, TdfH and TdfJ have been characterized and bind zinc-sequestering ligands, calprotectin and psoriasin, respectively, to release zinc into the periplasm. ZnuA in the periplasm aids in the transfer of the zinc substrate to the ATP machinery ZnuBC on the cytoplasmic membrane, ultimately releasing zinc into the cytoplasm of the zinc-starved cell (265, 268, 289). These genes are important virulence genes that enable *Ngo* to over zinc limitation during pathogenesis (284, 289). *znuA*, the gene encoding the zinc-substrate binding periplasmic protein, that is involved in shuttling zinc from the periplasm to the cytoplasm during zinc starvation, showed a high $\log_2$ fold-change of -5 whereas, *znuC* encoding for the ATP binding protein of the zinc ABC transport system, showed a lower $\log_2$ fold-change value of <-2 (Figure 6). *znuB,* which is a part of the *znuABC* polycistronic operon and encodes the metal ABC permease, although differentially regulated by zinc, showed a fold-change for zinc and Zur regulated expression <-2 (Figure 6). In most pathogens ZnuA has been associated with the primary means of overcoming calprotectin mediated zinc-limitation (221, 349, 350). The recent

implication of *znuA*'s importance during growth and attachment further complement the high transcript numbers from this study and the importance of this gene in overcoming zinc limitation in *Ngo* (321). *tdfH* and *tdfJ* have $\log_2$ fold-changes for gene expression of > -4, with *tdfJ* showing higher transcript numbers and a higher fold-change of -4.6 (Figure 6). This observation is in line with our understanding that *tdfH* is not as tightly regulated by zinc and Zur in FA1090 as compared to *tdfJ* (289) (Figure 6). Another gene that exhibited a high $\log_2$ fold-change value for expression of >-4, was *ngo1049*, a poorly characterized zinc responsive gene encoding for a hypothetical protein with unknown function and high affinity to zinc (Figure 6). The homologue of *ngo1049* in *Nme* was found to be the mostly highly zinc-regulated gene and was characterized to have specificity only to the zinc substrate. Similar preliminary bioinformatic characterizations and protein structure modeling in *Ngo,* have localized Ngo1049 in the periplasmic space much like ZnuA and highlighted its specificity to zinc (Liyayi IK and Criss AK., unpublished results).

The two most highly zinc- and Zur-regulated genes in this study were *ngo0930* (*rpmE2*) and *ngo0931* (*rpmJ2*) with the highest fold-change for expression at -6 and -7 respectively (Figure 6). *rpmE2* and *rpmJ2* are part of an operon and their expression is controlled by a single promoter that harbors a Zur-box through which Zur regulates expression. *rpmE2* and *rmpJ2* code for the 50S ribosomal L31 and L36 proteins that contain a CxxC motif, that is a designated zinc-ribbon signature. These ribosomal proteins are well described in *E. coli*, *Y. pestis* and *B. subtilis* and a mechanism of zinc replacement in different paralogs of these proteins have been noted for gene activation and ribosomal processing (351). It has been shown that Zur actively represses the L31p and L36p paralog forms of L31 and L36 protein during the presence of excess zinc. These Zur-box containing paralog forms are expressed during zinc-starvation and the L31p and L36p proteins

bind to a hairpin like structure preventing translation of the zinc-binding L31 and L36 proteins. When there is an abundance of zinc, the paralog forms are not made due to Zur repression and zinc containing L31 and L36 are liberated from the ribosome for translation. In *Ngo*, *rmpE2* and *rmpJ2* encode for the paralogous forms of L31 (RpmE) and L36 (RpmJ) that potentially control the ribosomal translation of these zinc-finger proteins. The zinc starvation response of replacing the zinc containing RpmE and RpmJ proteins with their non-zinc containing paralog forms RpmE2 and RpmJ2, could be a possible means of maintaining zinc homeostasis and enhance bacterial survival in the host (342, 352).

Genes encoding hypothetical proteins *ngo04165*, a sulfate ABC transporter substrate binding protein and *ngo0165*, defined as an integral membrane protein, were also differentially repressed by Zur in the presence of zinc by fold changes of approximately -1.5 (Figure 6).

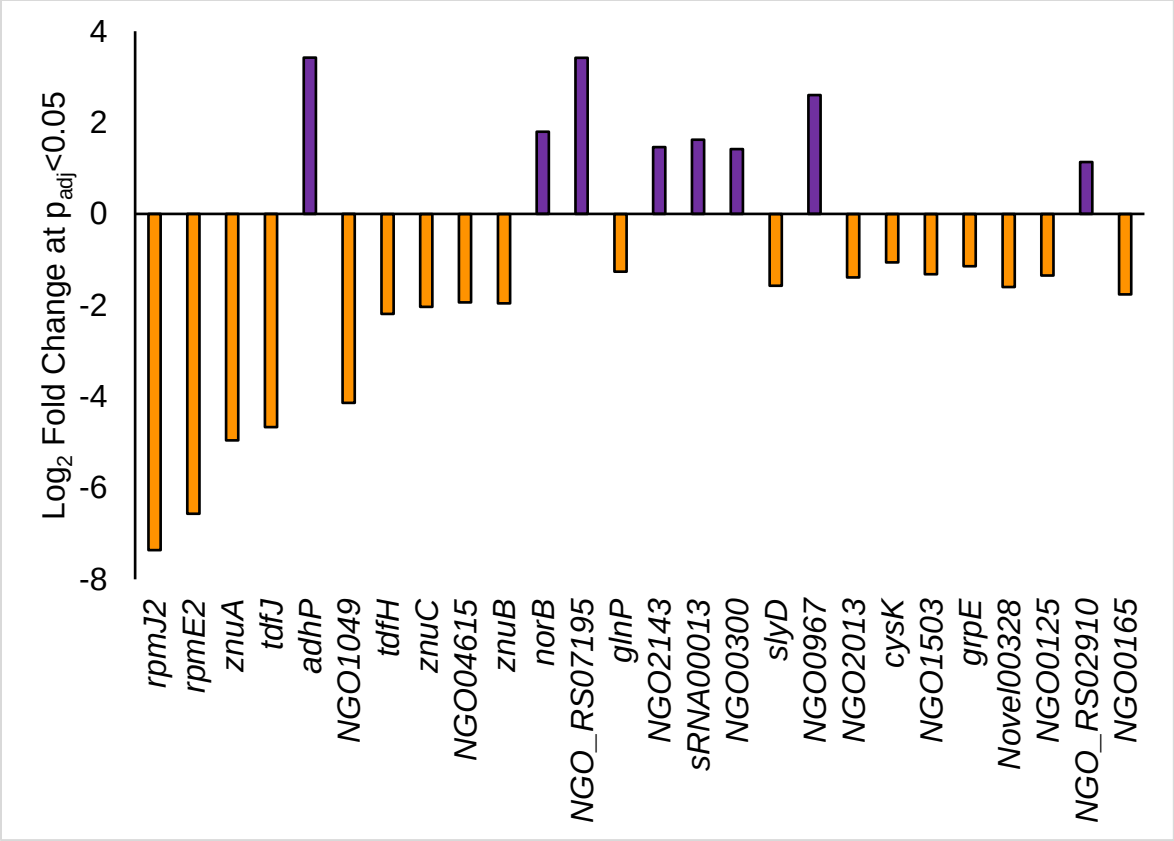

Figure 6. List of differentially expressed genes by Zur in *Ngo* FA1090 in response to zinc

Figure 6. List of differentially expressed genes by Zur in *Ngo* FA1090 in response to zinc. Log_2 fold-change for expression of genes repressed (orange) and activated (purple) by Zur in the presence of zinc in WT FA1090. *p* values were normalized to $p_{adjusted}$ values and significant expression with $p_{adjusted}$ <0.05 were considered as differentially expressed.

B. adhP and norB are Zn::Zur-activated Genes

ngo1442 (*adhP*), the gene that encodes the enzyme alcohol dehydrogenase in the family of zinc-binding dehydrogenases, was the most Zur induced and demonstrated a log_2 fold-change for expression of 3.4 in the presence of zinc. *adhP* is a propanol preferring alcohol dehydrogenase

which may be involved during anaerobic respiration. However alcohol utilization and synthesis pathways have not been defined in *Neisseria sp* (353). *adhP* was highly zinc induced in the *Nme* Zur regulon study and was also induced in an RNA seq study on genes in *Ngo* that were differentially regulated by Zur attachment to a surface (282, 321).The *Ngo* PerR regulon also showed an induction of *adhP* expression, although *Ngo* PerR is now considered Zur (354). The overlap between these different studies suggests an important role for *adhP* in zinc homeostasis.

ngo1275 (*norB*) is another gene induced in the presence of zinc and Zur with a $\log_2$ fold-change for expression of 1.8 (Figure 6). *norB* encodes for a nitric oxide reductase, which plays a pivotal role in nitrite utilization and anaerobic growth (355). In *Ngo*, the gonococcal denitrification apparatus consists of *norB* and a gene that precedes it *aniA*. *aniA* encodes for a nitrite reductase (AniA) that catalyzes the conversion of nitrite to nitric oxide (NO), which is subsequently reduced to nitrous oxide (N_2O) by NorB (356, 357). It has been shown that *Ngo norB* expression is induced in the presence of nitrite in anaerobic environments and that it is not regulated by the fumarate and nitrate regulator FNR or the nitrate/nitrite two component system, NarQ/NarP, unlike the *norB* homologue in *Nme* (355). *Ngo norB* has been shown to be directly regulated by NsrR, which acts as a repressor and binds to the *norB* promoter in the absence of NO (358). P_{norB} has been characterized in both *Ngo* and *Nme*, including the +1, -10, -35 promoter elements and a NsrR binding site downstream of the -10 region, along with a truncated FNR binding inverted repeat region (333, 355, 359). Adding to the list of regulators involved in the control of *norB* expression, it was further determined that Fur activates *norB* expression through an indirect mechanism and binds to a Fur-box upstream of the -35 sequence (333, 360). Interestingly, preliminary bioinformatic promoter analysis from this study revealed a

potential upstream Zur box, preceding the -35 region, that could explain the Zur induction of *norB* expression. This is the first study where Zur has been observed to activate *norB* expression in the presence of zinc and much is unknown regarding the Zur activation mechanisms in *Neisseria sp*.

ngo0967, a gene encoding a hypothetical protein was also found to be induced by Zur in the presence of zinc, contributing to a $\log_2$ fold-change for expression of 2.6 (Figure 6). Table 3 includes a comprehensive list of differentially Zur and Zinc regulated genes in *Ngo* FA1090, along with their respective $\log_2$ fold-change for expression.

Table 3. List of differentially expressed genes by Zur in FA1090

Gene locus	Symbol	L2FC Zn repressed by Zur WT Zn vs WT TPEN	L2FC CDM WT vs CDM zur	Definition
Repressed				
NGO_0931	*rpmJ2*	-7.360	(-)	type B 50S ribosomal protein L36
NGO_0930	*rpmE2*	-6.564	(-)	type B 50S ribosomal protein L31
NGO_0168	*znuA*	-4.957	(-)	zinc ABC transporter substrate-binding protein && PF01297:Zinc-uptake complex component A periplasmic
NGO_1205	*tdfJ*	-4.667	(-)	TonB-dependent receptor && PF07715:TonB-dependent Receptor Plug

				Domain|PF00593:TonB dependent receptor
NGO_1049	*ngo1049*	-4.136	(-)	DUF4198 domain-containing protein PF10670:Domain of unknown function (DUF4198)
NGO_0952	*tdfH*	-2.190	(-)	TonB-dependent receptor PF00593:TonB dependent receptor|PF07715:TonB-dependent Receptor Plug Domain
NGO_0170	*znuC*	-2.035	(-)	metal ABC transporter ATP-binding protein PF00005:ABC transporter
NGO_04615	*ngo04615*	-1.937	(-)	sulfate ABC transporter substrate-binding protein PF13531:Bacterial extracellular solute-binding protein

NGO_0169	*znuB*	-1.955	(-)	metal ABC transporter permease PF00950:ABC 3 transport family
NGO_2012	*glnP*	-1.264	(-)	amino acid ABC transporter permease PF00528:Binding-protein-dependent transport system inner membrane component
NGO_0981	*slyD*	-1.569	(-)	peptidylprolyl isomerase
NGO_2013	*ngo2013*	-1.393	(-)	amino acid ABC transporter ATP-binding protein && PF00005:ABC transporter
NGO_0340	*cysK*	-1.059	(-)	cysteine synthase A PF00291:Pyridoxal-phosphate dependent enzyme
NGO_1503	*ngo1503*	-1.322	(-)	Fic family protein PF02661:Fic/DOC family

NGO_1422	*grpE*	-1.147	(-)	nucleotide exchange factor GrpE PF01025:GrpE
NGO_0125	*ngo0125*	-1.346	(-)	hypothetical protein
NGO_0165	*ngo0165*	-1.758	(-)	hypothetical protein
NGO_0554	*ngo0554*	-1.230	1.708	hypothetical protein
NGO_0542	*zur*	(-)	1.712	transcriptional repressor

Induced

NGO_1442	*adhP*	3.421	2.018	alcohol dehydrogenase AdhP PF08240:Alcohol dehydrogenase GroES-like domain|PF00107:Zinc-binding dehydrogenase
NGO_1275	*norB*	1.799	(-)	nitric-oxide reductase large subunit && PF00115:Cytochrome C and Quinol oxidase polypeptide I
NGO_RS07195	*ngo_rs07195*	3.417	(-)	transposase
NGO_2143	*ngo2143*	1.462	(-)	ATP synthase subunit I

	sRNA00013	1.624	(-)	-
NGO_0300	*ngo0300*	1.419	(-)	very short patch repair endonuclease && PF03852:DNA mismatch endonuclease Vsr
NGO_0967	*ngo0967*	2.601	(-)	hypothetical protein
NGO_1684	*queF*	(-)	-1.275	preQ(1) synthase && PF14489:QueF-like protein
NGO_0129	*queC*	(-)	(-)	

Table 3. List of differentially expressed genes by Zur in *Ngo* FA1090 in response to zinc. Genes are categorized into repressed and induced and their respective Log_2 fold-changes (L2FC) for expression with $p_{adjusted}$ <0.05 are listed. L2FC for differential expression in FA1090 WT under zinc excess or TPEN condition and in CDM between a WT and *zur* mutant are displayed. Gene locus ID and predicted computational functions of differentially regulated genes are listed.

C. Comparison of Ngo Zur Regulon Genes with Other Transcriptomic Studies in Neisseria Sp

The Zur regulon (also known as PerR in the context of Manganese regulation) has been investigated in *Ngo* strain 1291 using a microarray analysis comparing a wildtype and a *zur* mutant strain, that revealed 12 differentially regulated genes which included zinc homeostasis genes *znuA (mntC)*, *znuB (mntB)*, *znuC(mntA)*, *tdfH*, *tdfJ*, *ngo1049* and the ribosomal L31 and L36 genes *rmpJ2* and *rmpE2*, which were all up-regulated in the *zur* mutant as compared to the wildtype and had fold-changes >2 (Table 4) (354). Only *adhP* was found to be downregulated in the *zur* mutant (354). Similarly, a microarray analysis performed in *Nme*, between a wildtype MC58 and *zur* mutant strain grown in CDM under zinc excess and zinc stress, also revealed a set of 17 differentially regulated genes of which *cbpA* (*tdfH*), *znuD* (*tdfJ*) and *znuA* were greatly Zur repressed and *adhP* was one of the two Zur-induced genes, the other a NosR-related protein family gene with no known characterization (Table 4) (282). Interestingly, our RNA sequencing study revealed *norB* as zinc- and Zur-induced apart from *adhP*, which has previously not been identified as Zur or zinc regulated. Prior studies on *norB* have focused on its regulation with respect to nitric oxide stress and regulation by the nitric oxide-sensitive repressor NsrR. NsrR binding sites have been mapped on the *aniA* (a nitrite reductase) and *norB* promoters in the gonococcal strain F62 (358). NsrR binds to a region downstream of the -10 region of the *norB* promoter and represses transcription in the absence of NO (358, 359). *norB* is additionally regulated by the Ferric uptake regulator (Fur) in F62, whereby, Fur activates *norB* expression in the presence of iron and binds to a region upstream of the -35 region (360). The predicted Zur binding site on the *norB* promoter lies about 20 base pairs downstream of the Fur-box and 1 base

pair upstream of the -35 region, in an ideal location to facilitate RNA polymerase recruitment activation when zinc is present. Currently the mechanism that facilitates this multi-regulatory process has not been studied, and this finding could be attributed to strain specific differences within *Neisseria* species, with *norB* Zur-activation being specific to FA1090. *tdfJ* is among the current set of genes that also shows a multi-regulation mechanism where is it Zur repressed, and zinc induced. *tdfJ* requires an iron enriched and zinc deficient environment, which is likely to be present in the female reproductive tract. A study focusing on the transcriptomic profile of *Ngo* during natural infection in men and women, showed that *tdfJ* expression was 5-fold higher in female subjects as compared to male subjects and that *norB* was 4-fold induced in the male subjects as compared to the female subjects (Table 4) (361). On the context of host relevant *Ngo* transcriptomes, a recent study exploring the interactions between primary human neutrophils and different strains of *Ngo*, unveiled differential regulation of several Zur-regulated genes and primary human neutrophils. These included *znuA*, *tdfJ*, *ngo1049* and *rpmE2*, with all four being induced upon *Ngo* exposure to neutrophils (362).

Table 4. Comparison of Zur regulon studies in *Ngo*

L2FC Zn repressed by Zur

Gene locus	Symbol	WT Zn vs WT TPEN	Jennings M Study PerR *N. gonorrhoeae*	MC Pawlik Study *N. meningitidis*	Ray JC Study *N. gonorrhoeae*	Criss AK Study *Ngo*+PMN	Genco CA Study *Ngo* Men vs Women
Repressed							
NGO_0931	*rpmJ2*	-7.360	(+) Zn Zur repressed	(+) Zn Zur repressed	ns		
NGO_0930	*rpmE2*	-6.564	(+) Zn Zur repressed	(+) Zn Zur repressed	(+) Adherence and Zn Zur regulated	✓	
NGO_0168	*znuA*	-4.957	(+) Zn Zur repressed	(+) Zn Zur repressed	(+) Adherence	✓	

					and Zn Zur regulated		
NGO_1205	*tdfJ*	-4.667	(+) Zn Zur repressed	(+) Zn Zur repressed	(+) Zn Zur regulation only	✓	✓
NGO_1049	*ngo1049*	-4.136	(+) Zn Zur repressed	(+) Zn Zur repressed	(+) Adherence and Zn Zur regulated	✓	
NGO_0952	*tdfH*	-2.190	(+) Zn Zur repressed	(+) Zn Zur repressed			
NGO_0170	*znuC*	-2.035	(+) Zn Zur repressed	(+) Zn Zur repressed	ns		
NGO_0169	*znuB*	-1.955	(+) Zn Zur repressed	(+) Zn Zur repressed	ns		

Induced

NGO_1442	*adhP*	3.421	(+) Induced under excess Zn	(+) Induced under excess Zn	(-) Zn induced by Zur and adherence	x	
NGO_1275	*norB*	1.799				✓ HO41 and FA1090	✓

Table 4. Comparison of differentially regulated genes in *Ngo* by Zur in other studies. Zur repressed and induced genes that overlap with other studies in Ngo under zinc starvation are listed**.** The conditions at which each of these Zur regulon genes are expressed in each of these studies are listed under each column for comparison. Differentially regulated genes that were differentially expressed in response to zinc or Zur in at least one of the 5 other studies were considered for further validation in this study. Log_2 fold-changes (L2FC) for expression with $p_{adjusted}$ <0.05 are listed for each gene.

D. Ribosomal Genes rpmE2/J2 Show the Highest Fold Change for Expression by RT-qPCR.

Based on overlapping information from the differentially regulated genes list in Table 2, we performed RT-qPCR for the six differentially expressed genes from this study. For zinc-dependent Zur repression, we found the zinc homeostasis genes *znuA*, *tdfJ*, *tdfH* and *ngo1049* were all significantly induced in the absence of zinc in the wildtype strain (Figure 7A). We found that the ribosomal genes *rpmE2* and *rpmJ2* were also greatly expressed in the absence of zinc in the wild type and showed the highest fold-changes for gene expression. *znuA* and *ngo1049* were 23-fold and 31-fold higher expressed in the absence of zinc, respectively, in wildtype FA1090 (Figure 7A). *tdfJ* showed a 10-fold increase in the absence of zinc in the wildtype while *tdfH* showed only a 3-fold increase in the absence of zinc in the wildtype strain (Figure 7A). *rpmE2* and *rmpJ2* on the other hand each showed 81- and 85-fold increase in expression respectively in the absence of zinc in the wildtype (Figure 7A). These expression and fold-changes are consisted with the $\log_2$ fold-change and FPKM values obtained from RNASeq analysis. *adhP* showed a 13-fold increase in expression in the presence of zinc in the wildtype and no significant difference in the *zur* mutant via RT-qPCR (Figure 7B). RT-qPCR for *norB* showed a 5-fold increase in the wildtype in the presence of zinc and no significant change in the *zur* mutant (Figure 7B). All RT-qPCR expression values were normalized to the expression of the house keeping gene *rmpM* and significance was calculated from biological and technical replicates.

A.

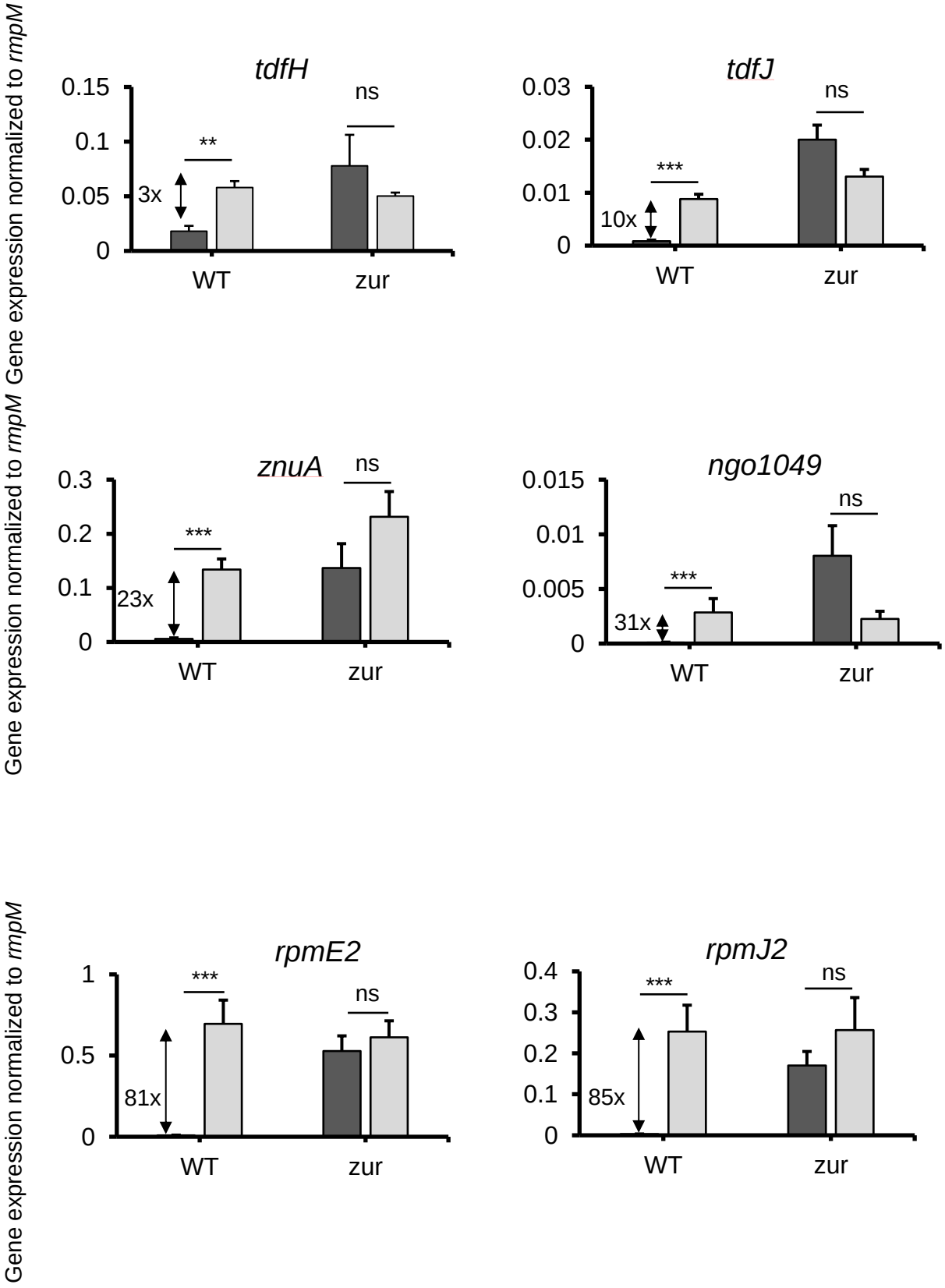
Gene expression normalized to rmpM
tdfH
0.15
0.1
0.05
0
**
ns
3x
WT
zur
tdfJ
0.03
0.02
0.01
0
***
ns
10x
WT
zur
znuA
0.3
0.2
0.1
0
***
ns
23x
WT
zur
ngo1049
0.015
0.01
0.005
0
***
ns
31x
WT
zur
Gene expression normalized to rmpM
rpmE2
1
0.5
0
***
ns
81x
WT
zur
rpmJ2
0.4
0.3
0.2
0.1
0
***
ns
85x
WT
zur

B.

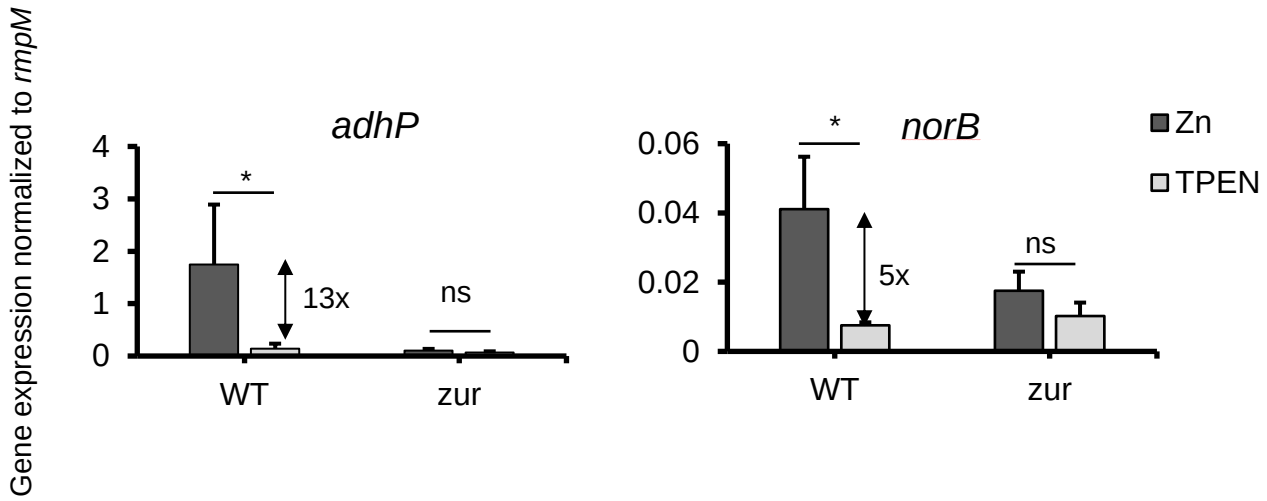

Figure 7. *rpmE2/J2* and *adhP* show high-fold change for expression among Zur repressed and induced genes in *Ngo*

Figure 7. *rpmE2/J2* and *adhP* show high fold-change for expression among Zur repressed and induced genes in *Ngo*. A. RT-qPCR bar graph for Zur-repressed genes in a WT and *zur* mutant. B. RT-qPCR bar graph for Zur induced genes in a WT and *zur* mutant. The zinc excess conditions are shown in dark grey and the zinc-deplete conditions upon treatment with TPEN, are shown in light grey. Gene expression normalized to the expression of *rmpM* is plotted in the bar graphs. Fold-changes for expression in the WT are depicted. Student T-test was used for determining statistical significance. *, $p<0.05$; **, $p<0.005$; ***, $p<0.0005$; *ns*, $p>0.05$

E. Zur Binds to the Zur Box Sequence on the Promoters of the Differentially Regulated Genes to Either Repress or Induce Expression

The Zur box consensus sequence has previously been established in *Nme* and further confirmed in *Ngo* FA1090 (282, 363). We aligned the predicted promoter regions of the above 8 Zur regulated genes, *tdfH*, *tdfJ*, *znuA*, *znuB*, *ngo1049*, *adhP*, *norB* and *rmpE2/J2* and mapped the extent of similarity or difference to the consensus. A consensus logo was prepared using the WebLogo 3 online software (Figure 8A). Among the Zur-repressed genes, *tdfH*, *ngo1049* and *rpmE2/J2* promoters had a 100% match to the established consensus Zur box of TGTTATDNHATAACA (Figure 8B). Interestingly *adhP,* a Zur induced gene, also had an exact match to this consensus, the difference being in the location of the Zur binding site with respect to the -10 and -35 promoter elements. Based on available literature on transcriptional regulators and their mechanism of regulation, genes with a Zur box overlapping the -10 and -35 region are repressed by Zur whereas genes with a Zur box upstream of the -35 region are Zur induced. The promoter region for *norB,* which is Zur induced, contains of a putative Zur box upstream of the -35 region and had a 75% match to the consensus (Figure 8B). The Zur box of *tdfH* was only a 16% match to the consensus while for the *znuA* promoter the Zur box was a 92% match with the consensus Zur box, once again signifying the RT-qPCR fold change for expression for *tdfH* and *znuA* (Figure 8B).

A.

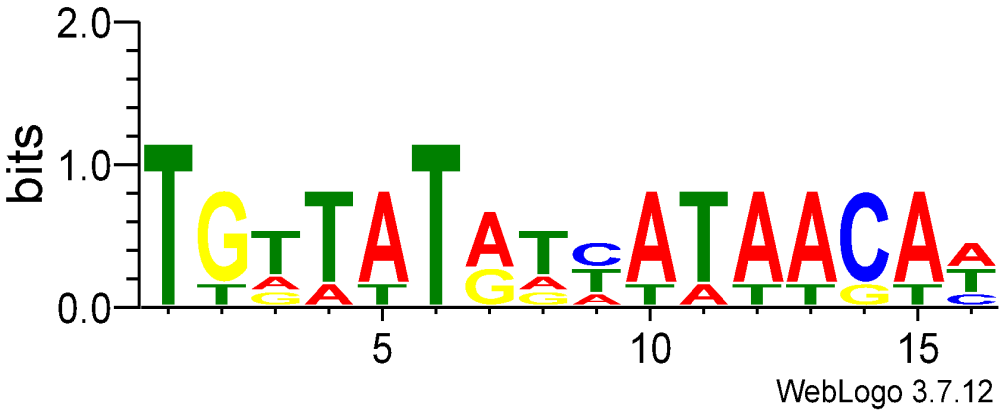

B.

ORF ID	Gene name	Zur box sequence	% Similarity
	Consensus	**TGTTAT**DNH**ATAACA**	
NGO0952	*tdfH*	**T**T**GATT**GTT**TATTGT**	16
NGO1205	*tdfJ*	**TGTTAT**ATA**ATAACA**	100
NGO0168	*znuA*	**TGATAT**AAC**ATAACA**	92
NGO1049	*ngo1049*	**TGTTAT**AGC**ATAACA**	100
NGO0930/31	*rmpE2/J2*	**TGTTAT**GTT**ATAACA**	100
NGO1442	*adhP*	**TGTTAT**AAT**ATAACA**	100
NGO1275	*norB*	**TGTT**T**G**AAC**A**A**AACA**	75

Figure 8. A Zur box consensus sequence for *Ngo* Zur

Figure 8. A Zur box consensus sequence for *Ngo* Zur. A. Consensus *Ngo* Zur box logo created using WebLogo 3.7.12. The consensus is an inverted repeat of 6-3-6 with a total of 15 base pair length. B. An alignment of Zur regulon genes predicted promoter region containing the Zur box. The matching nucleotides are bolded and shown in red while the mismatched nucleotides are bolded and depicted in black. The % similarity of the aligned Zur boxes to the consensus is included in the alignment.

F. Enrichment Analysis of Differentially Zinc Regulated Genes in the WT

A comparison of *Ngo* gene ontologies (GO) enriched in wildtype FA1090 under zinc restricted conditions were analyzed using an enrichment analysis. Gene functions were classified into three major processes, Biological Process (BP), Cellular Components (CC) and Metabolic Function (MF) (Figure 9A). Differentially expressed genes classified as Cellular Components were significantly enriched in membrane function in WT FA1090 under zinc starvation (Figure 4). Membrane GO's included genes involved in nutrient transport such as the TDTs, *tdfJ* and *tdfH* and genes responding to oxidative stress such as *norB* (Figure 9A). Biological Process GO's were enriched in oxidation-reduction and cell redox homeostasis responses, including *adhP*, *norB* and *msrAB*. *msrAB* encodes for the methionine sulfoxide reductase that reduces methionine sulfoxide residues back to methionine to repair proteins damaged by oxidative stress (Figure 9A) (364). In this study *msrA*B was differentially regulated by zinc and TPEN, but not by Zur and showed a $\log_2$ fold change of 1.5 in the presence of TPEN (Figure 7). *msrAB* was also found to exhibit the highest fold change upon exposure to PMNs, which are an environment of high oxidative stress and low zinc (362). Apart from the GO enrichment several KEGG pathways were enriched in the WT in response to zinc starvation (Figure 9B). Those significantly enriched include, genes involved in microbial metabolism, carbon metabolism, pentose phosphate pathway and pyruvate metabolism (Figure 9B). The zinc and Zur regulated genes enriched in these KEGG pathways were *norB* and a cysteine synthase gene (*cysK*) *ngo0340*, both of which are part of microbial and carbon metabolism pathways (Figure 9B). The KEGG enriched pathways in the *zur* mutant however do not include *norB* or *cysK*, suggesting that these two genes play an important role in *Ngo* metabolism during zinc starvation (data not shown).

A.

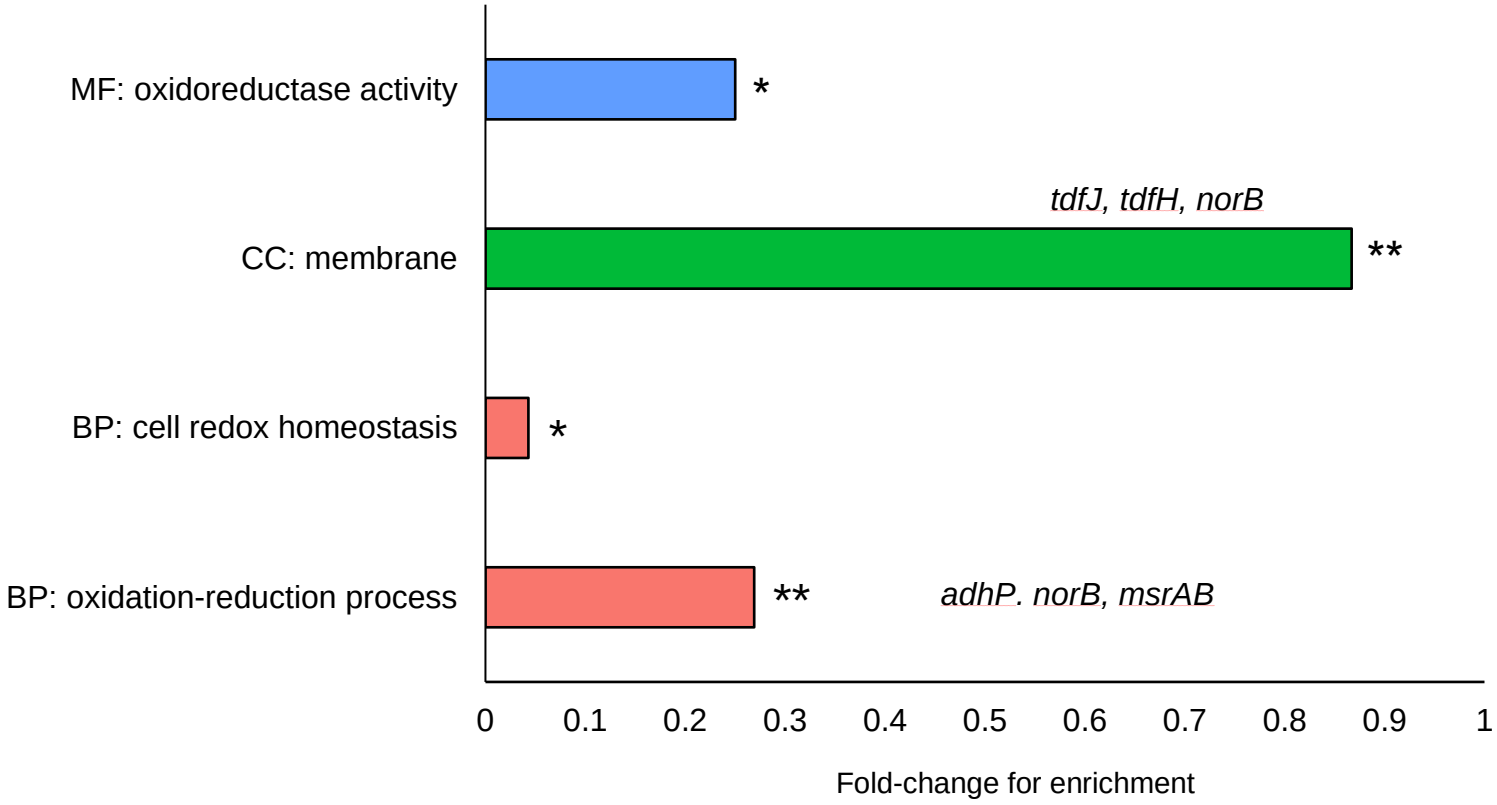

B.

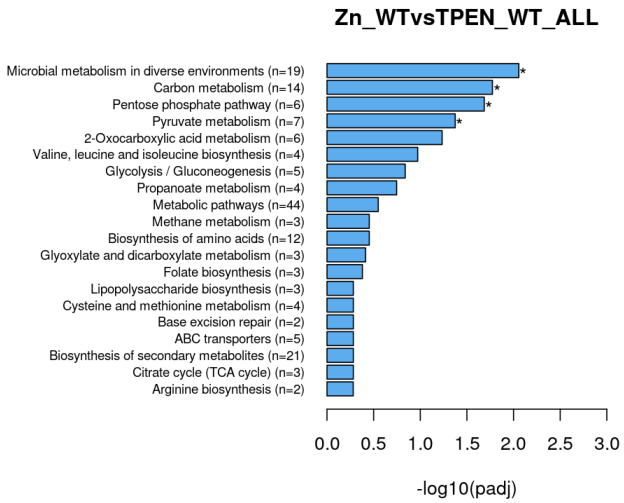

Figure 9. GO and KEGG enrichment analysis for Zur regulated genes in WT *Ngo*

Figure 9. GO and KEGG enrichment analysis for Zur regulated genes in WT *Ngo*. A. Gene Ontology enrichment of pathways in Metabolic Function (MF), Cellular Components (CC) and Biological Processes (BP). The Fold changes for enrichment in each pathway is on the X-axis. Statistical significance was obtained using p values. *,$p<0.05$; **, $p<0.005$. B. KEGG analysis of enriched pathways in the WT in response to zinc. The pathways and the number of genes involved are displayed on the Y-axis and the fold-change normalized to $p_{adjusted}$ values are on the X-axis. Here $p_{adjusted}<0.05$ were considered significant (*).

III. DISCUSSION

It is known that iron- and Fur-regulation in *Ngo* FA1090 modulate key genes necessary during *Ngo* pathogenesis (328, 361, 365). These genes include nutrient acquisition proteins such as TbpAB, a transferrin binding iron and Fur regulated bi-partite Fe-transporter which is important during infection and shows promise as a vaccine antigen (366). Other TDTs, including zinc uptake proteins such as TdfJ and TdfH, are also potentially valuable vaccine antigens. However, there has been little focus on the zinc transcriptome of *Ngo* FA1090 and the importance during pathogenesis. The male site for *Ngo* colonization is predominately zinc enriched while the female reproductive tract is zinc starved, suggesting importance for zinc and Zur regulation of genes in *Ngo*.

In this study we explored the global zinc and Zur transcriptome in FA1090 using RNA sequencing in a WT and *zur* mutant strain under zinc excess and zinc starvation. It appears that the present RNA seq analysis, exposes a primarily oxidative stress response in *Ngo* with Zur-regulated nutrient transport genes being differentially regulated. *norB* expression has primarily

been studied from the context of an oxidative stress response that involves nitric oxide and anaerobic growth in *Ngo* (355). Given its response to oxidative stress, the growth media in this study, CDM stimulates an oxidate stress within anaerobic conditions. CDM has been used in other studies including the Zur regulon of *Nme*, and a peroxide stress was induced for a manganese-dependent Zur (PerR) transcriptome in *Ngo*, however *norB* was not differentially expressed in either of these two studies (282, 354). A possible explanation for the differential expression of *norB* in this study could be the use of TPEN for zinc starvation. TPEN is a high affinity zinc chelator, but it can also chelate other metal ions including iron, which could potentially have an influence on overall transcriptional changes in *Ngo*. Studies have also shown that TPEN can affect membrane integrity as it is membrane permeable and has been demonstrated to enter *E. coli* cells which can cause the removal of not just extracellular but also intracellular metal ions (367). Another study in *E. coli* evaluated the effects of transcriptional changes in the presence of TPEN and noted a strong correlation with chelation of intracellular ions other than zinc and transcriptomic responses, identifying a major Fur regulated response in the study (368). This finding partially supports the *norB* regulation observed in this study as *norB* has been shown to harbor a Fur box and is shown to be regulated by iron (333). Surprisingly, an RT-qPCR to validate the *norB* zinc and Zur-dependent regulation, showed that it was indeed induced by zinc and Zur in the WT. Further bioinformatic promoter analysis identified a putative upstream Zur box in addition to an upstream Fur box in *norB*. This outcome of *norB* also has clinical relevance, because *norB* was found to be induced in H041, a multi-drug resistant clinical strain of *Ngo*, in the presence of PMNs (362). This suggests a critical role for *norB* not just in oxidative stress, but also zinc homeostasis which could be a strain specific or environment-based observation. This sheds

light on the results from this study and the hypothesis of dual and multi-regulatory effects on certain genes in the context of host metal availability. There is evidence that the female reproductive tract is more anaerobic than the male reproductive system, which may be potentially contributing to the greater percentage of asymptomatic infections seen in women (369). This is important to know because *norB* is involved in anaerobic respiration pathway which includes *aniA*, through nitrite reduction (355). This observation along with the differential regulation seen in women offer a potential critical role for *norB* in infections pertaining to women.

Gene Ontology (GO) analysis of these differentially zinc regulated genes showed a significant enrichment in cellular components in membrane function, among which are the TDT genes *tdfH* and *tdfJ*. Biological process genes responsible for oxidation reduction activity showed an enrichment of *adhP*, *norB* and *msrAB,* of which *msrAB* is only zinc or TPEN regulated but not by Zur. *msrAB* in other bacteria such as *Haemophilus influenzae*, has been shown to play a major role in virulence through the repair of damaged outer membrane and periplasmic proteins that are involved in nutrient acquisition much like the *Ngo* TDTs (370). *Ngo* incubation with PMNs, however, showed differential regulation of *msrAB* upon exposure (362). Once again, the effects of TPEN on the Zur transcriptome seems increasingly important to understand separate from the defined media (CDM) low in metals used in this study. Further investigation of several of the oxidative response genes such as *norB* and *msrAB* and the effects of TPEN on the *Ngo* transcriptome will be essential and important in understanding the host specific environmental changes during a gonorrhea infection.

From the context of natural infection there are the innate differences in disease presentation and responses between men and women. One aspect being the asymptomatic presentations of gonorrhea in women. Even if symptoms were present, they tend to be mild and often go undetected until dissemination of disease into the upper genital tract and distal organs (371). The reason for greater incidence of asymptomatic infections in women as compared to men is poorly understood, but we can suspect anatomy, immune response differences and nutrient availability as some of the factors. The lower genital tract, the site of primary infection, is zinc enriched in men and acutely zinc starved in women. The mucosal epithelium surrounding the female vagina, produces S100A7 (Psoriasin) that acts to restrict zinc availability, thereby mimicking a CDM or TPEN condition of zinc starvation used in this study (327). Transcriptomic analysis of these two sites during natural gonococcal infection, showed differential expression of genes that also stood out in this RNA Seq, which included *tdfJ* (*ngo1205*), *norB* (*ngo1275*) and *msrAB* (*ngo2059*), once again emphasizing an oxidative-stress and zinc starved response in the female genital tract. Zur is a regulator of oxidative stress in *Ngo* and further characterization of the genes overlapping a zinc and oxidative stress response, from the context of natural infection such as neutrophil influx or simulant media (vaginal and semen simulants), will guide the understanding of potential antigens for a vaccine and targets for therapeutics in the treatment of gonorrhea.

CHAPTER 5 THE ROLE OF THE GLOBAL REGULATOR ZUR AS AN ACTIVATOR AND REPRESSOR OF GENE EXPRESSION IN *NEISSERIA*

I. INTRODUCTION

Zinc is an important transition metal for enzymatic reactions, protein functions, DNA damage repair or immune response modulations not just in eukaryotic biology, but also in prokaryotes (372). Zinc was found to be essential for the survival of several bacterial pathogens, where efficient zinc acquisition and zinc tolerance were necessary to maintain virulence and pathogenicity (338). This ability of zinc to promote pathogenicity has been demonstrated in *Pseudomonas aeruginosa* by aiding biofilm formation (373). To emphasize its role in bacterial pathogenicity, zinc is required for the functional activity of metalloproteases that aid in the breakdown of host physiological barriers during invasion (228). In this battle between the pathogen and host, the host in turn mobilizes zinc through zinc -sequestration and withholding by nutritional immunity and trafficking within immune cells to induce zinc toxicity. High zinc concentrations within phagocyting macrophages and neutrophils may lead to mismetallation resulting in loading zinc into non-zinc binding sites within bacterial proteins, thereby preventing appropriate function and inducing zinc toxicity (374).

Pathogenic *Neisseria*, *N. gonorrhoeae* (*Ngo*) and *N. meningitidis* (*Nme*) have both been shown to subvert neutrophil-mediated zinc toxicity and zinc restriction by scavenging zinc from the host nutritional immunity protein calprotectin, enriched within neutrophils (229, 265, 289). TdfJ and TdfH are outer membrane TonB-Dependent Transporters (TDT) that shuttle the zinc to the periplasmic membrane where a zinc shuttle periplasmic protein ZnuA transports the zinc to

the cytoplasm with the help of the ABC transport system (268). ZnuA can bind zinc with very high affinity and has been identified as an important virulence protein necessary for survival in several pathogens including *Escherichia coli*, *Yersinia pestis* and *Salmonella enterica* (321, 340, 375, 376). During zinc excess these zinc shuttle and import proteins are downregulated and membrane porins and efflux pumps are expressed to overcome zinc toxicity. These carefully orchestrated graded expression of different set of proteins and systems to maintain zinc homeostasis within pathogens is done through the zinc-sensing zinc uptake metalloregulator, Zur. In principle, Zur functions by sensing and binding to free intracellular Zn^{2+} that enables it to bind to DNA and regulate gene expression of target genes. In low intracellular Zn^{2+} levels, Zur is unable to bind DNA, which modifies the set of target genes expressed (282, 325). These target genes that Zur regulates form the Zur regulon and several such Zur regulons have been described in bacterial pathogens. In this chapter, we review the structural and biochemical properties of *Neisseria* Zur that allow it to function as a global regulator and the properties that distinguish it from other bacterial Zur and their regulons, based on available crystallography and phylogenetic information.

Ngo is the causative agent of the sexually transmitted infection gonorrhea and an urgent threat pathogen. *Ngo* primarily infects the male and female reproductive organs, and upon a lack of treatment, can lead to irreversible outcomes such as infertility (348, 377). With no effective vaccine available and an increase in the number of antimicrobial resistant strains, it is imperative to explore new targets for therapeutics and treatment. The importance of Zur in virulence has been iterated among several pathogens in recent years and given its regulation of several virulence genes in pathogenic *Neisseria*, Zur is a potential target for therapeutic strategies. *Nme*

and *Ngo* Zur share a 100% protein sequence similarity and drive regulation of a similar set of homologous genes. In this review, we delve into the sequence-based intricacies of *Neisseria* Zur, examining their hypothesized structural makeup, properties, and typical mechanisms of action. Furthermore, we provide a comprehensive analysis of the genes regulated, shedding light on the potential dual role of *Neisseria* Zur as a transcriptional activator.

II. RESULTS

A. Structural and Mechanistic Insights into Neisseria Zur and its Conservation Among Gram Negative Pathogens.

Zur is a FUR-family regulator that has shown to predominantly act as a transcriptional repressor upon Zn^{2+} binding by blocking RNA polymerase transcription initiation (325). Like other FUR-family proteins Zur binds to a specific region on the DNA known as a Zur box, that often overlaps the promoter region to repress transcription. This Zur box sequence is a conserved sequence and consists of a 23 or 15 bp palindromic repeat (352). The *Neisseria sp*. Zur box is made up of a 15 bp repeat with variation in 3 nucleotides in the middle: 5' TGTTATDNHATAACA 3' (282). Zur binding to Zn^{2+} alters its conformation and therefore aids in its binding to the Zur box. The Zur protein crystal structure has been determined in a few gram-negative pathogens including that of *E. coli* (341). Using x-ray crystallography, the structure of the *E. coli* Zur protein complexed with the *znuABC* promoter was determined (341). *E. coli* Zur binds DNA as a dimer of dimers (four Zur monomers) and consists of two distinct zinc-binding sites on each monomer. Each monomer is made up of a helix-turn-helix (HTH) motif in the N-terminal DNA-binding domain which is attached to a C-terminal dimerization domain via a characteristic

winged-helix motif (341). At present, there is no available crystal structure of *Ngo* or *Nme* Zur and structure prediction modeling platforms such as Alpha Fold (378, 379) make predictions for *Neisseria* Zur based on the *E. coli* Zur structure (Figure 10A).

We performed a structure-based alignment of the *Ngo* and *Nme* Zur with the *E. coli* Zur and 7 other structurally characterized Zur protein sequences from gram negative pathogens. The sequence alignment showed a high degree of conservation of two C-X-X-C sulfur-rich motifs characterized in *E. coli* Zur as the tight zinc-binding sites (Figure 10B)(341). In *E. coli* Zur, the CXXC zinc binding site has been shown to flank the dimerization domain, thereby stabilizing the Zur dimer formation upon Zn^{2+} binding. The second zinc binding site is thought to stabilize the DNA-binding conformation of Zur upon Zn^{2+} occupancy (341). *E. coli* Zur in complex with DNA (P_{znuABC}) was the first Zur to be crystallized with bound DNA. This structure has provided evidence on the Zur residues that interact with DNA (325, 341). Figure 1B highlights the residues involved in DNA binding and this appears to be conserved among majority of the Zur protein species from other bacteria.

a.

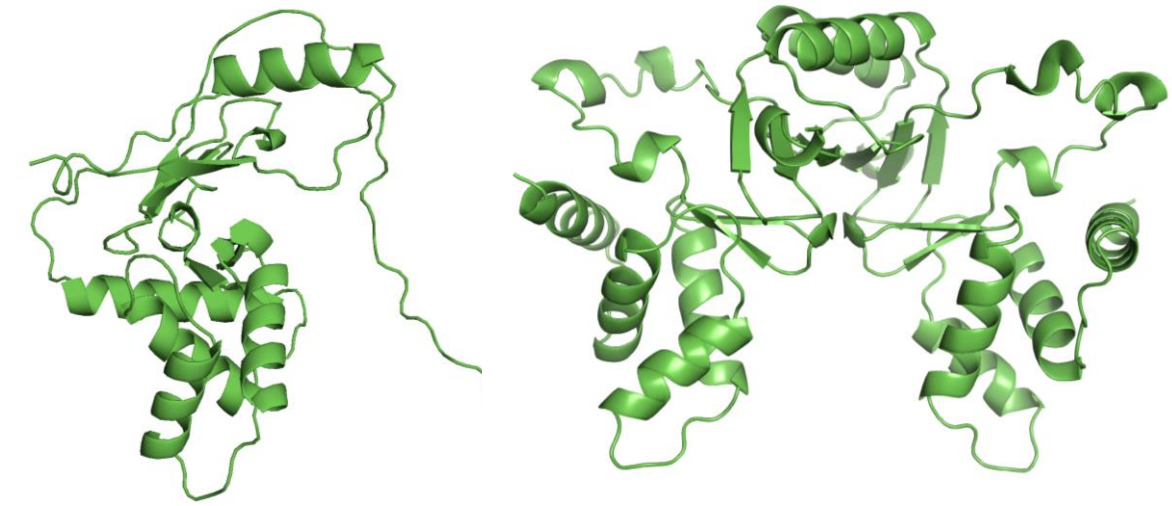

b.

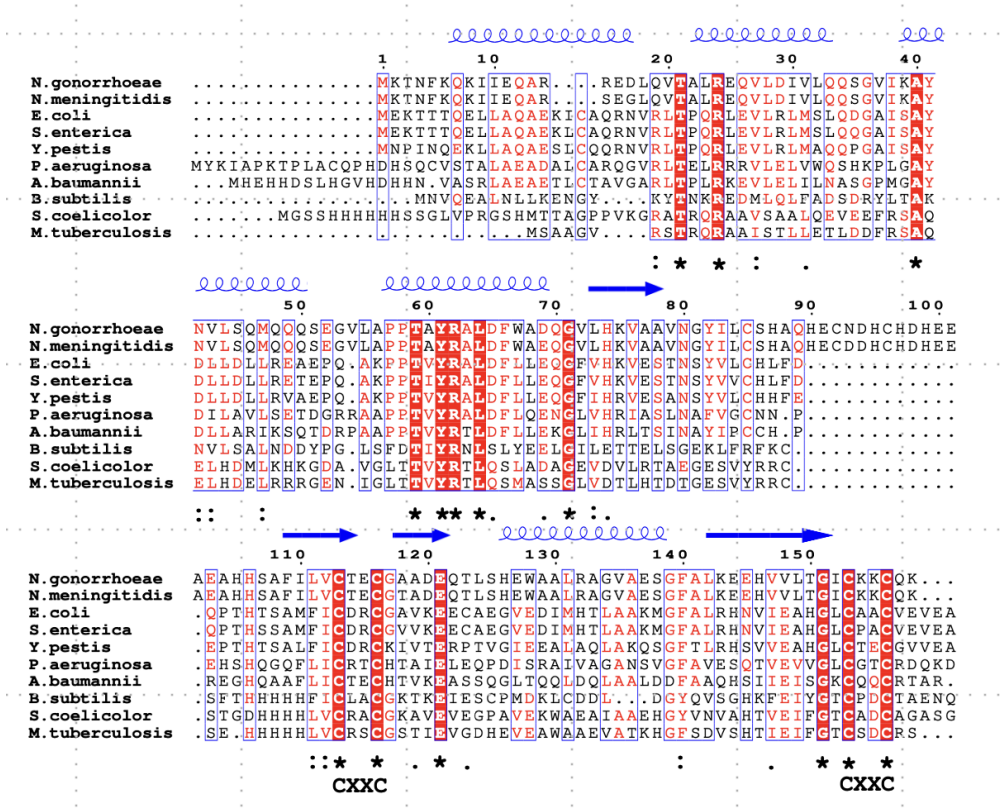

Figure 10. Predicted secondary structure and model of *Ngo* Zur

Figure 10. Predicted secondary structure and model of *Ngo* Zur. A) Alpha Fold DB predicted model of *Ngo* Zur monomer and homodimer based on the available *E. coli* Zur crystal structure (model created by Nunnally, N.S.). The residues unique to *Neisseria* Zur are highlighted in red in the drawing above the Alpha Fold model. B) A multiple sequence structural alignment of Zur sequences from bacterial pathogens and secondary structure predictions for *Neisseria* Zur, made with Clustal Omega. The conserved sequences are displayed in red and predicted α-helices and β-sheets drawn above in blue. ***** represents perfectly conserved residues while **:** and **.** represent well conserved residues.

B. Zur Box Consensus is Evolutionarily Conserved Across Pathogenic Bacteria

The protein sequence and structural similarities among the different Zur along with their ability to tetrahedrally co-ordinate Zn^{2+} also correlate with the DNA sequence (Zur box) recognized by different Zur. Phylogenetic analysis of the 10 Zur protein sequences analyzed in Figure 11, indicates how the Zur protein is distantly related in sequence identity. A study looking into the DNA binding sequence recognized by a functional Zur monomer in γ- proteobacteria, identified a 23 base pair palindrome of GAAATGTTAT-AWT-ATAACATTTC (352). Despite evolutionary and phylogenetic differences, the DNA-binding regions of these Zur proteins appear to have remained conserved.

Zur-DNA interactions are highly cooperative in most characterized Zur proteins and are thought to occur in two consecutive steps. WT *E. coli* Zur was found to consistently bind to the DNA duplex as a dimer and no intermediates of a single monomer bound to the DNA (341). The coordination for this mechanism involves a $(Zn_4{:}Zur_2)_2$ conformation, which refers to the tetrahedral coordination of Zn^{2+} by Zur. The first step involves a partially active state of a dimer of Zur bound to DNA and the final formation of the dimer of dimers for active repression, which presents the dissociation constant Kd for Zur. This cooperative binding has been partially observed for *Ngo* Zur binding to $P_{ngo1049}$ in preliminary DNA binding ELISA assays, with a purified form of recombinant His-tagged Zur bound to Zn^{2+} as $Zn_4{:}Zur_2$ (Data not shown)

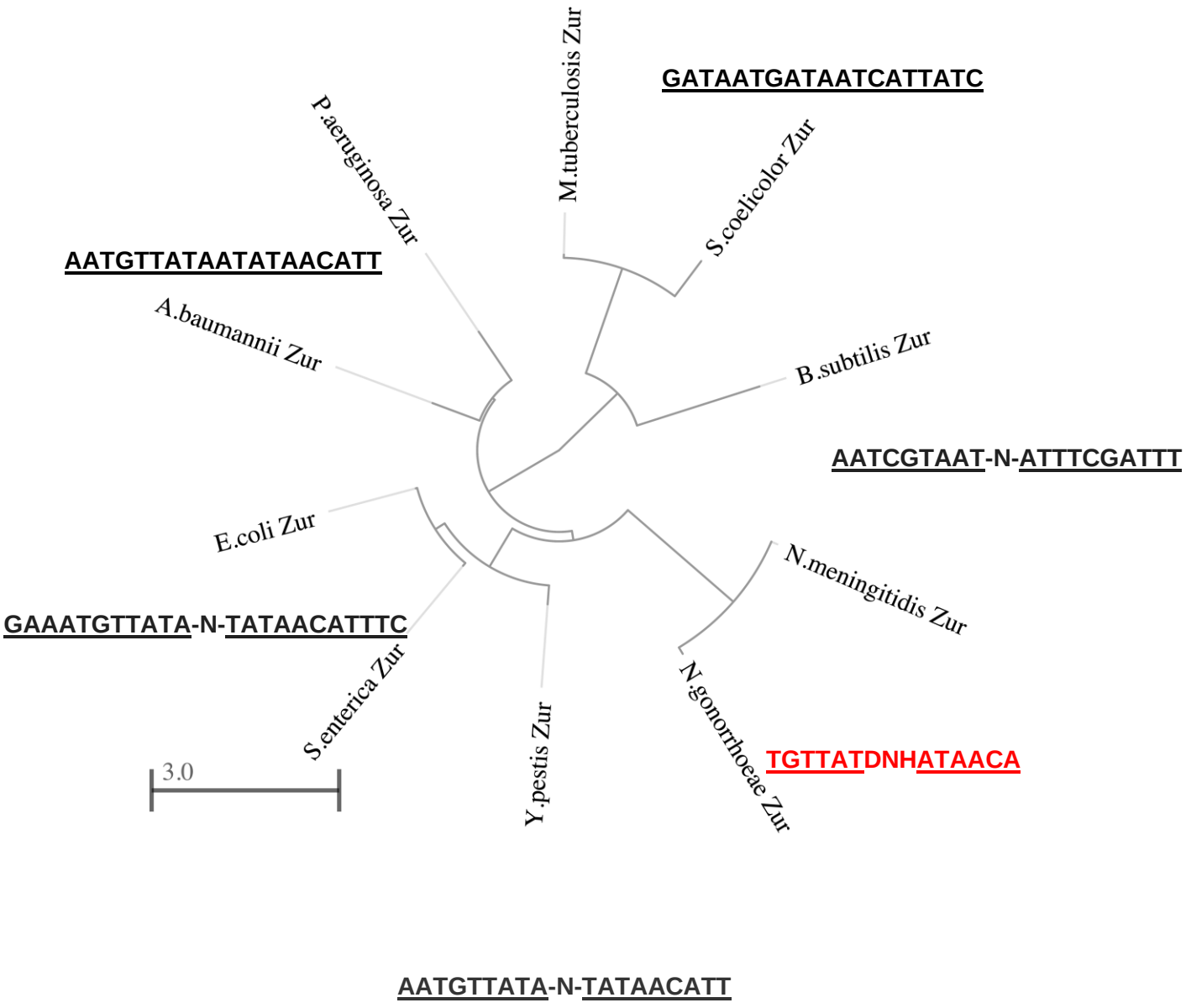

Figure 11. Evolutionary relationship among different Zur and their conserved Zur boxes

Figure 11. Evolutionary relationship among different Zur and their conserved Zur boxes. A circular tree showing grouping among proteobacteria from a multiple sequence alignment of their Zur protein sequence. The conserved Zur box consensus identified by each group on the target promoters is bolded and underlined for each closely related group of Zur. Zur consensus identified by *Neisseria* Zur is shown in red. Phylogenetic analysis was conducted in COBALT-NCBI.

C. Beyond the Role of Zur as a Repressor of Gene Expression- Mechanisms of Activation

The zinc-dependent Zur transcriptome of both *Ngo* and *Nme* Zur have identified Zur to behave primarily as a repressor of gene expression (282, 380). The Zur regulon of *Nme* consists of 17 genes of which 15 are Zur-repressed by zinc. The Zur regulon of *Ngo* consists of 18 genes that are Zur-repressed of the 26 differentially regulated by zinc (285). The remaining 2 genes of the *Nme* Zur and 8 genes of *Ngo* Zur were activated in the presence of zinc by their respective Zur proteins. This activation by a FUR family protein is increasingly being recognized in bacterial regulatory networks. Some factors that allow a repressor to activate gene expression include the location of the conserved regulatory/ consensus sequence with respect to the promoter, indirect activation in the form of repression of a secondary regulatory element and the activation signal.

An activator that activates via direct contact with RNA polymerase binds either upstream or overlapping the -35 promoter element on the target DNA (381-383). In *Ngo*, a direct mechanism of activation by the Ferric uptake regulator (Fur), among genes of the Fur regulatory network has been studied. *Ngo* Fur has been shown to bind directly to Fur-box consensus sequences found on the upstream region of at least six of the Fur-activated genes, including *nspA*

encoding for an outer membrane protein and *bfrA* that encodes for an iron storage protein bacterioferritin (277, 328). *nspA* has also been shown to be Fur-activated in *Nme* and *Nme* NspA has shown clinical significance in the vaccine development against meningococcal disease by eliciting an antibody response and protection against serogroup A, B and C (384).

The Genco study on mechanisms by Fur activates gene expression in *Ngo*, also noted that the Fur-box consensus sequence that Fur bound to for activation was not well conserved among the Fur-activated genes unlike the consensus Fur box for Fur repression, which was a well conserved 19 bp inverted repeat sequence (281, 385, 386). For the known Zur-activated genes in *Neisseria*, however, a well conserved 15 bp inverted repeat sequence that matches the Zur-box for repression was observed. The direct binding of Zur to these Zur-activated promoters have, however, not yet been demonstrated *in vitro* through binding assays. *Neisseria adhP* was the most highly Zur-activated gene in both *Ngo* and *Nme* and contains a Zur-box upstream of its -35 promoter element, suggesting a possible direct interaction with RNA polymerase for transcription initiation (282, 285).

The direct mechanism of activation by Fur described above is much less understood compared to the activation that involves occlusion of a repressor from binding, thereby initiating transcription. An example of this mechanism has been studied in the Fur-mediated activation of *Neisseria norB*, where the Fur-box overlaps the binding of another repressor AsrR. The binding of Fur to the Fur-box competes with ArsR binding, thereby resulting in de-repression of *norB* (333, 360). In *Ngo*, the Fur-box is located further upstream of the -35 region. Interestingly, *Ngo norB* is also activated by Zur in the presence of zinc (285). The *norB* promoter consists of a putative Zur-box just downstream of the predicted Fur-box, but upstream of and overlapping the -35 region

(285). This suggests a possible mechanism for Zur activation involving competition with the ArsR repressor, depending on the environmental signal. Due to its proximity to the -35 promoter element, it is possible Zur would also employ a direct mechanism by recruiting RNA polymerase to activate *norB* expression when the ArsR repressor is absent.

A third classical mechanism of indirect activation of gene expression can occur via repression of a negative regulator such as with small RNAs (sRNAs). This has been studied in both *Ngo* and *Nme*, where an sRNA *nrrF* is repressed by Fur, which in turn activates the genes *sdhA* and *sdhC* that were repressed by *nrrF* (387, 388). This mechanism has been studied in several other bacteria for Fur-mediated indirect activation including the repression of sRNA *rhyB* of *E. coli* and *Vibrio cholerae* and *prrF* of *P. aeruginosa* (286, 389-391). This form of indirect activation is less understood involving Zur; however, such a process cannot be discounted as RNA Sequencing analysis have revealed the presence of Zur regulated sRNAs in both *Ngo* and *Nme* (282, 285).

A structural mechanism for Zur-mediated activation has been evaluated in *Streptomyces coelicolor* Zur (ScZur). Crystal structure of ScZur bound to promoter DNA and RNA polymerase, was evaluated via structural and biochemical assays and found that ScZur oligomers cooperatively bind promoter DNA as a trimer of dimers and activates transcription via direct contact with RNA polymerase subunit (392). This study provides a framework for understanding activation of gene expression for not just Zur, but also other global regulators and will be necessary to explore in *Neisseria* as well.

D. Neisseria Zur is Not Self-regulated and is Transiently Expressed Under Zinc Restriction

Ngo zur was not found to be differentially regulated in the WT in the presence of zinc or TPEN from RNA seq analysis (285). However, differential regulation of *zur* was seen in the WT when grown in in a chemically defined medium that was chelex-treated to remove metals including zinc. This observation signifies that *Ngo zur* does not self-regulate itself and is instead regulated by another indirect and unknown mechanism to tightly maintain zinc homeostasis. In several bacteria, *zur* is known to autoregulate itself and this comes down to its location on the chromosome. In *Bacillus anthracis*, *P. aeruginosa*, *Y. pestis* and *S. aureus, zur* is in a polycistronic operon with *znuB* and *znuC* which is a part of the *znuABC* transport system, which is an essential zinc import machinery for the bacteria's survival (393-396). This proximity to the promoter of an ABC transporter allows zur to autoregulate its expression to allow strict control of zinc import and export and maintaining zinc homeostasis in these systems. However, in *Ngo* and *Nme* and other pathogens including *E. coli*, *B. subtilis*, *S. coelicolor* and *A. baumannii*, *zur* has its own promoter (monocistronic) and is not transcribed through a polycistronic operon (340, 343, 397-399). The *Ngo zur* promoter contains a Zur-box that is about a 50% match to the consensus and no other obvious regulatory sequences were found upstream that would regulate the expression of *zur*. It is possible that regulatory small RNAs play a role in shutting off and expressing *zur* in response to stimulus post-transcriptionally.

In *E. coli K-12*, *fur* is negatively regulated by the small RNA *ryhB* where RyhB inhibits the translation of *fur* under iron-rich conditions (400). This counterbalances the synthesis of *fur* mRNA by metalated Fur, keeping Fur translation steady under low iron conditions, never lagging. At present Zur-regulated small RNAs have been identified in *Neisseria*, however their role in

mitigating the zinc load in the cell is unknown, even in other bacterial pathogens. It is not evident if Zur bound to excess molar concentrations of zinc binds to itself to shut off expression and stays transcribed at low zinc levels. Upon comparing the *zur* expression in *Ngo* WT under excess zinc and CDM alone conditions, there is an increase in the $\log_2$ fold-change, however, this was not significant. Further experimental analysis is needed on the role of this transient expression of *zur* and is necessary for understanding its pathological significance in disease.

E. Apo-Zur Regulation and Biochemical Properties of Metal Selectivity of Neisseria Zur

As described previously, the structural basis of Zur regulation has been elucidated by x-ray crystallography of metal ion bound holo-Zur (active) form. Crystal structures of this zinc-bound Zur have been determined in *E. coli*, *S. coelicolor* and *M. tuberculosis* and all of these structures contain at least 3 zinc-bound sites on Zur (341, 392, 401). There is little-to-no evidence on the existence of an apo-form of Zur that regulates expression unlike other FUR family regulators like Fur that have shown to regulate gene expression even in the absence of metal binding (281). In *Helicobacter pylori* and *Vibrio vulnificus*, apo-Fur has been characterized to repress and activate gene expression respectively (402, 403). In the absence of iron, apo-Fur was shown to bind to the -10 and -35 regions to occlude RNA polymerase binding and therefore inhibit transcription. Whereas, in apo-Fur activation, the dimer was demonstrated to bind upstream to recruit RNA polymerase for induction (402, 403). In both of these cases apo-Fur forms a dimer to regulate gene expression. In the case of Zur, however, dimer formation has not been seen in the absence of metal ion. Recombinant purified *Ngo* Zur has been found to be unstable in laboratory conditions in the absence of zinc ions. Zur is stabilized after purified by supplementation with zinc in the dialysis buffer. Apo-Zur forms have been analyzed for regulatory

activity in *B. anthracis* and *S. coelicolor* Zur, and in both bacterial pathogens the apo-Zur is incapable of DNA-binding (393, 404). It is therefore unlikely that apo-Zur regulation is possible in *Neisseria*.

Neisseria Zur is expected to bind Zn^{2+} specifically in its structural and regulatory sites from the mutisequence alignment and modeling data (Figure 10). EMSA experiments with *Nme* Zur on Zur regulated promoters have shown that binding occurs only in the presence of Zn^{2+} (282). Similar selectivity has been shown in Zur from *Paracoccus denitrificans* and *Brucella abortus* (405, 406). However, Zur from *Corynebacterium glutamicum* and *Mycobacteria tuberculosis* have made Zur-DNA complexes in the presence of Mn and Cd (407, 408). *Ngo* Zur, also known as PerR, was identified as a Mn regulator, that allows Mn import through *znuABC* in *Ngo* 1291(354). However, preliminary RNA sequencing analysis, was inconclusive for Mn regulation of *znuABC* by *Ngo* FA1090 Zur (data not shown). Therefore, it is possible that metal selectivity of Zur in *Neisseria* is not conserved and is strain specific.

F. Physiological Significance of Zinc Availability and Zur in Pathogenesis

Zinc is the second most abundant transition metal in the host at 2 to 4 grams distributed throughout the body (409). However, during inflammation and infection the bioavailability of zinc drops as part of host induced nutritional immunity (410). This host-mediated zinc restriction is both cell-mediated and extracellular. The cell-mediated zinc restriction occurs through zinc transporters expressed by immune cells such as ZIP8 that restricts the lysosomal Zn^{2+} levels for pathogens phagocytosed (411). Extracellular restriction is carried out through S100 proteins, such as Psoriasin and Calprotectin which are enriched within cells and epithelial mucosal

surfaces, which are predominant sites of infection and pathogenesis (412). The mobilization of zinc during pathogenesis is done not just to restrict the zinc availability, but to also to overload the bacterial cells with zinc imparting zinc toxicity. This host-mechanism of combating intracellular pathogens is especially seen in immune cells such as PMNs and neutrophils that are enriched in zinc and trap pathogens in neutrophil extracellular traps (346). This makes zinc regulation and homeostasis in pathogens extremely important for survival. Bacteria, including *Neisseria,* employ strictly controlled strategies to overcome zinc toxicity and restriction by regulating the genes in response to zinc availability (282, 289). Zn-dependent regulation involves the zinc uptake regulator, Zur, which has been increasingly implicated as a global regulator that not only regulates genes essential for maintaining zinc homeostasis but also crucial in the regulation of virulence genes in several bacterial pathogens. Zur therefore, is essential for maintaining the survival of pathogens within the host. An example of this regulation in *Neisseria* is Zur regulation of virulence genes encoding for TDTs that are important vaccine antigens for the prevention of both gonococcal and meningococcal disease (229, 266, 289, 304, 322, 329). Zur regulates the expression of *tdfH*/*cbpA*, *tdfJ*/*znuD* which are essential for overcoming zinc restriction imposed by calprotectin and psoriasin respectively (229, 322). Zur also regulates the expression of *znuABC*, and *znuA* has been demonstrated to be essential for *Neisseria's* survival within the host, where a *znuA* mutant has a survival defect in epithelial cell infections (285, 321, 380). Zur performs several moonlighting functions in other bacterial pathogens; in *Salmonella typhimurium*, Zur was found to be necessary for regulating invasion genes such as *filAZ* and disruption of Zur in the *zur* mutant lead to a 50% increase in the lethal for mice infections (376, 413). Similarly, in uropathogenic *E. coli*, Zur was shown to repress the expression of the *hlyCABD*

operon which encodes for the important virulence factor α-hemolysin (414). A *zur* mutant in *Acinetobacter baumannii* was unable to cause a disseminated pneumonia infection in a mouse model, including the failure to upregulate several secreted proteins and virulence factors (398).

III. CONCLUSION

Zur is a major zinc sensing protein in both gram negative and gram-positive bacterial pathogens and primarily functions to sense both intercellular and extracellular zinc and to regulate genes in order to maintain zinc homeostasis and prevent metal toxicity. The peptide sequence of Zur is conserved among pathogens investigated, with similar residues coordinating DNA binding and dimerization (Figure 10). Protein structure modeling has allowed prediction of sensory zinc binding sites for *Neisseria* Zur that lacks a crystal structure at present. The Zur-box recognized by Zur for DNA binding is also evolutionarily conserved among these pathogens and allows Zur to either repress or activate gene expression. The localization of the Zur-box on the promoter of Zur-regulated genes, along with the ability of the protein to multimerize at high zinc concentrations, appear to determine whether Zur functions as a repressor or an activator similar to other regulators. Zur metal specificity in *Neisseria* appears to be restricted to Zn^{2+} and DNA binding occurs only upon zinc binding. With the absence of autoregulation of Zur in *Neisseria*, the molecular mechanisms involved in regulating Zur need to be identified. This is especially important as we have highlighted the crucial role Zur plays in virulence. There is much to be understood on the molecular structure and dynamics of Zur regulation and this study provides a microscopic view on Zur ‘s multifaceted role in pathogenic *Neisseria*. Due to its role in the regulation of several virulence genes, Zur is an attractive candidate for antimicrobial and therapeutic targets. Antimicrobial peptides and small molecule inhibitors have been developed

against Fur in *E. coli* and these small peptide inhibitors show a reduction in IC_{50} levels in a fly infection model (415). Given the rise in the number of antibiotic resistant strains of *Ngo*, and the lack of an effective vaccine, it is imperative to seek other strategies for therapeutics. These anti-peptide inhibitors are a novel approach and can be applied to Zur to be used in the treatment of gonococcal and meningococcal infections.

CHAPTER 6 SUMMARY AND PERSPECTIVES

Neisseria gonorrhoeae (Ngo), the causative agent of the sexually transmitted disease gonorrhea, is a public health concern and has evolved with the host for centuries, dating as far back as 1550 BC (416). It is not surprising that *Ngo* have adapted so well to their only host, humans; *Ngo* successfully evade immune clearance and don't elicit immunological memory (417). The number of cases has only been rising over the years, with an estimated 106 million cases reported each year across the globe (418). Prior obstacles of identifying effective vaccine antigens against *Ngo*, have left antibiotics as the only option to combat uncomplicated gonococcal infections. However, strains have emerged with increasing resistance to all available classes of antibiotics ranging from sulfonamides to cephalosporins, currently leaving only a single dose of ceftriaxone for treatment (348, 419). Soon we will be faced with untreatable gonorrhea unless alternate strategies for identifying effective vaccine antigens to prevent gonorrhea are developed. Due to the high incidence of disease and the dwindling treatment options, the World health Organization (WHO) has elevated *Ngo* to the status of an urgent threat and a high priority pathogen. This status calls for more research into therapeutic options and vaccine development, and a greater vigilance on the correct use of antibiotic therapy (420). TonB-dependent outer membrane transporters (TDTs) have received much attention in the recent past and fit the bid as effective vaccine targets. Not only are they well conserved across all gonococcal strains, but they are also not antigenically variable, surface exposed, and some are essential for nutrient acquisition and bacterial survival (421). In *Ngo*, these TDTs are essential proteins in maintaining transition metal homeostasis within the bacterial cell. In the gonococcus they function through

metal piracy to hijack iron and zinc from host nutritional immunity proteins overcoming metal limitation (268).

In our study, we focused on zinc limitation at the host-pathogen interface and the regulatory pathways involved in maintaining zinc homeostasis. The zinc import TDTs have been characterized in *Ngo* as TdfH and TdfJ which bind to their host ligands calprotectin (S100A8/A9) and psoriasin (S100A7), respectively, to extract the bound zinc (289). This zinc is then shuttled across the periplasm and through the cytoplasmic membrane via an ABC transporter (ZnuABC) (290, 322). The expression of the genes in response to zinc concentration is controlled by the Zinc uptake regulator (Zur) in *Ngo*. Here we show that *Ngo* Zur regulates gene expression by binding to specific conserved sequences within the promoters of *tdfH*, *tdfJ* and *znuABC* to repress expression in the presence of intracellular zinc. This conserved sequence is a 15 base pair inverted repeat of TGTTAT-DNH-ATAACA which appears to be conserved between both pathogenic *Neisseria* species (282). Previous studies in both *Nme* and *Ngo* have recognized that several virulence genes are differentially regulated in response to zinc and oxidative stress and controlled by Zur, also referred to as PerR in relation to regulation in response to Mn concentrations (282, 354).

Zur from *Escherichia coli*, *Acinetobacter baumanii*, *Pseudomonas aeruginosa*, *Bacillus subtilis*, and others, regulates the expression of genes; the absence of Zur can be detrimental to growth and survival due to oxidative stress from zinc toxicity (340, 343, 368, 398, 422). We characterize the Zur regulon in *Ngo* and identified 26 genes that were differentially regulated between a wildtype strain FA1090 and a *zur* mutant strain. We found that Zur, in addition to functioning as a repressor, is also able to activate certain genes under high zinc environments.

Among the several regulators known to function as a master regulator to both repress and activate is the Ferric uptake regulator (Fur) (281). Fur is primarily a repressor of gene expression and upon iron binding, dimerizes on target promoters at the consensus Fur-box region to repress expression (423). Fur also functions to indirectly repress gene expression which involves small RNAs like RhyB (424). The *rhyB* homologue *nrrf* in *Ngo* is repressed under iron-replete conditions, thereby allowing Fur to indirectly activate genes, however in the absence of iron *nrrf* represse Fur activity, finetuning mRNA turnover (425). The sequence to which Fur binds when upregulating gene expression is not well conserved and is less specific, spanning about 30 bp (328, 330). Upon analysis of the global regulatory circuit of Zur in our RNASeq dataset, we found that *Ngo* Zur, binds to the same conserved sequence on target promoters when acting as an activator or repressor of gene expression. The signal for activation versus repression, appears to be dependent on the localization of this conserved Zur box with respect to the -35 and -10 promoter elements. Our RT-qPCR analysis of zinc- and Zur-dependent gene expression showed that among the TDTs, *tdfJ* demonstrated high fold-changes for expression while also having a 100% match to the *Ngo* Zur box consensus, which was corroborated by the Western blotting analysis. TdfJ protein production directly correlated with the gene expression data with TdfJ only found under zinc deprivation conditions (380).

Ngo TdfJ, and the homologous protein in *Neisseria meningitidis* (*Nme)* ZnuD, has potential as an important vaccine antigen (266). Disruption of the ability to acquire zinc from S100A7 via TdfJ resulted in a survival defect in *Ngo* (304, 329). The same study found that TdfJ expression in defined media low in both iron and zinc was further enhanced upon addition of excess iron. The same increase in protein production upon addition of excess iron to the zinc restricted media was

observed for *Nme* ZnuD (332). The dual regulation of TdfJ is significant from the context of site of infection. The gonococcus is faced with varying levels of transition metals as it infects different mucosal surfaces within the host. For instance, when Ngo enter the urogenital mucosa in men, the cells are faced with a zinc-enriched environment due to the abundance of zinc in the seminal fluid (426). This would suggest Zur repression of zinc import genes, including TdfJ, TdfH, and ZnuABC. However, in the female genital tract, the mucosal epithelium lining the ecto-cervix, is enriched in calprotectin and S100A7, zinc restricting nutritional immunity proteins (327, 427, 428). Additionally, cervical secretions are also abundant in calprotectin and S100A7, leaving the female genital mucosa a zinc deprived environment, requiring the use of the TDTs TdfH and TdfJ for zinc acquisition. Therefore, in this zinc-limited environment, Zur is expected to de-represses the promoters of these TDTs to enhance protein production. Further, the female genital tract can also be iron rich when the endometrium sheds during menstruation, allowing iron availability to the gonococci. This culminates with the possibility for the female genital tract to be both Zinc-starved and iron enriched, much like the observation for iron induced expression of *tdfJ*. Preliminary studies in the lab have shown indications for the ability of TdfJ to also aid in invasion of epithelial cells, especially ME180 cells that line the ecto-cervix (data not published) (429). Taking together the dual regulation and invasion capabilities of TdfJ, we characterized the *tdfJ* promoter in response to iron and zinc to understand the molecular mechanism behind this regulation (56).

Based on the iron-induction data, it was hypothesized that *tdfJ* is dually regulated by iron and zinc, being induced through regulation by Fur-Fe^{2+}, and repressed by Zur:Zn; however, prior characterizations of this mechanism by measuring gene expression of *tdfJ* in a WT and *fur* mutant

strain were not fruitful due to the lack of a complete *fur* deletion mutant of *Ngo* FA1090 (284). In *Ngo* F62, this Fur activation of *tdfJ* was verified by DNA-binding EMSAs, which recognized a large fragment upstream on the promoter, about 300 bp in length, while failing to determine a binding affinity of Fur for the *tdfJ* promoter (328). We characterized the promoter elements of *tdfJ* and mapped the +1, -10, -35 regions and the Zur box. Based on computational RNAseq analysis of differentially iron regulated genes, we determined the Fur box consensus in *Ngo* FA1090 for iron regulation. Using this information, we were able to map two regions on the *tdfJ* promoter with potential Fur-binding activity, one upstream of the -35 region and one overlapping the Zur box. Through DNA binding ELISAs we determined the binding affinity (K_D) for Fur binding to the *tdfJ* promoter. We also analyzed the specificity of Fur for the two Fur box regions and found that the Fur box 1, the region upstream the -35, had the most substantial impact on binding when the region was disrupted. This is the first study to determine the Fur-box consensus, and its location on the *tdfJ* promoter, in *Ngo* FA1090. Although, disruption of Fur-box 1 had the greatest fold-change for binding, disruption of Fur-box 2 showed a significant reduction in Fur binding as well.

Through this study, we have uncovered a clue into the mechanism by which Fur regulates gene expression, which may include weaker binding during induction of expression, and may not be as sensitive to the recognition of the exact consensus Fur box. Due to the unstable properties of the reduced form of iron in the Fe^{2+} state, we tested a more stable Fur: Mn^{2+} for Fur for binding experiments (430). Zur on the other hand is known to bind the Zur box with high specificity and only in the presence of Zn^{2+} ions as seen in *Nme* Zur binding EMSAs (282). Future experiments will involve characterizing the *Ngo* Zur binding affinities and specificity for the *tdfJ* promoter.

Direct interaction of both Fur and Zur should also be tested using EMSAs or Surface Plasmon Resonance (SPR) techniques to investigate how the two regulators act to dually regulate *tdfJ* expression. Crystallization of *Ngo* Zur will also determine the important Zn-binding residues and a co-crystal structure with DNA, will reveal essential DNA-binding residues. At present, the coordination by *Ngo* Zur is not well understand, but we can make informed conclusions from available literature and secondary structure alignments that Zur tetrahedrally coordinates zinc in Ngo and binds DNA as a dimer of dimers. This has been determined in the case of *E. coli* Zur that was co-crystalized with promoter DNA (341). This information will be crucial for *Ngo* Zur regulation of *tdfJ* and will inform us of the possibility of stearic hinderance if Fur coordinates iron and tries to bind the *tdfJ* promoter simultaneously.

The scope of this study extends beyond the dual regulation of *tdfJ* and provides fruitful information for vaccine and therapeutic development. Structure and function-based characterization of the gonococcal vaccine candidate TdfJ, show specific loops and loop residues within TdfJ are necessary for binding to human S100A7 and acquisition of zinc. Proline mutations were especially significant in generating TdfJ non-binding mutants. Non-binding TdfJ may be more visible to immune cells, because it is not masked by S100A7 and, therefore elicit adaptive immune response to an infection and develop immunological memory (431). This was first demonstrated in *Heamophilus parasuis* and the effectiveness of non-binding transferrin binding protein TDT, TbpA (431). Similar efforts have since been carried out for gonococcal transferrin binding TDT, TbpA (366), which is currently being tested in a transgenic mouse model of infection. An observation detail that stemmed from the TbpAB and TdfJ characterizations is the conservation of an extracellular loop that appears to be the most important for human ligand

interactions signifying an evolutionary adaptation in gonococci, however this is not necessarily true for all TDTs (304). The effectiveness of TdfJ has been evaluated in preliminary experimental lower genital tract infection studies where hybrid loop antigens of TdfJ generated cross-reactive antibodies with specific identifiable functions (329). These studies will be further evaluated in transgenic S100A7 mouse models of infection for promise in generating correlates of protection against gonorrhea. Monoclonal antibodies with blocking function against TdfJ have also showed great promise as a therapeutic and treatment option (Stoudenmire, J., unpublished data).

Our *tdfJ* promoter characterization combined with the functional studies on the effectiveness of TdfJ as a vaccine antigen together iterate the importance of this TDT. Owing to the dual control of the *tdfJ* promoter, P_{tdfJ} holds the potential to be an important molecular tool in evaluation of the sites of colonization for metal restriction. A reporter using the *tdfJ* promoter, could be useful in visualization of cellular metal content in animal models of infection with *Staphylococcus aureus* (432). A reporter constituting the *tdfJ* promoter that holds both its upstream Fur and Zur elements, would be powerful in investigating the difference in nutrient availability, specifically iron and zinc availability, between a male and female urogenital tissue in experimental transgenic mouse models of infection. Some questions that may be answered with these *tdfJ* reporter studies would be whether TdfJ plays specific roles in infections between men and women and whether TdfJ is an invasin and how it adapts or influence pathogenesis in the female reproductive tract, prone to asymptomatic infections. At present experimental evidence indicates only TdfF, a TDT with an unknown ligand and thought to import iron, is essential for intracellular survival in ME180 cervical epithelial cells (267). Re-evaluation of these studies by incorporating what we have identified from the context of zinc-restriction may change the

outcome. A study focusing on differential expression of genes from male and female patients with gonococcal infection showed that TdfJ was differentially expressed in women, highlighting our framework for prospects of *tdfJ* reporter studies (361).

The main obstacle for vaccine development strategies in *Ngo* is whether protective immunity and memory can be achieved from immunizations with promising TDTs. *Ngo* is a facultative intracellular pathogen, and it readily skews immune response towards an innate response rather than an adaptive one. This process involves immunomodulatory effects of the gonococcus which include IL-10, TGF-β and Type 1 T_{reg} dependent suppression of Th1 and Th2 T cell development (70, 130). Other factors contributing to immune evasion include NLRP3 dependent apoptosis of antigen presenting cells, induced by gonococci and inhibition of B-cell proliferation upon *Ngo* opa binding to CEACAMs (129, 433). This would be one area to explore to ensure development of TDT vaccines that can overcome these obstacles and induce immunological memory. It is also essential to note that several TDTs expressed by Ngo import the same nutrient, that is TbpA, HpuB, LbpA, TdfF, FetA all import iron, while both TdfH and TdfJ import zinc within the same strain, causing potential redundancy between these systems when only a single TDT is targeted. This was demonstrated in the sufficiency of lactoferrin utilization in the absence of TbpA (252). It is therefore necessary to expand characterizations to multiple *Ngo* TDTs for establishment of long-term protection. It is also important to remember that different metal sources may be available at different locations. Therefore, targeting something that is only localized in one infection site, will not protect at a different infection site, will not protect at a different infection site.

The effectiveness of a gonococcal vaccine hinges on various factors such as method of delivery, the target demographic and timing of vaccination. Clinical trials would be one way to provide valuable information on effective vaccine combinations, routes of delivery, etc. Moreover, initial recipients of the gonococcal vaccine would play a pivotal role in shaping the trajectory of disease incidence. For example, a recent study utilizing a site-specific mathematical model predicted that immunizing 30% of a population of 10,000 men who have sex with men (MSM) could result in a 62% reduction in disease prevalence within a span of 2 years (434). The vaccine efficacy was estimated at 50% or 94% reduction with a fully protective vaccine. This study also suggested that with access to vaccine boosters, gonorrhea could potentially be eradicated provided the vaccine maintains a 50% efficacy or higher, with long-term protection of at least 2 years. These findings underscore the significant impact even a moderately protective vaccine can have when strategically implemented and reduce the burden of gonorrhea. The timing of administration would require focus on the disproportionate disease incidence rate among young adults in the age group of 15-24 years. However, with recent focus on anti-vaccination groups and policies in the light of the COVID-19 pandemic, evaluation of vaccine acceptance is necessary to the successful roll out and precise predictions for gonococcal vaccines.

In summary, this study on *tdfJ* regulation in response to both iron and zinc and its differentially expression in female gonorrhea patient samples, provides a clue for its possible role in infecting the female reproductive tract. This is crucial information and shows the potential for *tdfJ* to be a molecular tool to help assess the bioavailability of iron and zinc or both in various niches. This will certainly expand our understanding towards vaccine development strategies from the context of nutrient availability and possible targets for an effective gonococcal vaccine.

TdfJ has demonstrated superior quality in its potential to be a vaccine antigen itself and future transgenic mice experiments will shed light on the immunological determinants to consider for long-term protection from gonorrhea. Apart from TdfJ, we have showed in this study that Zur is a master regulator controlling the expression of several virulence and oxidative stress response genes essential for survival of *Ngo* within neutrophils, macrophages, and zinc deprived environments. Blocking the function of Zur using small molecule peptides has a potential role as a therapeutic and added function in along with a vaccine to effectively combat and prevent the spread of gonorrhea. Further understanding the role of TdfJ and NorB in contributing to asymptomatic gonorrhea infections in women is crucial, which may aid in the development of effective detection and treatment of infection in women.

REFERENCES

1. Rossau R, Vandenbussche G, Thielemans S, Segers P, Grosch H, Göthe E, Mannheim W, De Ley J. 1989. Ribosomal Ribonucleic Acid Cistron Similarities and Deoxyribonucleic Acid Homologies of Neisseria, Kingella, Eikenella, Simonsiella, Alysiella, and Centers for Disease Control Groups EF-4 and M-5 in the Emended Family Neisseriaceae. International Journal of Systematic and Evolutionary Microbiology 39:185-198.
2. Rossau R, Van Landschoot A, Mannheim W, De Ley J. 1986. Inter- and Intrageneric Similarities of Ribosomal Ribonucleic Acid Cistrons of the Neisseriaceae. International Journal of Systematic and Evolutionary Microbiology 36:323-332.
3. Harmsen D, Singer C, Rothgänger J, Tønjum T, de Hoog GS, Shah H, Albert J, Frosch M. 2001. Diagnostics of neisseriaceae and moraxellaceae by ribosomal DNA sequencing: ribosomal differentiation of medical microorganisms. J Clin Microbiol 39:936-42.
4. Morse SA. 1996. Neisseria, Moraxella, Kingella and Eikenella. *In* Baron S (ed), Medical Microbiology. University of Texas Medical Branch at Galveston

5. Johnson AP. 1983. The pathogenic potential of commensal species of Neisseria. J Clin Pathol 36:213-23.
6. Platt DJ. 1976. Carbon dioxide requirement of Neisseria gonorrhoeae growing on a solid medium. J Clin Microbiol 4:129-32.
7. Knapp JS. 1988. Historical perspectives and identification of Neisseria and related species. Clin Microbiol Rev 1:415-31.

8. Cartwright KA, Stuart JM, Jones DM, Noah ND. 1987. The Stonehouse survey: nasopharyngeal carriage of meningococci and Neisseria lactamica. Epidemiol Infect 99:591-601.

9. Liu G, Tang CM, Exley RM. 2015. Non-pathogenic Neisseria: members of an abundant, multi-habitat, diverse genus. Microbiology (Reading) 161:1297-1312.

10. Caugant DA, Høiby EA, Magnus P, Scheel O, Hoel T, Bjune G, Wedege E, Eng J, Frøholm LO. 1994. Asymptomatic carriage of Neisseria meningitidis in a randomly sampled population. J Clin Microbiol 32:323-30.

11. Greenfield S, Sheehe PR, Feldman HA. 1971. Meningococcal carriage in a population of "normal" families. J Infect Dis 123:67-73.

12. Andersen J, Berthelsen L, Bech Jensen B, Lind I. 1998. Dynamics of the meningococcal carrier state and characteristics of the carrier strains: a longitudinal study within three cohorts of military recruits. Epidemiol Infect 121:85-94.

13. Yazdankhah SP, Caugant DA. 2004. Neisseria meningitidis: an overview of the carriage state. J Med Microbiol 53:821-832.

14. Tzeng YL, Stephens DS. 2000. Epidemiology and pathogenesis of Neisseria meningitidis. Microbes Infect 2:687-700.

15. Fischer M, Hedberg K, Cardosi P, Plikaytis BD, Hoesly FC, Steingart KR, Bell TA, Fleming DW, Wenger JD, Perkins BA. 1997. Tobacco smoke as a risk factor for meningococcal disease. Pediatr Infect Dis J 16:979-83.

16. Stephens DS, Greenwood B, Brandtzaeg P. 2007. Epidemic meningitis, meningococcaemia, and Neisseria meningitidis. Lancet 369:2196-2210.

17. Greenwood BM, Blakebrough IS, Bradley AK, Wali S, Whittle HC. 1984. Meningococcal disease and season in sub-Saharan Africa. Lancet 1:1339-42.

18. Molesworth AM, Thomson MC, Connor SJ, Cresswell MP, Morse AP, Shears P, Hart CA, Cuevas LE. 2002. Where is the meningitis belt? Defining an area at risk of epidemic meningitis in Africa. Trans R Soc Trop Med Hyg 96:242-9.

19. Harrison LH, Trotter CL, Ramsay ME. 2009. Global epidemiology of meningococcal disease. Vaccine 27 Suppl 2:B51-63.

20. Rouphael NG, Stephens DS. 2012. Neisseria meningitidis: biology, microbiology, and epidemiology. Methods Mol Biol 799:1-20.

21. Stephens DS, Hoffman LH, McGee ZA. 1983. Interaction of Neisseria meningitidis with human nasopharyngeal mucosa: attachment and entry into columnar epithelial cells. J Infect Dis 148:369-76.

22. Aycock WL, Mueller JH. 1950. Meningococcus carrier rates and meningitis incidence. Bacteriol Rev 14:115-60.

23. Rosenstein NE, Perkins BA, Stephens DS, Popovic T, Hughes JM. 2001. Meningococcal disease. N Engl J Med 344:1378-88.

24. Millar BC, Banks L, Bourke TW, Cunningham M, Dooley J, Elshibly S, Goldsmith CE, Fairley D, Jackson K, Lamont S, Jessop L, McCrudden E, McConnell D, McAuley K, McKenna JP, Moore P, Smithson R, Stirling J, Shields M, Moore JE. 2018. Meningococcal Disease Section 3: Diagnosis and Management: MeningoNI Forum. Ulster Med J 87:94-98.

25. CDC. 2022. Diagnosis, Treatment, and Complications. https://www.cdc.gov/meningococcal/about/diagnosis-treatment.html#:~:text=Meningococcal%20disease%20can%20be%20difficult,to%20a%20laboratory%20for%20testing.

26. Fox AJ, Taha MK, Vogel U. 2007. Standardized nonculture techniques recommended for European reference laboratories. FEMS Microbiol Rev 31:84-8.

27. Quagliarello VJ, Scheld WM. 1997. Treatment of bacterial meningitis. N Engl J Med 336:708-16.

28. Flexner S. 1913. THE RESULTS OF THE SERUM TREATMENT IN THIRTEEN HUNDRED CASES OF EPIDEMIC MENINGITIS. J Exp Med 17:553-76.

29. Edwards MS, Baker CJ. 1981. Complications and sequelae of meningococcal infections in children. J Pediatr 99:540-5.

30. Kirsch EA, Barton RP, Kitchen L, Giroir BP. 1996. Pathophysiology, treatment and outcome of meningococcemia: a review and recent experience. Pediatr Infect Dis J 15:967-78; quiz 979.

31. Dillon JR, Pauzé M, Yeung KH. 1983. Spread of penicillinase-producing and transfer plasmids from the gonococcus to Neisseria meningitidis. Lancet 1:779-81.

32. Woods CR, Smith AL, Wasilauskas BL, Campos J, Givner LB. 1994. Invasive disease caused by Neisseria meningitidis relatively resistant to penicillin in North Carolina. J Infect Dis 170:453-6.

33. Brigham KS, Sandora TJ. 2009. Neisseria meningitidis: epidemiology, treatment and prevention in adolescents. Curr Opin Pediatr 21:437-43.

34. Blakebrough IS, Greenwood BM, Whittle HC, Bradley AK, Gilles HM. 1983. Failure of meningococcal vaccination to stop the transmission of meningococci in Nigerian schoolboys. Ann Trop Med Parasitol 77:175-8.

35. Rosenstein N, Levine O, Taylor JP, Evans D, Plikaytis BD, Wenger JD, Perkins BA. 1998. Efficacy of meningococcal vaccine and barriers to vaccination. Jama 279:435-9.

36. Pace D, Pollard AJ. 2007. Meningococcal A, C, Y and W-135 polysaccharide-protein conjugate vaccines. Arch Dis Child 92:909-15.

37. Myers TR, McNeil MM. 2018. Current safety issues with quadrivalent meningococcal conjugate vaccines. Hum Vaccin Immunother 14:1175-1178.

38. Leca M, Bornet C, Montana M, Curti C, Vanelle P. 2015. Meningococcal vaccines: Current state and future outlook. Pathol Biol (Paris) 63:144-51.

39. Liu TY, Gotschlich EC, Jonssen EK, Wysocki JR. 1971. Studies on the meningococcal polysaccharides. I. Composition and chemical properties of the group A polysaccharide. J Biol Chem 246:2849-58.

40. Liu TY, Gotschlich EC, Dunne FT, Jonssen EK. 1971. Studies on the meningococcal polysaccharides. II. Composition and chemical properties of the group B and group C polysaccharide. J Biol Chem 246:4703-12.

41. Finne J, Leinonen M, Mäkelä PH. 1983. Antigenic similarities between brain components and bacteria causing meningitis. Implications for vaccine development and pathogenesis. Lancet 2:355-7.

42. Sette A, Rappuoli R. 2010. Reverse vaccinology: developing vaccines in the era of genomics. Immunity 33:530-41.

43. Feavers IM, Maiden MCJ. 2017. Recent Progress in the Prevention of Serogroup B Meningococcal Disease. Clin Vaccine Immunol 24.

44. Snape MD, Medini D, Halperin SA, DeTora L, Drori J, Moxon ER. 2012. The challenge of post-implementation surveillance for novel meningococcal vaccines. Vaccine 30 Suppl 2:B67-72.

45. Donnelly J, Medini D, Boccadifuoco G, Biolchi A, Ward J, Frasch C, Moxon ER, Stella M, Comanducci M, Bambini S, Muzzi A, Andrews W, Chen J, Santos G, Santini L, Boucher P, Serruto D, Pizza M, Rappuoli R, Giuliani MM. 2010. Qualitative and quantitative assessment of meningococcal antigens to evaluate the potential strain coverage of protein-based vaccines. Proc Natl Acad Sci U S A 107:19490-5.

46. Shirley M, Taha MK. 2018. MenB-FHbp Meningococcal Group B Vaccine (Trumenba(®)): A Review in Active Immunization in Individuals Aged ≥ 10 Years. Drugs 78:257-268.

47. Mbaeyi S, Pondo T, Blain A, Yankey D, Potts C, Cohn A, Hariri S, Shang N, MacNeil JR. 2020. Incidence of Meningococcal Disease Before and After Implementation of Quadrivalent Meningococcal Conjugate Vaccine in the United States. JAMA Pediatr 174:843-851.

48. WHO. 2021. Gonorrhoea: latest antimicrobial global surveillance results and guidance for vaccine development published. https://www.who.int/news/item/22-11-2021-gonorrhoea-antimicrobial-resistance-results-and-guidance-vaccine-development#:~:text=WHO%20estimates%20that%2082.4%20million,curable%20when%20treated%20with%20antibiotics.

49. CDC. 2023. National Overview of STDs, 2021. Prevention CfDCa, https://www.cdc.gov/std/statistics/2021/overview.htm#Gonorrhea.

50. CDC. 2021. Sexually Transmitted Infections Prevalence, Incidence, and Cost Estimates in the United States. https://www.cdc.gov/std/statistics/prevalence-2020-at-a-glance.htm.

51. Liu Y, Feinen B, Russell MW. 2011. New concepts in immunity to *Neisseria gonorrhoeae*: innate responses and suppression of adaptive immunity favor the pathogen, not the host. Front Microbiol 2:52.

52. Cohen MS, Hoffman IF, Royce RA, Kazembe P, Dyer JR, Daly CC, Zimba D, Vernazza PL, Maida M, Fiscus SA, Eron JJ, Jr. 1997. Reduction of concentration of HIV-1 in semen after treatment of urethritis: implications for prevention of sexual transmission of HIV-1. AIDSCAP Malawi Research Group. Lancet 349:1868-73.

53. McClelland RS, Wang CC, Mandaliya K, Overbaugh J, Reiner MT, Panteleeff DD, Lavreys L, Ndinya-Achola J, Bwayo JJ, Kreiss JK. 2001. Treatment of cervicitis is associated with decreased cervical shedding of HIV-1. Aids 15:105-10.

54. Malott RJ, Keller BO, Gaudet RG, McCaw SE, Lai CC, Dobson-Belaire WN, Hobbs JL, St Michael F, Cox AD, Moraes TF, Gray-Owen SD. 2013. Neisseria gonorrhoeae-

derived heptose elicits an innate immune response and drives HIV-1 expression. Proc Natl Acad Sci U S A 110:10234-9.

55. Lyss SB, Kamb ML, Peterman TA, Moran JS, Newman DR, Bolan G, Douglas JM, Jr., Iatesta M, Malotte CK, Zenilman JM, Ehret J, Gaydos C, Newhall WJ. 2003. Chlamydia trachomatis among patients infected with and treated for Neisseria gonorrhoeae in sexually transmitted disease clinics in the United States. Ann Intern Med 139:178-85.
56. Walker CK, Sweet RL. 2011. Gonorrhea infection in women: prevalence, effects, screening, and management. Int J Womens Health 3:197-206.
57. Farley TA, Cohen DA, Elkins W. 2003. Asymptomatic sexually transmitted diseases: the case for screening. Prev Med 36:502-9.
58. Workowski K. 2013. In the clinic. Chlamydia and gonorrhea. Ann Intern Med 158:Itc2-1.
59. Higashi DL, Lee SW, Snyder A, Weyand NJ, Bakke A, So M. 2007. Dynamics of Neisseria gonorrhoeae attachment: microcolony development, cortical plaque formation, and cytoprotection. Infect Immun 75:4743-53.
60. Walker E, van Niekerk S, Hanning K, Kelton W, Hicks J. 2023. Mechanisms of host manipulation by Neisseria gonorrhoeae. Front Microbiol 14:1119834.
61. Portnoy J, Mendelson J, Clecner B, Heisler L. 1974. Asymptomatic gonorrhea in the male. Can Med Assoc J 110:169 passim.
62. Mayor MT, Roett MA, Uduhiri KA. 2012. Diagnosis and management of gonococcal infections. Am Fam Physician 86:931-8.
63. McCormack WM, Stumacher RJ, Johnson K, Donner A. 1977. Clinical spectrum of gonococcal infection in women. Lancet 1:1182-5.
64. Vidaurrazaga MM, Perlman DC. 2020. A case of purulent gonococcal arthritis. IDCases 19:e00662.
65. Douedi S, Dattadeen J, Akoluk A, Liu E. 2020. Disseminated Neisseria gonorrhea of the wrist. IDCases 20:e00763.

66. Anan TJ, Culik DA. 1989. Neisseria gonorrhoeae dissemination and gonococcal meningitis. J Am Board Fam Pract 2:123-5.

67. de Campos FP, Kawabata VS, Bittencourt MS, Lovisolo SM, Felipe-Silva A, de Lemos AP. 2016. Gonococcal endocarditis: an ever-present threat. Autops Case Rep 6:19-25.

68. Bro-Jorgensen A, Jensen T. 1973. Gonococcal pharyngeal infections. Report of 110 cases. Br J Vener Dis 49:491-9.

69. Moran JS. 1995. Treating uncomplicated Neisseria gonorrhoeae infections: is the anatomic site of infection important? Sex Transm Dis 22:39-47.

70. Liu Y, Islam EA, Jarvis GA, Gray-Owen SD, Russell MW. 2012. Neisseria gonorrhoeae selectively suppresses the development of Th1 and Th2 cells, and enhances Th17 cell responses, through TGF-β-dependent mechanisms. Mucosal Immunol 5:320-31.

71. Stevens JS, Criss AK. 2018. Pathogenesis of Neisseria gonorrhoeae in the female reproductive tract: neutrophilic host response, sustained infection, and clinical sequelae. Curr Opin Hematol 25:13-21.

72. Liu Y, Hammer LA, Liu W, Hobbs MM, Zielke RA, Sikora AE, Jerse AE, Egilmez NK, Russell MW. 2017. Experimental vaccine induces Th1-driven immune responses and resistance to Neisseria gonorrhoeae infection in a murine model. Mucosal Immunol 10:1594-1608.

73. Liu Y, Russell MW. 2011. Diversion of the immune response to Neisseria gonorrhoeae from Th17 to Th1/Th2 by treatment with anti-transforming growth factor β antibody generates immunological memory and protective immunity. mBio 2:e00095-11.

74. Russell MW, Jerse AE, Gray-Owen SD. 2019. Progress Toward a Gonococcal Vaccine: The Way Forward. Front Immunol 10:2417.

75. Ramsey KH, Schneider H, Cross AS, Boslego JW, Hoover DL, Staley TL, Kuschner RA, Deal CD. 1995. Inflammatory cytokines produced in response to experimental human gonorrhea. J Infect Dis 172:186-91.

76. Hedges SR, Mayo MS, Mestecky J, Hook EW, Russell MW. 1999. Limited local and systemic antibody responses to Neisseria gonorrhoeae during uncomplicated genital infections. Infect Immun 67:3937-46.

77. West D, Reddin K, Matheson M, Heath R, Funnell S, Hudson M, Robinson A, Gorringe A. 2001. Recombinant Neisseria meningitidis transferrin binding protein A protects against experimental meningococcal infection. Infect Immun 69:1561-7.

78. Price GA, Hobbs MM, Cornelissen CN. 2004. Immunogenicity of gonococcal transferrin binding proteins during natural infections. Infect Immun 72:277-83.

79. de Vries FP, van Der Ende A, van Putten JP, Dankert J. 1996. Invasion of primary nasopharyngeal epithelial cells by Neisseria meningitidis is controlled by phase variation of multiple surface antigens. Infect Immun 64:2998-3006.

80. Ohnishi M, Golparian D, Shimuta K, Saika T, Hoshina S, Iwasaku K, Nakayama S, Kitawaki J, Unemo M. 2011. Is Neisseria gonorrhoeae initiating a future era of untreatable gonorrhea?: detailed characterization of the first strain with high-level resistance to ceftriaxone. Antimicrob Agents Chemother 55:3538-45.

81. Unemo M, Golparian D, Nicholas R, Ohnishi M, Gallay A, Sednaoui P. 2012. High-level cefixime- and ceftriaxone-resistant Neisseria gonorrhoeae in France: novel penA mosaic allele in a successful international clone causes treatment failure. Antimicrob Agents Chemother 56:1273-80.

82. Unemo M, Lahra MM, Cole M, Galarza P, Ndowa F, Martin I, Dillon JR, Ramon-Pardo P, Bolan G, Wi T. 2019. World Health Organization Global Gonococcal Antimicrobial Surveillance Program (WHO GASP): review of new data and evidence to inform international collaborative actions and research efforts. Sex Health 16:412-425.

83. Singh A, Turner JM, Tomberg J, Fedarovich A, Unemo M, Nicholas RA, Davies C. 2020. Mutations in penicillin-binding protein 2 from cephalosporin-resistant Neisseria

gonorrhoeae hinder ceftriaxone acylation by restricting protein dynamics. J Biol Chem 295:7529-7543.

84. CDC. 2007. Update to CDC's Sexually Transmitted Diseases Treatment Guidelines, 2006: Fluoroquinolones No Longer Recommended for Treatment of Gonococcal Infections. https://www.cdc.gov/mmwr/preview/mmwrhtml/mm5614a3.htm.

85. CDC. 2012. Update to CDC's Sexually Transmitted Diseases Treatment Guidelines, 2010: Oral Cephalosporins No Longer a Recommended Treatment for Gonococcal Infections. https://www.cdc.gov/mmwr/preview/mmwrhtml/mm6131a3.htm.

86. Unemo M, Shafer WM. 2014. Antimicrobial resistance in Neisseria gonorrhoeae in the 21st century: past, evolution, and future. Clin Microbiol Rev 27:587-613.

87. CaliforniaDepartmentofPublicHealth. 2023. Antibiotic-Resistant Gonorrhea Center of Excellence. https://www.cdph.ca.gov/Programs/CID/DCDC/Pages/Antibiotic-Resistant-Gonorrhea-Center-of-Excellence.aspx.

88. Springer C, Salen P. 2023. Gonorrhea, StatPearls. StatPearls Publishing

89. St Cyr S, Barbee L, Workowski KA, Bachmann LH, Pham C, Schlanger K, Torrone E, Weinstock H, Kersh EN, Thorpe P. 2020. Update to CDC's Treatment Guidelines for Gonococcal Infection, 2020. MMWR Morb Mortal Wkly Rep 69:1911-1916.

90. Kirkcaldy RD, Weinstock HS, Moore PC, Philip SS, Wiesenfeld HC, Papp JR, Kerndt PR, Johnson S, Ghanem KG, Hook EW, 3rd. 2014. The efficacy and safety of gentamicin plus azithromycin and gemifloxacin plus azithromycin as treatment of uncomplicated gonorrhea. Clin Infect Dis 59:1083-91.

91. Workowski KA, Bolan GA. 2015. Sexually transmitted diseases treatment guidelines, 2015. MMWR Recomm Rep 64:1-137.

92. Semchenko EA, Tan A, Borrow R, Seib KL. 2019. The Serogroup B Meningococcal Vaccine Bexsero Elicits Antibodies to Neisseria gonorrhoeae. Clin Infect Dis 69:1101-1111.

93. Kirkcaldy RD, Harvey A, Papp JR, Del Rio C, Soge OO, Holmes KK, Hook EW, 3rd, Kubin G, Riedel S, Zenilman J, Pettus K, Sanders T, Sharpe S, Torrone E. 2016. Neisseria gonorrhoeae Antimicrobial Susceptibility Surveillance - The Gonococcal Isolate Surveillance Project, 27 Sites, United States, 2014. MMWR Surveill Summ 65:1-19.

94. Soto GE, Hultgren SJ. 1999. Bacterial adhesins: common themes and variations in architecture and assembly. J Bacteriol 181:1059-71.

95. Merz AJ, So M. 2000. Interactions of pathogenic neisseriae with epithelial cell membranes. Annu Rev Cell Dev Biol 16:423-57.

96. Carbonnelle E, Helaine S, Nassif X, Pelicic V. 2006. A systematic genetic analysis in Neisseria meningitidis defines the Pil proteins required for assembly, functionality, stabilization and export of type IV pili. Mol Microbiol 61:1510-22.

97. Hung MC, Christodoulides M. 2013. The biology of Neisseria adhesins. Biology (Basel) 2:1054-109.

98. Tønjum T, Koomey M. 1997. The pilus colonization factor of pathogenic neisserial species: organelle biogenesis and structure/function relationships--a review. Gene 192:155-63.

99. Forest KT, Tainer JA. 1997. Type-4 pilus-structure: outside to inside and top to bottom--a minireview. Gene 192:165-9.

100. Wolfgang M, van Putten JP, Hayes SF, Dorward D, Koomey M. 2000. Components and dynamics of fiber formation define a ubiquitous biogenesis pathway for bacterial pili. EMBO J 19:6408-18.

101. Scheuerpflug I, Rudel T, Ryll R, Pandit J, Meyer TF. 1999. Roles of PilC and PilE proteins in pilus-mediated adherence of Neisseria gonorrhoeae and Neisseria meningitidis to human erythrocytes and endothelial and epithelial cells. Infect Immun 67:834-43.

102. Merz AJ, So M, Sheetz MP. 2000. Pilus retraction powers bacterial twitching motility. Nature 407:98-102.

103. Maier B, Potter L, So M, Long CD, Seifert HS, Sheetz MP. 2002. Single pilus motor forces exceed 100 pN. Proc Natl Acad Sci U S A 99:16012-7.

104. Fussenegger M, Rudel T, Barten R, Ryll R, Meyer TF. 1997. Transformation competence and type-4 pilus biogenesis in Neisseria gonorrhoeae--a review. Gene 192:125-34.

105. Hamilton HL, Dillard JP. 2006. Natural transformation of Neisseria gonorrhoeae: from DNA donation to homologous recombination. Mol Microbiol 59:376-85.

106. Hagblom P, Segal E, Billyard E, So M. 1985. Intragenic recombination leads to pilus antigenic variation in Neisseria gonorrhoeae. Nature 315:156-8.

107. Segal E, Hagblom P, Seifert HS, So M. 1986. Antigenic variation of gonococcal pilus involves assembly of separated silent gene segments. Proc Natl Acad Sci U S A 83:2177-81.

108. Jonsson AB, Nyberg G, Normark S. 1991. Phase variation of gonococcal pili by frameshift mutation in pilC, a novel gene for pilus assembly. EMBO J 10:477-88.

109. Swanson J. 1978. Studies on gonococcus infection. XII. Colony color and opacity varienats of gonococci. Infect Immun 19:320-31.

110. Swanson J. 1982. Colony opacity and protein II compositions of gonococci. Infect Immun 37:359-68.

111. Bhat KS, Gibbs CP, Barrera O, Morrison SG, Jähnig F, Stern A, Kupsch EM, Meyer TF, Swanson J. 1992. The opacity proteins of Neisseria gonorrhoeae strain MS11 are encoded by a family of 11 complete genes. Mol Microbiol 6:1073-6.

112. Hauck CR, Meyer TF. 2003. 'Small' talk: Opa proteins as mediators of Neisseria-host-cell communication. Curr Opin Microbiol 6:43-9.

113. Stern A, Brown M, Nickel P, Meyer TF. 1986. Opacity genes in Neisseria gonorrhoeae: control of phase and antigenic variation. Cell 47:61-71.

114. Stern A, Meyer TF. 1987. Common mechanism controlling phase and antigenic variation in pathogenic neisseriae. Mol Microbiol 1:5-12.

115. Swanson J, Belland RJ, Hill SA. 1992. Neisserial surface variation: how and why? Curr Opin Genet Dev 2:805-11.

116. Jerse AE, Cohen MS, Drown PM, Whicker LG, Isbey SF, Seifert HS, Cannon JG. 1994. Multiple gonococcal opacity proteins are expressed during experimental urethral infection in the male. J Exp Med 179:911-20.

117. Swanson J, Barrera O, Sola J, Boslego J. 1988. Expression of outer membrane protein II by gonococci in experimental gonorrhea. J Exp Med 168:2121-9.

118. Hill SA, Masters TL, Wachter J. 2016. Gonorrhea - an evolving disease of the new millennium. Microb Cell 3:371-389.

119. Makino S, van Putten JP, Meyer TF. 1991. Phase variation of the opacity outer membrane protein controls invasion by Neisseria gonorrhoeae into human epithelial cells. EMBO J 10:1307-15.

120. van Putten JP, Paul SM. 1995. Binding of syndecan-like cell surface proteoglycan receptors is required for Neisseria gonorrhoeae entry into human mucosal cells. EMBO J 14:2144-54.

121. Chen T, Belland RJ, Wilson J, Swanson J. 1995. Adherence of pilus- Opa+ gonococci to epithelial cells in vitro involves heparan sulfate. J Exp Med 182:511-7.

122. Chen T, Gotschlich EC. 1996. CGM1a antigen of neutrophils, a receptor of gonococcal opacity proteins. Proc Natl Acad Sci U S A 93:14851-6.

123. Virji M, Makepeace K, Ferguson DJ, Watt SM. 1996. Carcinoembryonic antigens (CD66) on epithelial cells and neutrophils are receptors for Opa proteins of pathogenic neisseriae. Mol Microbiol 22:941-50.

124. Chen T, Grunert F, Medina-Marino A, Gotschlich EC. 1997. Several carcinoembryonic antigens (CD66) serve as receptors for gonococcal opacity proteins. J Exp Med 185:1557-64.

125. Islam EA, Anipindi VC, Francis I, Shaik-Dasthagirisaheb Y, Xu S, Leung N, Sintsova A, Amin M, Kaushic C, Wetzler LM, Gray-Owen SD. 2018. Specific Binding to Differentially Expressed Human Carcinoembryonic Antigen-Related Cell Adhesion Molecules Determines the Outcome of Neisseria gonorrhoeae Infections along the Female Reproductive Tract. Infect Immun 86.

126. Sarantis H, Gray-Owen SD. 2007. The specific innate immune receptor CEACAM3 triggers neutrophil bactericidal activities via a Syk kinase-dependent pathway. Cell Microbiol 9:2167-80.

127. Alcott AM, Werner LM, Baiocco CM, Belcher Dufrisne M, Columbus L, Criss AK. 2022. Variable Expression of Opa Proteins by Neisseria gonorrhoeae Influences Bacterial Association and Phagocytic Killing by Human Neutrophils. J Bacteriol 204:e0003522.

128. Boulton IC, Gray-Owen SD. 2002. Neisserial binding to CEACAM1 arrests the activation and proliferation of CD4+ T lymphocytes. Nat Immunol 3:229-36.

129. Pantelic M, Kim YJ, Bolland S, Chen I, Shively J, Chen T. 2005. Neisseria gonorrhoeae kills carcinoembryonic antigen-related cellular adhesion molecule 1 (CD66a)-expressing human B cells and inhibits antibody production. Infect Immun 73:4171-9.

130. Liu Y, Liu W, Russell MW. 2014. Suppression of host adaptive immune responses by Neisseria gonorrhoeae: role of interleukin 10 and type 1 regulatory T cells. Mucosal Immunol 7:165-76.

131. Britigan BE, Cohen MS, Sparling PF. 1985. Gonococcal infection: a model of molecular pathogenesis. N Engl J Med 312:1683-94.

132. Sandstrom EG, Chen KC, Buchanan TM. 1982. Serology of Neisseria gonorrhoeae: coagglutination serogroups WI and WII/III correspond to different outer membrane protein I molecules. Infect Immun 38:462-70.

133. Cannon JG, Buchanan TM, Sparling PF. 1983. Confirmation of association of protein I serotype of Neisseria gonorrhoeae with ability to cause disseminated infection. Infect Immun 40:816-9.

134. Gotschlich EC, Seiff ME, Blake MS, Koomey M. 1987. Porin protein of Neisseria gonorrhoeae: cloning and gene structure. Proc Natl Acad Sci U S A 84:8135-9.

135. Feavers IM, Maiden MC. 1998. A gonococcal porA pseudogene: implications for understanding the evolution and pathogenicity of Neisseria gonorrhoeae. Mol Microbiol 30:647-56.

136. Sandström EG, Knapp JS, Reller LB, Thompson SE, Hook EW, Holmes KK. 1984. Serogrouping of Neisseria gonorrhoeae: correlation of serogroup with disseminated gonococcal infection. Sex Transm Dis 11:77-80.

137. Benz R. 1988. Structure and function of porins from gram-negative bacteria. Annu Rev Microbiol 42:359-93.

138. Haines KA, Yeh L, Blake MS, Cristello P, Korchak H, Weissmann G. 1988. Protein I, a translocatable ion channel from Neisseria gonorrhoeae, selectively inhibits exocytosis from human neutrophils without inhibiting O2- generation. J Biol Chem 263:945-51.

139. Mosleh IM, Huber LA, Steinlein P, Pasquali C, Günther D, Meyer TF. 1998. Neisseria gonorrhoeae porin modulates phagosome maturation. J Biol Chem 273:35332-8.

140. Lynch EC, Blake MS, Gotschlich EC, Mauro A. 1984. Studies of Porins: Spontaneously Transferred from Whole Cells and Reconstituted from Purified Proteins of Neisseria gonorrhoeae and Neisseria meningitidis. Biophys J 45:104-7.

141. Ram S, McQuillen DP, Gulati S, Elkins C, Pangburn MK, Rice PA. 1998. Binding of complement factor H to loop 5 of porin protein 1A: a molecular mechanism of serum resistance of nonsialylated Neisseria gonorrhoeae. J Exp Med 188:671-80.

142. Ram S, Cullinane M, Blom AM, Gulati S, McQuillen DP, Monks BG, O'Connell C, Boden R, Elkins C, Pangburn MK, Dahlbäck B, Rice PA. 2001. Binding of C4b-binding protein to porin: a molecular mechanism of serum resistance of Neisseria gonorrhoeae. J Exp Med 193:281-95.

143. Ram S, Cullinane M, Blom AM, Gulati S, McQuillen DP, Boden R, Monks BG, O'Connell C, Elkins C, Pangburn MK, Dahlbäck B, Rice PA. 2001. C4bp binding to porin mediates stable serum resistance of Neisseria gonorrhoeae. Int Immunopharmacol 1:423-32.

144. Schneider H, Griffiss JM, Boslego JW, Hitchcock PJ, Zahos KM, Apicella MA. 1991. Expression of paragloboside-like lipooligosaccharides may be a necessary component of gonococcal pathogenesis in men. J Exp Med 174:1601-5.

145. Harvey HA, Ketterer MR, Preston A, Lubaroff D, Williams R, Apicella MA. 1997. Ultrastructural analysis of primary human urethral epithelial cell cultures infected with Neisseria gonorrhoeae. Infect Immun 65:2420-7.

146. Harvey HA, Porat N, Campbell CA, Jennings M, Gibson BW, Phillips NJ, Apicella MA, Blake MS. 2000. Gonococcal lipooligosaccharide is a ligand for the asialoglycoprotein receptor on human sperm. Mol Microbiol 36:1059-70.

147. Harvey HA, Swords WE, Apicella MA. 2001. The mimicry of human glycolipids and glycosphingolipids by the lipooligosaccharides of pathogenic neisseria and haemophilus. J Autoimmun 16:257-62.

148. Parsons NJ, Patel PV, Tan EL, Andrade JR, Nairn CA, Goldner M, Cole JA, Smith H. 1988. Cytidine 5'-monophospho-N-acetyl neuraminic acid and a low molecular weight factor from human blood cells induce lipopolysaccharide alteration in gonococci when conferring resistance to killing by human serum. Microb Pathog 5:303-9.

149. Smith H, Parsons NJ, Cole JA. 1995. Sialylation of neisserial lipopolysaccharide: a major influence on pathogenicity. Microb Pathog 19:365-77.

150. Parsons NJ, Curry A, Fox AJ, Jones DM, Cole JA, Smith H. 1992. The serum resistance of gonococci in the majority of urethral exudates is due to sialylated lipopolysaccharide seen as a surface coat. FEMS Microbiol Lett 69:295-9.

151. Lewis LA, Choudhury B, Balthazar JT, Martin LE, Ram S, Rice PA, Stephens DS, Carlson R, Shafer WM. 2009. Phosphoethanolamine substitution of lipid A and resistance of Neisseria gonorrhoeae to cationic antimicrobial peptides and complement-mediated killing by normal human serum. Infect Immun 77:1112-20.

152. Cox AD, Wright JC, Li J, Hood DW, Moxon ER, Richards JC. 2003. Phosphorylation of the lipid A region of meningococcal lipopolysaccharide: identification of a family of transferases that add phosphoethanolamine to lipopolysaccharide. J Bacteriol 185:3270-7.

153. Packiam M, Yedery RD, Begum AA, Carlson RW, Ganguly J, Sempowski GD, Ventevogel MS, Shafer WM, Jerse AE. 2014. Phosphoethanolamine decoration of Neisseria gonorrhoeae lipid A plays a dual immunostimulatory and protective role during experimental genital tract infection. Infect Immun 82:2170-9.

154. Liu M, John CM, Jarvis GA. 2010. Phosphoryl moieties of lipid A from Neisseria meningitidis and N. gonorrhoeae lipooligosaccharides play an important role in activation of both MyD88- and TRIF-dependent TLR4-MD-2 signaling pathways. J Immunol 185:6974-84.

155. Gotschlich EC. 1994. Genetic locus for the biosynthesis of the variable portion of Neisseria gonorrhoeae lipooligosaccharide. J Exp Med 180:2181-90.

156. Yang QL, Gotschlich EC. 1996. Variation of gonococcal lipooligosaccharide structure is due to alterations in poly-G tracts in lgt genes encoding glycosyl transferases. J Exp Med 183:323-7.

157. van Putten JP. 1993. Phase variation of lipopolysaccharide directs interconversion of invasive and immuno-resistant phenotypes of Neisseria gonorrhoeae. EMBO J 12:4043-51.

158. Pohlner J, Halter R, Beyreuther K, Meyer TF. 1987. Gene structure and extracellular secretion of Neisseria gonorrhoeae IgA protease. Nature 325:458-62.

159. Plaut AG, Gilbert JV, Artenstein MS, Capra JD. 1975. Neisseria gonorrhoeae and neisseria meningitidis: extracellular enzyme cleaves human immunoglobulin A. Science 190:1103-5.

160. Plaut AG, Gilbert JV, Wistar R. 1977. Loss of antibody activity in human immunoglobulin A exposed extracellular immunoglobulin A proteases of Neisseria gonorrhoeae and Streptococcus sanguis. Infect Immun 17:130-5.

161. Roussel-Jazédé V, Arenas J, Langereis JD, Tommassen J, van Ulsen P. 2014. Variable processing of the IgA protease autotransporter at the cell surface of Neisseria meningitidis. Microbiology (Reading) 160:2421-2431.

162. Lin L, Ayala P, Larson J, Mulks M, Fukuda M, Carlsson SR, Enns C, So M. 1997. The Neisseria type 2 IgA1 protease cleaves LAMP1 and promotes survival of bacteria within epithelial cells. Mol Microbiol 24:1083-94.

163. Brooks GF, Lammel CJ, Blake MS, Kusecek B, Achtman M. 1992. Antibodies against IgA1 protease are stimulated both by clinical disease and asymptomatic carriage of serogroup A Neisseria meningitidis. J Infect Dis 166:1316-21.

164. Hopper S, Vasquez B, Merz A, Clary S, Wilbur JS, So M. 2000. Effects of the immunoglobulin A1 protease on Neisseria gonorrhoeae trafficking across polarized T84 epithelial monolayers. Infect Immun 68:906-11.

165. Johannsen DB, Johnston DM, Koymen HO, Cohen MS, Cannon JG. 1999. A Neisseria gonorrhoeae immunoglobulin A1 protease mutant is infectious in the human challenge model of urethral infection. Infect Immun 67:3009-13.

166. Lieu PT, Heiskala M, Peterson PA, Yang Y. 2001. The roles of iron in health and disease. Mol Aspects Med 22:1-87.

167. Liu Z, Ren Z, Zhang J, Chuang CC, Kandaswamy E, Zhou T, Zuo L. 2018. Role of ROS and Nutritional Antioxidants in Human Diseases. Front Physiol 9:477.

168. Hood MI, Skaar EP. 2012. Nutritional immunity: transition metals at the pathogen-host interface. Nat Rev Microbiol 10:525-37.

169. Luck AN, Mason AB. 2012. Transferrin-mediated cellular iron delivery. Curr Top Membr 69:3-35.

170. Park I, Schaeffer E, Sidoli A, Baralle FE, Cohen GN, Zakin MM. 1985. Organization of the human transferrin gene: direct evidence that it originated by gene duplication. Proc Natl Acad Sci U S A 82:3149-53.

171. Aisen P, Leibman A, Zweier J. 1978. Stoichiometric and site characteristics of the binding of iron to human transferrin. J Biol Chem 253:1930-7.

172. Williams J, Moreton K. 1980. The distribution of iron between the metal-binding sites of transferrin human serum. Biochem J 185:483-8.

173. Sun H, Li H, Sadler PJ. 1999. Transferrin as a metal ion mediator. Chem Rev 99:2817-42.

174. Mason AB, Byrne SL, Everse SJ, Roberts SE, Chasteen ND, Smith VC, MacGillivray RT, Kandemir B, Bou-Abdallah F. 2009. A loop in the N-lobe of human serum transferrin

is critical for binding to the transferrin receptor as revealed by mutagenesis, isothermal titration calorimetry, and epitope mapping. J Mol Recognit 22:521-9.

175. Masson PL, Heremans JF, Schonne E. 1969. Lactoferrin, an iron-binding protein in neutrophilic leukocytes. J Exp Med 130:643-58.

176. Morgan EH, Appleton TC. 1969. Autoradiographic localization of 125-I-labelled transferrin in rabbit reticulocytes. Nature 223:1371-2.

177. González-Chávez SA, Arévalo-Gallegos S, Rascón-Cruz Q. 2009. Lactoferrin: structure, function and applications. Int J Antimicrob Agents 33:301.e1-8.

178. Wang B, Timilsena YP, Blanch E, Adhikari B. 2019. Lactoferrin: Structure, function, denaturation and digestion. Crit Rev Food Sci Nutr 59:580-596.

179. Conneely OM. 2001. Antiinflammatory activities of lactoferrin. J Am Coll Nutr 20:389S-395S; discussion 396S-397S.

180. Masson PL, Heremans JF. 1971. Lactoferrin in milk from different species. Comp Biochem Physiol B 39:119-29.

181. Bennett RM, Kokocinski T. 1978. Lactoferrin content of peripheral blood cells. Br J Haematol 39:509-21.

182. Metz-Boutigue MH, Jollès J, Mazurier J, Schoentgen F, Legrand D, Spik G, Montreuil J, Jollès P. 1984. Human lactotransferrin: amino acid sequence and structural comparisons with other transferrins. Eur J Biochem 145:659-76.

183. Aisen P, Leibman A. 1972. Lactoferrin and transferrin: a comparative study. Biochim Biophys Acta 257:314-23.

184. Levay PF, Viljoen M. 1995. Lactoferrin: a general review. Haematologica 80:252-67.

185. Bellamy W, Takase M, Wakabayashi H, Kawase K, Tomita M. 1992. Antibacterial spectrum of lactoferricin B, a potent bactericidal peptide derived from the N-terminal region of bovine lactoferrin. J Appl Bacteriol 73:472-9.

186. Bellamy W, Takase M, Yamauchi K, Wakabayashi H, Kawase K, Tomita M. 1992. Identification of the bactericidal domain of lactoferrin. Biochim Biophys Acta 1121:130-6.

187. Farnaud S, Evans RW. 2003. Lactoferrin--a multifunctional protein with antimicrobial properties. Mol Immunol 40:395-405.

188. Saito H, Miyakawa H, Tamura Y, Shimamura S, Tomita M. 1991. Potent bactericidal activity of bovine lactoferrin hydrolysate produced by heat treatment at acidic pH. J Dairy Sci 74:3724-30.

189. Runyen-Janecky LJ. 2013. Role and regulation of heme iron acquisition in gram-negative pathogens. Front Cell Infect Microbiol 3:55.

190. Anzaldi LL, Skaar EP. 2010. Overcoming the heme paradox: heme toxicity and tolerance in bacterial pathogens. Infect Immun 78:4977-89.

191. Ahmed MH, Ghatge MS, Safo MK. 2020. Hemoglobin: Structure, Function and Allostery. Subcell Biochem 94:345-382.

192. Schryvers AB, Stojiljkovic I. 1999. Iron acquisition systems in the pathogenic Neisseria. Mol Microbiol 32:1117-23.

193. Nielsen MJ, Møller HJ, Moestrup SK. 2010. Hemoglobin and heme scavenger receptors. Antioxid Redox Signal 12:261-73.

194. Kristiansen M, Graversen JH, Jacobsen C, Sonne O, Hoffman HJ, Law SK, Moestrup SK. 2001. Identification of the haemoglobin scavenger receptor. Nature 409:198-201.

195. Andersen CBF, Stødkilde K, Sæderup KL, Kuhlee A, Raunser S, Graversen JH, Moestrup SK. 2017. Haptoglobin. Antioxid Redox Signal 26:814-831.

196. Parrow NL, Fleming RE, Minnick MF. 2013. Sequestration and scavenging of iron in infection. Infect Immun 81:3503-14.

197. Hintze KJ, Theil EC. 2006. Cellular regulation and molecular interactions of the ferritins. Cell Mol Life Sci 63:591-600.

198. Aisen P, Enns C, Wessling-Resnick M. 2001. Chemistry and biology of eukaryotic iron metabolism. Int J Biochem Cell Biol 33:940-59.

199. Koorts AM, Viljoen M. 2007. Ferritin and ferritin isoforms I: Structure-function relationships, synthesis, degradation and secretion. Arch Physiol Biochem 113:30-54.

200. Plays M, Müller S, Rodriguez R. 2021. Chemistry and biology of ferritin. Metallomics 13.

201. Richter GW. 1986. Studies of iron overload. Lysosomal proteolysis of rat liver ferritin. Pathol Res Pract 181:159-67.

202. Rudeck M, Volk T, Sitte N, Grune T. 2000. Ferritin oxidation in vitro: implication of iron release and degradation by the 20S proteasome. IUBMB Life 49:451-6.

203. Ferreira C, Bucchini D, Martin ME, Levi S, Arosio P, Grandchamp B, Beaumont C. 2000. Early embryonic lethality of H ferritin gene deletion in mice. J Biol Chem 275:3021-4.

204. Maret W. 2017. Zinc in Cellular Regulation: The Nature and Significance of "Zinc Signals". Int J Mol Sci 18.

205. THIERS RE, VALLEE BL. 1957. Distribution of metals in subcellular fractions of rat liver. J Biol Chem 226:911-20.

206. Krezel A, Maret W. 2006. Zinc-buffering capacity of a eukaryotic cell at physiological pZn. J Biol Inorg Chem 11:1049-62.

207. Tamaki M, Fujitani Y, Hara A, Uchida T, Tamura Y, Takeno K, Kawaguchi M, Watanabe T, Ogihara T, Fukunaka A, Shimizu T, Mita T, Kanazawa A, Imaizumi MO, Abe T, Kiyonari H, Hojyo S, Fukada T, Kawauchi T, Nagamatsu S, Hirano T, Kawamori R, Watada H. 2013. The diabetes-susceptible gene SLC30A8/ZnT8 regulates hepatic insulin clearance. J Clin Invest 123:4513-24.

208. Potts BC, Smith J, Akke M, Macke TJ, Okazaki K, Hidaka H, Case DA, Chazin WJ. 1995. The structure of calcyclin reveals a novel homodimeric fold for S100 Ca(2+)-binding proteins. Nat Struct Biol 2:790-6.

209. Heizmann CW, Fritz G, Schäfer BW. 2002. S100 proteins: structure, functions and pathology. Front Biosci 7:d1356-68.

210. Hunter MJ, Chazin WJ. 1998. High level expression and dimer characterization of the S100 EF-hand proteins, migration inhibitory factor-related proteins 8 and 14. J Biol Chem 273:12427-35.

211. Foell D, Wittkowski H, Vogl T, Roth J. 2007. S100 proteins expressed in phagocytes: a novel group of damage-associated molecular pattern molecules. J Leukoc Biol 81:28-37.

212. Leclerc E, Fritz G, Vetter SW, Heizmann CW. 2009. Binding of S100 proteins to RAGE: an update. Biochim Biophys Acta 1793:993-1007.

213. Vogl T, Tenbrock K, Ludwig S, Leukert N, Ehrhardt C, van Zoelen MA, Nacken W, Foell D, van der Poll T, Sorg C, Roth J. 2007. Mrp8 and Mrp14 are endogenous activators of Toll-like receptor 4, promoting lethal, endotoxin-induced shock. Nat Med 13:1042-9.

214. Ghavami S, Rashedi I, Dattilo BM, Eshraghi M, Chazin WJ, Hashemi M, Wesselborg S, Kerkhoff C, Los M. 2008. S100A8/A9 at low concentration promotes tumor cell growth via RAGE ligation and MAP kinase-dependent pathway. J Leukoc Biol 83:1484-92.

215. Sunahori K, Yamamura M, Yamana J, Takasugi K, Kawashima M, Yamamoto H, Chazin WJ, Nakatani Y, Yui S, Makino H. 2006. The S100A8/A9 heterodimer amplifies proinflammatory cytokine production by macrophages via activation of nuclear factor kappa B and p38 mitogen-activated protein kinase in rheumatoid arthritis. Arthritis Res Ther 8:R69.

216. Broome AM, Ryan D, Eckert RL. 2003. S100 protein subcellular localization during epidermal differentiation and psoriasis. J Histochem Cytochem 51:675-85.

217. Gläser R, Harder J, Lange H, Bartels J, Christophers E, Schröder JM. 2005. Antimicrobial psoriasin (S100A7) protects human skin from Escherichia coli infection. Nat Immunol 6:57-64.

218. Schmid KW, Lügering N, Stoll R, Brinkbäumer P, Winde G, Domschke W, Böcker W, Sorg C. 1995. Immunohistochemical demonstration of the calcium-binding proteins MRP8 and MRP14 and their heterodimer (27E10 antigen) in Crohn's disease. Hum Pathol 26:334-7.

219. Reid PA, McAllister DA, Boyd AC, Innes JA, Porteous D, Greening AP, Gray RD. 2015. Measurement of serum calprotectin in stable patients predicts exacerbation and lung function decline in cystic fibrosis. Am J Respir Crit Care Med 191:233-6.

220. Corbin BD, Seeley EH, Raab A, Feldmann J, Miller MR, Torres VJ, Anderson KL, Dattilo BM, Dunman PM, Gerads R, Caprioli RM, Nacken W, Chazin WJ, Skaar EP. 2008. Metal chelation and inhibition of bacterial growth in tissue abscesses. Science 319:962-5.

221. Liu JZ, Jellbauer S, Poe AJ, Ton V, Pesciaroli M, Kehl-Fie TE, Restrepo NA, Hosking MP, Edwards RA, Battistoni A, Pasquali P, Lane TE, Chazin WJ, Vogl T, Roth J, Skaar EP, Raffatellu M. 2012. Zinc sequestration by the neutrophil protein calprotectin enhances Salmonella growth in the inflamed gut. Cell Host Microbe 11:227-39.

222. Wang J, Lonergan ZR, Gonzalez-Gutierrez G, Nairn BL, Maxwell CN, Zhang Y, Andreini C, Karty JA, Chazin WJ, Trinidad JC, Skaar EP, Giedroc DP. 2019. Multi-metal Restriction by Calprotectin Impacts De Novo Flavin Biosynthesis in Acinetobacter baumannii. Cell Chem Biol 26:745-755.e7.

223. Gaddy JA, Radin JN, Loh JT, Piazuelo MB, Kehl-Fie TE, Delgado AG, Ilca FT, Peek RM, Cover TL, Chazin WJ, Skaar EP, Scott Algood HM. 2014. The host protein calprotectin modulates the Helicobacter pylori cag type IV secretion system via zinc sequestration. PLoS Pathog 10:e1004450.

224. Mildner M, Stichenwirth M, Abtin A, Eckhart L, Sam C, Gläser R, Schröder JM, Gmeiner R, Mlitz V, Pammer J, Geusau A, Tschachler E. 2010. Psoriasin (S100A7) is a major Escherichia coli-cidal factor of the female genital tract. Mucosal Immunol 3:602-9.

225. Kambe T, Tsuji T, Hashimoto A, Itsumura N. 2015. The Physiological, Biochemical, and Molecular Roles of Zinc Transporters in Zinc Homeostasis and Metabolism. Physiol Rev 95:749-84.

226. Hara T, Takeda TA, Takagishi T, Fukue K, Kambe T, Fukada T. 2017. Physiological roles of zinc transporters: molecular and genetic importance in zinc homeostasis. J Physiol Sci 67:283-301.

227. Coyle P, Philcox JC, Carey LC, Rofe AM. 2002. Metallothionein: the multipurpose protein. Cell Mol Life Sci 59:627-47.

228. Capdevila DA, Edmonds KA, Giedroc DP. 2017. Metallochaperones and metalloregulation in bacteria. Essays Biochem 61:177-200.

229. Maurakis S, Keller K, Maxwell CN, Pereira K, Chazin WJ, Criss AK, Cornelissen CN. 2019. The novel interaction between Neisseria gonorrhoeae TdfJ and human S100A7 allows gonococci to subvert host zinc restriction. PLoS Pathog 15:e1007937.

230. Chimento DP, Kadner RJ, Wiener MC. 2005. Comparative structural analysis of TonB-dependent outer membrane transporters: implications for the transport cycle. Proteins 59:240-51.

231. Noinaj N, Guillier M, Barnard TJ, Buchanan SK. 2010. TonB-dependent transporters: regulation, structure, and function. Annu Rev Microbiol 64:43-60.

232. Noinaj N, Easley NC, Oke M, Mizuno N, Gumbart J, Boura E, Steere AN, Zak O, Aisen P, Tajkhorshid E, Evans RW, Gorringe AR, Mason AB, Steven AC, Buchanan SK. 2012. Structural basis for iron piracy by pathogenic Neisseria. Nature 483:53-8.

233. Cornelissen CN, Biswas GD, Tsai J, Paruchuri DK, Thompson SA, Sparling PF. 1992. Gonococcal transferrin-binding protein 1 is required for transferrin utilization and is homologous to TonB-dependent outer membrane receptors. J Bacteriol 174:5788-97.

234. Cornelissen CN. 2003. Transferrin-iron uptake by Gram-negative bacteria. Front Biosci 8:d836-47.

235. Kenney CD, Cornelissen CN. 2002. Demonstration and characterization of a specific interaction between gonococcal transferrin binding protein A and TonB. J Bacteriol 184:6138-45.

236. Noto JM, Cornelissen CN. 2008. Identification of TbpA residues required for transferrin-iron utilization by Neisseria gonorrhoeae. Infect Immun 76:1960-9.

237. Banerjee S, Siburt CJ, Mistry S, Noto JM, DeArmond P, Fitzgerald MC, Lambert LA, Cornelissen CN, Crumbliss AL. 2012. Evidence of Fe3+ interaction with the plug domain of the outer membrane transferrin receptor protein of Neisseria gonorrhoeae: implications for Fe transport. Metallomics 4:361-72.

238. Cornelissen CN, Sparling PF. 1996. Binding and surface exposure characteristics of the gonococcal transferrin receptor are dependent on both transferrin-binding proteins. J Bacteriol 178:1437-44.

239. Anderson JE, Sparling PF, Cornelissen CN. 1994. Gonococcal transferrin-binding protein 2 facilitates but is not essential for transferrin utilization. J Bacteriol 176:3162-70.

240. DeRocco AJ, Yost-Daljev MK, Kenney CD, Cornelissen CN. 2009. Kinetic analysis of ligand interaction with the gonococcal transferrin-iron acquisition system. Biometals 22:439-51.

241. Noinaj N, Buchanan SK, Cornelissen CN. 2012. The transferrin-iron import system from pathogenic Neisseria species. Mol Microbiol 86:246-57.

242. Calmettes C, Alcantara J, Yu RH, Schryvers AB, Moraes TF. 2012. The structural basis of transferrin sequestration by transferrin-binding protein B. Nat Struct Mol Biol 19:358-60.

243. Marri PR, Paniscus M, Weyand NJ, Rendón MA, Calton CM, Hernández DR, Higashi DL, Sodergren E, Weinstock GM, Rounsley SD, So M. 2010. Genome sequencing reveals widespread virulence gene exchange among human Neisseria species. PLoS One 5:e11835.

244. Ronpirin C, Jerse AE, Cornelissen CN. 2001. Gonococcal genes encoding transferrin-binding proteins A and B are arranged in a bicistronic operon but are subject to differential expression. Infect Immun 69:6336-47.

245. Cornelissen CN, Anderson JE, Boulton IC, Sparling PF. 2000. Antigenic and sequence diversity in gonococcal transferrin-binding protein A. Infect Immun 68:4725-35.

246. Cornelissen CN, Anderson JE, Sparling PF. 1997. Characterization of the diversity and the transferrin-binding domain of gonococcal transferrin-binding protein 2. Infect Immun 65:822-8.

247. Cornelissen CN, Kelley M, Hobbs MM, Anderson JE, Cannon JG, Cohen MS, Sparling PF. 1998. The transferrin receptor expressed by gonococcal strain FA1090 is required for the experimental infection of human male volunteers. Mol Microbiol 27:611-6.

248. Noinaj N, Cornelissen CN, Buchanan SK. 2013. Structural insight into the lactoferrin receptors from pathogenic Neisseria. J Struct Biol 184:83-92.

249. Biswas GD, Sparling PF. 1995. Characterization of lbpA, the structural gene for a lactoferrin receptor in Neisseria gonorrhoeae. Infect Immun 63:2958-67.

250. Biswas GD, Anderson JE, Chen CJ, Cornelissen CN, Sparling PF. 1999. Identification and functional characterization of the Neisseria gonorrhoeae lbpB gene product. Infect Immun 67:455-9.

251. Morgenthau A, Partha SK, Adamiak P, Schryvers AB. 2014. The specificity of protection against cationic antimicrobial peptides by lactoferrin binding protein B. Biometals 27:923-33.

252. Anderson JE, Hobbs MM, Biswas GD, Sparling PF. 2003. Opposing selective forces for expression of the gonococcal lactoferrin receptor. Mol Microbiol 48:1325-37.

253. Harrison OB, Bennett JS, Derrick JP, Maiden MCJ, Bayliss CD. 2013. Distribution and diversity of the haemoglobin-haptoglobin iron-acquisition systems in pathogenic and non-pathogenic Neisseria. Microbiology (Reading) 159:1920-1930.

254. Chen CJ, Sparling PF, Lewis LA, Dyer DW, Elkins C. 1996. Identification and purification of a hemoglobin-binding outer membrane protein from *Neisseria gonorrhoeae*. Infect Immun 64:5008-14.

255. Lewis LA, Gray E, Wang YP, Roe BA, Dyer DW. 1997. Molecular characterization of hpuAB, the haemoglobin-haptoglobin-utilization operon of *Neisseria meningitidis*. Mol Microbiol 23:737-49.

256. Lewis LA, Dyer DW. 1995. Identification of an iron-regulated outer membrane protein of *Neisseria meningitidis* involved in the utilization of hemoglobin complexed to haptoglobin. J Bacteriol 177:1299-306.

257. Chen CJ, McLean D, Thomas CE, Anderson JE, Sparling PF. 2002. Point mutations in HpuB enable gonococcal HpuA deletion mutants to grow on hemoglobin. J Bacteriol 184:420-6.

258. Chen CJ, Elkins C, Sparling PF. 1998. Phase variation of hemoglobin utilization in *Neisseria gonorrhoeae*. Infect Immun 66:987-93.

259. Lewis LA, Gipson M, Hartman K, Ownbey T, Vaughn J, Dyer DW. 1999. Phase variation of HpuAB and HmbR, two distinct haemoglobin receptors of *Neisseria meningitidis* DNM2. Mol Microbiol 32:977-89.

260. Anderson JE, Leone PA, Miller WC, Chen C, Hobbs MM, Sparling PF. 2001. Selection for expression of the gonococcal hemoglobin receptor during menses. J Infect Dis 184:1621-3.

261. Kramer J, Özkaya Ö, Kümmerli R. 2020. Bacterial siderophores in community and host interactions. Nat Rev Microbiol 18:152-163.

262. Carson SD, Klebba PE, Newton SM, Sparling PF. 1999. Ferric enterobactin binding and utilization by Neisseria gonorrhoeae. J Bacteriol 181:2895-901.

263. Hollander A, Mercante AD, Shafer WM, Cornelissen CN. 2011. The iron-repressed, AraC-like regulator MpeR activates expression of fetA in Neisseria gonorrhoeae. Infect Immun 79:4764-76.

264. Carson SD, Stone B, Beucher M, Fu J, Sparling PF. 2000. Phase variation of the gonococcal siderophore receptor FetA. Mol Microbiol 36:585-93.

265. Stork M, Grijpstra J, Bos MP, Mañas Torres C, Devos N, Poolman JT, Chazin WJ, Tommassen J. 2013. Zinc piracy as a mechanism of Neisseria meningitidis for evasion of nutritional immunity. PLoS Pathog 9:e1003733.

266. Stork M, Bos MP, Jongerius I, de Kok N, Schilders I, Weynants VE, Poolman JT, Tommassen J. 2010. An outer membrane receptor of Neisseria meningitidis involved in zinc acquisition with vaccine potential. PLoS Pathog 6:e1000969.

267. Hagen TA, Cornelissen CN. 2006. Neisseria gonorrhoeae requires expression of TonB and the putative transporter TdfF to replicate within cervical epithelial cells. Mol Microbiol 62:1144-57.

268. Cornelissen CN. 2018. Subversion of nutritional immunity by the pathogenic Neisseriae. Pathog Dis 76.

269. Sauter A, Howard SP, Braun V. 2003. In vivo evidence for TonB dimerization. J Bacteriol 185:5747-54.

270. Gresock MG, Kastead KA, Postle K. 2015. From Homodimer to Heterodimer and Back: Elucidating the TonB Energy Transduction Cycle. J Bacteriol 197:3433-45.

271. Kaserer WA, Jiang X, Xiao Q, Scott DC, Bauler M, Copeland D, Newton SM, Klebba PE. 2008. Insight from TonB hybrid proteins into the mechanism of iron transport through the outer membrane. J Bacteriol 190:4001-16.

272. Josts I, Veith K, Tidow H. 2019. Ternary structure of the outer membrane transporter FoxA with resolved signalling domain provides insights into TonB-mediated siderophore uptake. Elife 8.

273. Klebba PE. 2016. ROSET Model of TonB Action in Gram-Negative Bacterial Iron Acquisition. J Bacteriol 198:1013-21.

274. Postle K, Larsen RA. 2007. TonB-dependent energy transduction between outer and cytoplasmic membranes. Biometals 20:453-65.

275. Krewulak KD, Vogel HJ. 2008. Structural biology of bacterial iron uptake. Biochim Biophys Acta 1778:1781-804.

276. Rees DC, Johnson E, Lewinson O. 2009. ABC transporters: the power to change. Nat Rev Mol Cell Biol 10:218-27.

277. Chen CY, Berish SA, Morse SA, Mietzner TA. 1993. The ferric iron-binding protein of pathogenic Neisseria spp. functions as a periplasmic transport protein in iron acquisition from human transferrin. Mol Microbiol 10:311-8.

278. Siburt CJ, Roulhac PL, Weaver KD, Noto JM, Mietzner TA, Cornelissen CN, Fitzgerald MC, Crumbliss AL. 2009. Hijacking transferrin bound iron: protein-receptor interactions involved in iron transport in *N. gonorrhoeae*. Metallomics 1:249-55.

279. Ammendola S, Pasquali P, Pistoia C, Petrucci P, Petrarca P, Rotilio G, Battistoni A. 2007. High-affinity Zn2+ uptake system ZnuABC is required for bacterial zinc homeostasis in intracellular environments and contributes to the virulence of Salmonella enterica. Infect Immun 75:5867-76.

280. Gabbianelli R, Scotti R, Ammendola S, Petrarca P, Nicolini L, Battistoni A. 2011. Role of ZnuABC and ZinT in Escherichia coli O157:H7 zinc acquisition and interaction with epithelial cells. BMC Microbiol 11:36.

281. Yu C, Genco CA. 2012. Fur-mediated global regulatory circuits in pathogenic Neisseria species. J Bacteriol 194:6372-81.

282. Pawlik MC, Hubert K, Joseph B, Claus H, Schoen C, Vogel U. 2012. The zinc-responsive regulon of Neisseria meningitidis comprises 17 genes under control of a Zur element. J Bacteriol 194:6594-603.

283. Fillat MF. 2014. The FUR (ferric uptake regulator) superfamily: diversity and versatility of key transcriptional regulators. Arch Biochem Biophys 546:41-52.

284. Jean S. 2015. Characterizarion of the Regulation and Function of Neisseria Gonorrhoeae TonB-dependent Transporters: TdfG, TdfH and TdfJ. Doctor of Philosophy. Virginia Commonwealth University, VCU.

285. Padmanabhan S, Branch AH, Stoudenmire JL, Cornelissen CN. 2024. RNA Sequencing analysis for the Zinc and Zur-dependent transcriptome of N*eisseria gonorrhoeae* FA1090. Georgia State University, Doctoral Dissertation Thesis- Chapter 4.

286. Massé E, Gottesman S. 2002. A small RNA regulates the expression of genes involved in iron metabolism in Escherichia coli. Proc Natl Acad Sci U S A 99:4620-5.

287. Minato Y, Fassio SR, Wolfe AJ, Häse CC. 2013. Central metabolism controls transcription of a virulence gene regulator in Vibrio cholerae. Microbiology (Reading) 159:792-802.

288. Nachamkin I, Cannon JG, Mittler RS. 1981. Monoclonal antibodies against Neisseria gonorrhoeae: production of antibodies directed against a strain-specific cell surface antigen. Infect Immun 32:641-8.

289. Jean S, Juneau RA, Criss AK, Cornelissen CN. 2016. Neisseria gonorrhoeae Evades Calprotectin-Mediated Nutritional Immunity and Survives Neutrophil Extracellular Traps by Production of TdfH. Infect Immun 84:2982-94.

290. Maurakis S, Cornelissen CN. 2020. Metal-Limited Growth of Neisseria gonorrhoeae for Characterization of Metal-Responsive Genes and Metal Acquisition from Host Ligands. J Vis Exp.

291. Macherey N. User Manual - NucleoProtect RNA, *on* Macherey- Nagel. https://www.bioke.com/blobs/downloads/Macherey-Nagel/MAN-MN-NucleoProtect%20RNA.pdf. Accessed

292. Werner F, Fröndt R. 2016. Automated Purification of RNA from Cells or

Tissue with the MACHEREY-NAGEL NucleoMag®

RNA Kit on the epMotion® 5075. Eppendorf, Eppendorf.

293. Invitrogen. 29 June 2018. TURBO DNA-free Kit User Guide, vol Catalog Number: AM1907. Thermo Fischer Scientific, Thermo Fischer Scientific.

294. Scientific TF. 12 May 2023. SuperScript IV First-Strand Synthesis System Catalog No: 18091050.

295. Aranda PS, LaJoie DM, Jorcyk CL. 2012. Bleach gel: a simple agarose gel for analyzing RNA quality. Electrophoresis 33:366-9.

296. IDT. OligoAnalyzer™ Tool- Primer Design, *on* Integrated DNA Technologies (IDT). https://www.idtdna.com/pages/tools/oligoanalyzer?returnurl=%2Fcalc%2Fanalyzer. Accessed

297. Bio-Rad. 2006. Real-Time PCR Applications Guide. 4.2.3.2(Real-Time PCR Data Analysis):42.

298. Invitrogen. 6 December 2004. 5' Rapid Amplification of cDNA Ends Version 2.0, vol 18374-058. Invitrogen, Invitrogen Life Technologies.

299. NEB. 2024 PCR Protocol for Phusion® High-Fidelity DNA Polymerase (M0530).

300. ThermoFischer. 14 February 2014 2014. Zero Blunt TOPO PCR Cloning Kit. B(32.

301. Davis MW, Jorgensen EM. 2022. ApE, A Plasmid Editor: A Freely Available DNA Manipulation and Visualization Program. Frontiers in Bioinformatics 2.

302. SnapGene. SnapGene Viewer Software, www.snapgene.com.

303. BioRad. Stain Free Imaging Technology. https://www.bio-rad.com/en-us/applications-technologies/stain-free-imaging-technology?ID=NZ0G1815. Accessed

304. Maurakis SA, Stoudenmire JL, Rymer JK, Chazin WJ, Cornelissen CN. 2022. Mutagenesis of the Loop 3 α-Helix of Neisseria gonorrhoeae TdfJ Inhibits S100A7 Binding and Utilization. mBio 13:e0167022.

305. Brand LH, Kirchler T, Hummel S, Chaban C, Wanke D. 2010. DPI-ELISA: a fast and versatile method to specify the binding of plant transcription factors to DNA in vitro. Plant Methods 6:25.

306. 3.0.0 GPV. 2023. Linear Regression Model Curve Fitting using Hill Equation, PRISM, GraphPad PRISM.

307. Cassiano MHA, Silva-Rocha R. 2020. Benchmarking Bacterial Promoter Prediction Tools: Potentialities and Limitations. mSystems 5.

308. Dudek CA, Jahn D. 2022. PRODORIC: state-of-the-art database of prokaryotic gene regulation. Nucleic Acids Res 50:D295-D302.

309. Bailey TL, Johnson J, Grant CE, Noble WS. 2015. The MEME Suite. Nucleic Acids Res 43:W39-49.

310. Ma W, Noble WS, Bailey TL. 2014. Motif-based analysis of large nucleotide data sets using MEME-ChIP. Nat Protoc 9:1428-50.

311. GeneiousPrime. 2016. Geneious Primer 2016 (https://www.geneious.com), Geneious. https://www.geneious.com.

312. Crooks GE, Hon G, Chandonia JM, Brenner SE. 2004. WebLogo: a sequence logo generator. Genome Res 14:1188-90.

313. World Health Organization. 2023. Gonorrhea (N*eisseria gonorrhoeae* infection), *on* World Health Organization. https://www.who.int/news-room/fact-sheets/detail/gonorrhoea-(neisseria-gonorrhoeae-infection). Accessed 18 July 2023.

314. Workowski KA, Bachmann LH, Chan PA, Johnston CM, Muzny CA, Park I, Reno H, Zenilman JM, Bolan GA. 2021. Sexually Transmitted Infections Treatment Guidelines, 2021. MMWR Recomm Rep 70:1-187.

315. CDC. 2019. Antibiotic Resistance Threats in the United States. US Department of Health and Human Services Atlanta, GA.

316. Brill JR. 2010. Diagnosis and treatment of urethritis in men. Am Fam Physician 81:873-8.

317. Edwards JL, Apicella MA. 2004. The molecular mechanisms used by Neisseria gonorrhoeae to initiate infection differ between men and women. Clin Microbiol Rev 17:965-81, table of contents.

318. Cohen MS, Sparling PF. 1992. Mucosal infection with Neisseria gonorrhoeae. Bacterial adaptation and mucosal defenses. J Clin Invest 89:1699-705.

319. Criss AK, Seifert HS. 2012. A bacterial siren song: intimate interactions between Neisseria and neutrophils. Nat Rev Microbiol 10:178-90.

320. Kehl-Fie TE, Skaar EP. 2010. Nutritional immunity beyond iron: a role for manganese and zinc. Curr Opin Chem Biol 14:218-24.

321. Ray JC, Smirnov A, Maurakis SA, Harrison SA, Ke E, Chazin WJ, Cornelissen CN, Criss AK. 2022. Adherence Enables Neisseria gonorrhoeae to Overcome Zinc Limitation Imposed by Nutritional Immunity Proteins. Infect Immun 90:e0000922.

322. Kammerman MT, Bera A, Wu R, Harrison SA, Maxwell CN, Lundquist K, Noinaj N, Chazin WJ, Cornelissen CN. 2020. Molecular Insight into TdfH-Mediated Zinc Piracy from Human Calprotectin by Neisseria gonorrhoeae. mBio 11.

323. Maurakis SA, Cornelissen CN. 2022. Recent Progress Towards a Gonococcal Vaccine. Front Cell Infect Microbiol 12:881392.

324. Kandari D, Joshi H, Bhatnagar R. 2021. Zur: Zinc-Sensing Transcriptional Regulator in a Diverse Set of Bacterial Species. Pathogens 10.

325. Mikhaylina A, Ksibe AZ, Scanlan DJ, Blindauer CA. 2018. Bacterial zinc uptake regulator proteins and their regulons. Biochem Soc Trans 46:983-1001.

326. Agarwal S, Sebastian S, Szmigielski B, Rice PA, Genco CA. 2008. Expression of the gonococcal global regulatory protein Fur and genes encompassing the Fur and iron regulon during in vitro and in vivo infection in women. J Bacteriol 190:3129-39.

327. Mildner M, Stichenwirth M, Abtin A, Eckhart L, Sam C, Gl ä ser R, Schr ö der J-M, Gmeiner R, Mlitz V, Pammer J, A Geusau A, Tschachler E. 2010. Psoriasin (S100A7) is

a major E*scherichia coli*-cidal factor of the female genital tract. Mucosal Immunology 3:602-609.

328. Yu C, Genco CA. 2012. Fur-mediated activation of gene transcription in the human pathogen Neisseria gonorrhoeae. J Bacteriol 194:1730-42.

329. Maurakis S. 2022. Functional and Immune Characterization of the Gonococcal Zinc Importer TdfJ. Dissertation. Georgia State University, https://doi.org/10.57709/31312707, 2022.

330. Grifantini R, Sebastian S, Frigimelica E, Draghi M, Bartolini E, Muzzi A, Rappuoli R, Grandi G, Genco CA. 2003. Identification of iron-activated and -repressed Fur-dependent genes by transcriptome analysis of Neisseria meningitidis group B. Proc Natl Acad Sci U S A 100:9542-7.

331. Jackson LA, Ducey TF, Day MW, Zaitshik JB, Orvis J, Dyer DW. 2010. Transcriptional and functional analysis of the Neisseria gonorrhoeae Fur regulon. J Bacteriol 192:77-85.

332. Kumar P, Sannigrahi S, Tzeng YL. 2012. The Neisseria meningitidis ZnuD zinc receptor contributes to interactions with epithelial cells and supports heme utilization when expressed in Escherichia coli. Infect Immun 80:657-67.

333. Isabella V, Wright LF, Barth K, Spence JM, Grogan S, Genco CA, Clark VL. 2008. cis- and trans-acting elements involved in regulation of norB (norZ), the gene encoding nitric oxide reductase in Neisseria gonorrhoeae. Microbiology (Reading) 154:226-239.

334. Browning DF, Busby SJ. 2004. The regulation of bacterial transcription initiation. Nat Rev Microbiol 2:57-65.

335. Wong WY, Thomas CMG, Merkus JMWM, Zielhuis GA, Steegers-Theunissen RPM. 1999. Male factor subfertility: possible causes

and the impact of nutritional factors. FERTILITY AND STERILITY 73:435-442.

336. Owen DH, Katz DF. 1999. A vaginal fluid simulant. Contraception 59:91-5.

337. Mildner M, Stichenwirth M, Abtin A, Eckhart L, Sam C, Gläser R, Schröder J, Gmeiner R, Mlitz V, Pammer J, Geusau A, Tschachler E. 2010. Psoriasin (S100A7) is a major Escherichia coli-cidal

factor of the female genital tract. Mucosal Immunology- Nature Publishing group 3:602-609.

338. Capdevila DA, Wang J, Giedroc DP. 2016. Bacterial Strategies to Maintain Zinc Metallostasis at the Host-Pathogen Interface. J Biol Chem 291:20858-20868.

339. Ong CL, Gillen CM, Barnett TC, Walker MJ, McEwan AG. 2014. An antimicrobial role for zinc in innate immune defense against group A streptococcus. J Infect Dis 209:1500-8.

340. Patzer SI, Hantke K. 1998. The ZnuABC high-affinity zinc uptake system and its regulator Zur in Escherichia coli. Mol Microbiol 28:1199-210.

341. Gilston BA, Wang S, Marcus MD, Canalizo-Hernández MA, Swindell EP, Xue Y, Mondragón A, O'Halloran TV. 2014. Structural and mechanistic basis of zinc regulation across the E. coli Zur regulon. PLoS Biol 12:e1001987.

342. Rasmussen RA, Wang S, Camarillo JM, Sosnowski V, Cho BK, Goo YA, Lucks JB, O'Halloran TV. 2022. Zur and zinc increase expression of E. coli ribosomal protein L31 through RNA-mediated repression of the repressor L31p. Nucleic Acids Res 50:12739-12753.

343. Shin JH, Helmann JD. 2016. Molecular logic of the Zur-regulated zinc deprivation response in Bacillus subtilis. Nat Commun 7:12612.

344. Li Y, Qiu Y, Gao H, Guo Z, Han Y, Song Y, Du Z, Wang X, Zhou D, Yang R. 2009. Characterization of Zur-dependent genes and direct Zur targets in Yersinia pestis. BMC Microbiol 9:128.

345. CDC. 2015. Gonorrhea – CDC Detailed Fact Sheet. Center for Disease Control and Prevention Web Archive.

346. Rosales C, Lowell CA, Schnoor M, Uribe-Querol E. 2017. Neutrophils: Their Role in Innate and Adaptive Immunity 2017. J Immunol Res 2017:9748345.

347. Johnson MB, Criss AK. 2011. Resistance of Neisseria gonorrhoeae to neutrophils. Front Microbiol 2:77.

348. Unemo M, Nicholas RA. 2012. Emergence of multidrug-resistant, extensively drug-resistant and untreatable gonorrhea. Future Microbiol 7:1401-22.

349. Hood MI, Mortensen BL, Moore JL, Zhang Y, Kehl-Fie TE, Sugitani N, Chazin WJ, Caprioli RM, Skaar EP. 2012. Identification of an Acinetobacter baumannii zinc acquisition system that facilitates resistance to calprotectin-mediated zinc sequestration. PLoS Pathog 8:e1003068.

350. Hesse LE, Lonergan ZR, Beavers WN, Skaar EP. 2019. The Acinetobacter baumannii Znu System Overcomes Host-Imposed Nutrient Zinc Limitation. Infect Immun 87.

351. Nanamiya H, Akanuma G, Natori Y, Murayama R, Kosono S, Kudo T, Kobayashi K, Ogasawara N, Park SM, Ochi K, Kawamura F. 2004. Zinc is a key factor in controlling alternation of two types of L31 protein in the Bacillus subtilis ribosome. Mol Microbiol 52:273-83.

352. Panina EM, Mironov AA, Gelfand MS. 2003. Comparative genomics of bacterial zinc regulons: enhanced ion transport, pathogenesis, and rearrangement of ribosomal proteins. Proc Natl Acad Sci U S A 100:9912-7.

353. Jordan PW, Saunders NJ. 2009. Host iron binding proteins acting as niche indicators for Neisseria meningitidis. PLoS One 4:e5198.

354. Wu HJ, Seib KL, Srikhanta YN, Kidd SP, Edwards JL, Maguire TL, Grimmond SM, Apicella MA, McEwan AG, Jennings MP. 2006. PerR controls Mn-dependent resistance to oxidative stress in Neisseria gonorrhoeae. Mol Microbiol 60:401-16.

355. Householder TC, Fozo EM, Cardinale JA, Clark VL. 2000. Gonococcal nitric oxide reductase is encoded by a single gene, norB, which is required for anaerobic growth and is induced by nitric oxide. Infect Immun 68:5241-6.

356. Barth KR, Isabella VM, Clark VL. 2009. Biochemical and genomic analysis of the denitrification pathway within the genus Neisseria. Microbiology (Reading) 155:4093-4103.

357. Tzeng YL, Sannigrahi S, Berman Z, Bourne E, Edwards JL, Bazan JA, Turner AN, Moir JWB, Stephens DS. 2023. Acquisition of Gonococcal AniA-NorB Pathway by the Neisseria meningitidis Urethritis Clade Confers Denitrifying and Microaerobic Respiration Advantages for Urogenital Adaptation. Infect Immun 91:e0007923.

358. Overton TW, Whitehead R, Li Y, Snyder LA, Saunders NJ, Smith H, Cole JA. 2006. Coordinated regulation of the Neisseria gonorrhoeae-truncated denitrification pathway by the nitric oxide-sensitive repressor, NsrR, and nitrite-insensitive NarQ-NarP. J Biol Chem 281:33115-26.

359. Rodionov DA, Dubchak IL, Arkin AP, Alm EJ, Gelfand MS. 2005. Dissimilatory metabolism of nitrogen oxides in bacteria: comparative reconstruction of transcriptional networks. PLoS Comput Biol 1:e55.

360. Delany I, Rappuoli R, Scarlato V. 2004. Fur functions as an activator and as a repressor of putative virulence genes in Neisseria meningitidis. Mol Microbiol 52:1081-90.

361. Nudel K, McClure R, Moreau M, Briars E, Abrams AJ, Tjaden B, Su XH, Trees D, Rice PA, Massari P, Genco CA. 2018. Transcriptome Analysis of Neisseria gonorrhoeae during Natural Infection Reveals Differential Expression of Antibiotic Resistance Determinants between Men and Women. mSphere 3.

362. Vonetta L. Edwards ADP, Adonis D'Mello , Mary C. Gray , Amol C. Shetty ,, Xuechu Zhao KMH, Stephanie A. Ragland , Alison K. Criss , Hervé Tettelin. 2022. Dual

species transcriptomics reveals core metabolic and immunologic processes in the interaction

between primary human neutrophils and Neisseria gonorrhoeae strains. bioRxiv 482360.

363. Padmanabhan S, Stoudenmire J, Branch A, Cornelissen C. 2024. Transcriptional control of the dual regulated t*dfJ* promoter by zinc and iron in N*eisseria gonorrhoeae*. mBIO.

364. Weissbach H, Resnick L, Brot N. 2005. Methionine sulfoxide reductases: history and cellular role in protecting against oxidative damage. Biochim Biophys Acta 1703:203-12.

365. McClure R, Sunkavalli A, Balzano PM, Massari P, Cho C, Nauseef WM, Apicella MA, Genco CA. 2020. Global Network Analysis of Neisseria gonorrhoeae Identifies Coordination between Pathways, Processes, and Regulators Expressed during Human Infection. mSystems 5.

366. Greenawalt AN, Stoudenmire J, Lundquist K, Noinaj N, Gumbart JC, Cornelissen CN. 2022. Point Mutations in TbpA Abrogate Human Transferrin Binding in Neisseria gonorrhoeae. Infect Immun 90:e0041422.

367. Haase H, Hebel S, Engelhardt G, Rink L. 2013. Application of Zinpyr-1 for the investigation of zinc signals in Escherichia coli. Biometals 26:167-77.

368. Sigdel TK, Easton JA, Crowder MW. 2006. Transcriptional response of Escherichia coli to TPEN. J Bacteriol 188:6709-13.

369. Falsetta ML, McEwan AG, Jennings MP, Apicella MA. 2010. Anaerobic metabolism occurs in the substratum of gonococcal biofilms and may be sustained in part by nitric oxide. Infect Immun 78:2320-8.

370. Nasreen M, Nair RP, McEwan AG, Kappler U. 2022. The Peptide Methionine Sulfoxide Reductase (MsrAB) of. Antioxidants (Basel) 11.

371. Stupiansky NW, Van Der Pol B, Williams JA, Weaver B, Taylor SE, Fortenberry JD. 2011. The natural history of incident gonococcal infection in adolescent women. Sex Transm Dis 38:750-4.

372. Andreini C, Banci L, Bertini I, Rosato A. 2006. Zinc through the three domains of life. J Proteome Res 5:3173-8.

373. Marguerettaz M, Dieppois G, Que YA, Ducret V, Zuchuat S, Perron K. 2014. Sputum containing zinc enhances carbapenem resistance, biofilm formation and virulence of Pseudomonas aeruginosa. Microb Pathog 77:36-41.

374. Braymer JJ, Giedroc DP. 2014. Recent developments in copper and zinc homeostasis in bacterial pathogens. Curr Opin Chem Biol 19:59-66.

375. Bobrov AG, Kirillina O, Fetherston JD, Miller MC, Burlison JA, Perry RD. 2014. The Yersinia pestis siderophore, yersiniabactin, and the ZnuABC system both contribute to zinc acquisition and the development of lethal septicaemic plague in mice. Mol Microbiol 93:759-75.

376. Campoy S, Jara M, Busquets N, Pérez De Rozas AM, Badiola I, Barbé J. 2002. Role of the high-affinity zinc uptake znuABC system in Salmonella enterica serovar typhimurium virulence. Infect Immun 70:4721-5.

377. Unemo M, Seifert HS, Hook EW, Hawkes S, Ndowa F, Dillon JR. 2019. Gonorrhoea. Nat Rev Dis Primers 5:79.

378. Jumper J, Evans R, Pritzel A, Green T, Figurnov M, Ronneberger O, Tunyasuvunakool K, Bates R, Žídek A, Potapenko A, Bridgland A, Meyer C, Kohl SAA, Ballard AJ, Cowie A, Romera-Paredes B, Nikolov S, Jain R, Adler J, Back T, Petersen S, Reiman D, Clancy E, Zielinski M, Steinegger M, Pacholska M, Berghammer T, Bodenstein S, Silver D, Vinyals O, Senior AW, Kavukcuoglu K, Kohli P, Hassabis D. 2021. Highly accurate protein structure prediction with AlphaFold. Nature 596:583-589.

379. Varadi M, Anyango S, Deshpande M, Nair S, Natassia C, Yordanova G, Yuan D, Stroe O, Wood G, Laydon A, Žídek A, Green T, Tunyasuvunakool K, Petersen S, Jumper J, Clancy E, Green R, Vora A, Lutfi M, Figurnov M, Cowie A, Hobbs N, Kohli P, Kleywegt G, Birney E, Hassabis D, Velankar S. 2022. AlphaFold Protein Structure Database: massively expanding the structural coverage of protein-sequence space with high-accuracy models. Nucleic Acids Res 50:D439-D444.

380. Padmanabhan S, Stoudenmire J, Branch A, Cornelissen C. 2024. Transcriptional control of the dual regulated t*dfJ* promoter by zinc and iron in N*eisseria gonorrhoeae*. Unpublished.

381. Busby S, Ebright RH. 1994. Promoter structure, promoter recognition, and transcription activation in prokaryotes. Cell 79:743-6.

382. Hochschild A, Dove SL. 1998. Protein-protein contacts that activate and repress prokaryotic transcription. Cell 92:597-600.

383. Pérez-Rueda E, Gralla JD, Collado-Vides J. 1998. Genomic position analyses and the transcription machinery. J Mol Biol 275:165-70.

384. Lewis LA, Ngampasutadol J, Wallace R, Reid JE, Vogel U, Ram S. 2010. The meningococcal vaccine candidate neisserial surface protein A (NspA) binds to factor H and enhances meningococcal resistance to complement. PLoS Pathog 6:e1001027.

385. Escolar L, Pérez-Martín J, de Lorenzo V. 1998. Binding of the fur (ferric uptake regulator) repressor of Escherichia coli to arrays of the GATAAT sequence. J Mol Biol 283:537-47.

386. Baichoo N, Helmann JD. 2002. Recognition of DNA by Fur: a reinterpretation of the Fur box consensus sequence. J Bacteriol 184:5826-32.

387. Mellin JR, Goswami S, Grogan S, Tjaden B, Genco CA. 2007. A novel fur- and iron-regulated small RNA, NrrF, is required for indirect fur-mediated regulation of the sdhA and sdhC genes in Neisseria meningitidis. J Bacteriol 189:3686-94.

388. Mellin JR, McClure R, Lopez D, Green O, Reinhard B, Genco C. 2010. Role of Hfq in iron-dependent and -independent gene regulation in Neisseria meningitidis. Microbiology (Reading) 156:2316-2326.

389. Massé E, Vanderpool CK, Gottesman S. 2005. Effect of RyhB small RNA on global iron use in Escherichia coli. J Bacteriol 187:6962-71.

390. Davis BM, Quinones M, Pratt J, Ding Y, Waldor MK. 2005. Characterization of the small untranslated RNA RyhB and its regulon in Vibrio cholerae. J Bacteriol 187:4005-14.

391. Wilderman PJ, Sowa NA, FitzGerald DJ, FitzGerald PC, Gottesman S, Ochsner UA, Vasil ML. 2004. Identification of tandem duplicate regulatory small RNAs in Pseudomonas aeruginosa involved in iron homeostasis. Proc Natl Acad Sci U S A 101:9792-7.

392. Yang X, Wang Y, Liu G, Deng Z, Lin S, Zheng J. 2022. Structural basis of Streptomyces transcription activation by zinc uptake regulator. Nucleic Acids Res 50:8363-8376.

393. Kandari D, Gopalani M, Gupta M, Joshi H, Bhatnagar S, Bhatnagar R. 2018. Identification, Functional Characterization, and Regulon Prediction of the Zinc Uptake Regulator (Front Microbiol 9:3314.

394. Pederick VG, Eijkelkamp BA, Begg SL, Ween MP, McAllister LJ, Paton JC, McDevitt CA. 2015. ZnuA and zinc homeostasis in Pseudomonas aeruginosa. Sci Rep 5:13139.

395. Desrosiers DC, Bearden SW, Mier I, Abney J, Paulley JT, Fetherston JD, Salazar JC, Radolf JD, Perry RD. 2010. Znu is the predominant zinc importer in Yersinia pestis during in vitro growth but is not essential for virulence. Infect Immun 78:5163-77.

396. Kallifidas D, Pascoe B, Owen GA, Strain-Damerell CM, Hong HJ, Paget MS. 2010. The zinc-responsive regulator Zur controls expression of the coelibactin gene cluster in Streptomyces coelicolor. J Bacteriol 192:608-11.

397. Ellison ML, Farrow JM, Parrish W, Danell AS, Pesci EC. 2013. The transcriptional regulator Np20 is the zinc uptake regulator in Pseudomonas aeruginosa. PLoS One 8:e75389.

398. Mortensen BL, Rathi S, Chazin WJ, Skaar EP. 2014. Acinetobacter baumannii response to host-mediated zinc limitation requires the transcriptional regulator Zur. J Bacteriol 196:2616-26.

399. Shin JH, Oh SY, Kim SJ, Roe JH. 2007. The zinc-responsive regulator Zur controls a zinc uptake system and some ribosomal proteins in Streptomyces coelicolor A3(2). J Bacteriol 189:4070-7.

400. Vecerek B, Moll I, Bläsi U. 2007. Control of Fur synthesis by the non-coding RNA RyhB and iron-responsive decoding. EMBO J 26:965-75.

401. Lucarelli D, Russo S, Garman E, Milano A, Meyer-Klaucke W, Pohl E. 2007. Crystal structure and function of the zinc uptake regulator FurB from Mycobacterium tuberculosis. J Biol Chem 282:9914-9922.

402. Miles S, Carpenter BM, Gancz H, Merrell DS. 2010. Helicobacter pylori apo-Fur regulation appears unconserved across species. J Microbiol 48:378-86.

403. Lee HJ, Bang SH, Lee KH, Park SJ. 2007. Positive regulation of fur gene expression via direct interaction of fur in a pathogenic bacterium, Vibrio vulnificus. J Bacteriol 189:2629-36.

404. Shin JH, Jung HJ, An YJ, Cho YB, Cha SS, Roe JH. 2011. Graded expression of zinc-responsive genes through two regulatory zinc-binding sites in Zur. Proc Natl Acad Sci U S A 108:5045-50.

405. Neupane DP, Jacquez B, Sundararajan A, Ramaraj T, Schilkey FD, Yukl ET. 2017. Zinc-Dependent Transcriptional Regulation in. Front Microbiol 8:569.

406. Sheehan LM, Budnick JA, Roop RM, Caswell CC. 2015. Coordinated zinc homeostasis is essential for the wild-type virulence of Brucella abortus. J Bacteriol 197:1582-91.

407. Schröder J, Jochmann N, Rodionov DA, Tauch A. 2010. The Zur regulon of Corynebacterium glutamicum ATCC 13032. BMC Genomics 11:12.

408. Maciag A, Dainese E, Rodriguez GM, Milano A, Provvedi R, Pasca MR, Smith I, Palù G, Riccardi G, Manganelli R. 2007. Global analysis of the Mycobacterium tuberculosis Zur (FurB) regulon. J Bacteriol 189:730-40.

409. Eggleton WG. 1940. The zinc and copper contents of the organs and tissues of Chinese subjects. Biochem J 34:991-7.

410. Palmer LD, Skaar EP. 2016. Transition Metals and Virulence in Bacteria. Annu Rev Genet 50:67-91.

411. Pyle CJ, Azad AK, Papp AC, Sadee W, Knoell DL, Schlesinger LS. 2017. Elemental Ingredients in the Macrophage Cocktail: Role of ZIP8 in Host Response to Mycobacterium tuberculosis. Int J Mol Sci 18.

412. Zackular JP, Chazin WJ, Skaar EP. 2015. Nutritional Immunity: S100 Proteins at the Host-Pathogen Interface. J Biol Chem 290:18991-8.

413. Iyoda S, Kamidoi T, Hirose K, Kutsukake K, Watanabe H. 2001. A flagellar gene fliZ regulates the expression of invasion genes and virulence phenotype in Salmonella enterica serovar Typhimurium. Microb Pathog 30:81-90.

414. Velasco E, Wang S, Sanet M, Fernández-Vázquez J, Jové D, Glaría E, Valledor AF, O'Halloran TV, Balsalobre C. 2018. A new role for Zinc limitation in bacterial pathogenicity: modulation of α-hemolysin from uropathogenic Escherichia coli. Sci Rep 8:6535.

415. Cissé C, Mathieu SV, Abeih MB, Flanagan L, Vitale S, Catty P, Boturyn D, Michaud-Soret I, Crouzy S. 2014. Inhibition of the ferric uptake regulator by peptides derived from anti-FUR peptide aptamers: coupled theoretical and experimental approaches. ACS Chem Biol 9:2779-86.

416. Nickel JC. 2005. Management of urinary tract infections: historical perspective and current strategies: Part 1--Before antibiotics. J Urol 173:21-6.

417. Quillin SJ, Seifert HS. 2018. Neisseria gonorrhoeae host adaptation and pathogenesis. Nat Rev Microbiol 16:226-240.

418. Ong JJ, Baggaley RC, Wi TE, Tucker JD, Fu H, Smith MK, Rafael S, Anglade V, Falconer J, Ofori-Asenso R, Terris-Prestholt F, Hodges-Mameletzis I, Mayaud P. 2019. Global Epidemiologic Characteristics of Sexually Transmitted Infections Among Individuals Using Preexposure Prophylaxis for the Prevention of HIV Infection: A Systematic Review and Meta-analysis. JAMA Netw Open 2:e1917134.

419. Unemo M, Shafer WM. 2011. Antibiotic resistance in Neisseria gonorrhoeae: origin, evolution, and lessons learned for the future. Ann N Y Acad Sci 1230:E19-28.

420. WHO. 27 February 2017 2017. List of antibiotic-resistant "priority pathogens" – a catalogue of 12 families of bacteria that pose the greatest threat to human health.

421. Wang J, Xiong K, Pan Q, He W, Cong Y. 2020. Application of TonB-Dependent Transporters in Vaccine Development of Gram-Negative Bacteria. Front Cell Infect Microbiol 10:589115.

422. Kim M, Hwang S, Ryu S, Jeon B. 2011. Regulation of perR expression by iron and PerR in Campylobacter jejuni. J Bacteriol 193:6171-8.

423. Troxell B, Hassan HM. 2013. Transcriptional regulation by Ferric Uptake Regulator (Fur) in pathogenic bacteria. Front Cell Infect Microbiol 3:59.

424. Delany I, Spohn G, Rappuoli R, Scarlato V. 2001. The Fur repressor controls transcription of iron-activated and -repressed genes in Helicobacter pylori. Mol Microbiol 42:1297-309.

425. Jackson LA, Day M, Allen J, Scott E, Dyer DW. 2017. Iron-regulated small RNA expression as Neisseria gonorrhoeae FA 1090 transitions into stationary phase growth. BMC Genomics 18:317.

426. Foresta C, Garolla A, Cosci I, Menegazzo M, Ferigo M, Gandin V, De Toni L. 2014. Role of zinc trafficking in male fertility: from germ to sperm. Hum Reprod 29:1134-45.

427. Uhlén M, Fagerberg L, Hallström BM, Lindskog C, Oksvold P, Mardinoglu A, Sivertsson Å, Kampf C, Sjöstedt E, Asplund A, Olsson I, Edlund K, Lundberg E, Navani S, Szigyarto CA, Odeberg J, Djureinovic D, Takanen JO, Hober S, Alm T, Edqvist PH, Berling H, Tegel H, Mulder J, Rockberg J, Nilsson P, Schwenk JM, Hamsten M, von Feilitzen K, Forsberg M, Persson L, Johansson F, Zwahlen M, von Heijne G, Nielsen J, Pontén F. 2015. Proteomics. Tissue-based map of the human proteome. Science 347:1260419.

428. Bastian FB, Roux J, Niknejad A, Comte A, Fonseca Costa SS, de Farias TM, Moretti S, Parmentier G, de Laval VR, Rosikiewicz M, Wollbrett J, Echchiki A, Escoriza A, Gharib WH, Gonzales-Porta M, Jarosz Y, Laurenczy B, Moret P, Person E, Roelli P, Sanjeev K, Seppey M, Robinson-Rechavi M. 2021. The Bgee suite: integrated curated expression atlas and comparative transcriptomics in animals. Nucleic Acids Res 49:D831-D847.

429. Hagen T. 2006. Mechanisms of Iron Acquisition Employed by Neisseria Gonorrhoeae for Survival within Cervical Epithelial Cells. Doctor of Philosophy. Virginia Commonwealth University, VCU.

430. Adrait A, Jacquamet L, Le Pape L, Gonzalez de Peredo A, Aberdam D, Hazemann JL, Latour JM, Michaud-Soret I. 1999. Spectroscopic and saturation magnetization properties of the manganese- and cobalt-substituted Fur (ferric uptake regulation) protein from Escherichia coli. Biochemistry 38:6248-60.

431. Ramos Prigol S, Klein R, Chaudhuri S, Paraboni Frandoloso G, Guizzo JA, Gutiérrez Martín CB, Schryvers AB, Kreutz LC, Frandoloso R. 2022. TbpB. Pathogens 11.

432. Miller RJ, Crosby HA, Schilcher K, Wang Y, Ortines RV, Mazhar M, Dikeman DA, Pinsker BL, Brown ID, Joyce DP, Zhang J, Archer NK, Liu H, Alphonse MP, Czupryna J, Anderson WR, Bernthal NM, Fortuno-Miranda L, Bulte JWM, Francis KP, Horswill AR,

Miller LS. 2019. Development of a Staphylococcus aureus reporter strain with click beetle red luciferase for enhanced in vivo imaging of experimental bacteremia and mixed infections. Sci Rep 9:16663.

433. Duncan JA, Gao X, Huang MT, O'Connor BP, Thomas CE, Willingham SB, Bergstralh DT, Jarvis GA, Sparling PF, Ting JP. 2009. Neisseria gonorrhoeae activates the proteinase cathepsin B to mediate the signaling activities of the NLRP3 and ASC-containing inflammasome. J Immunol 182:6460-9.

434. Hui BB, Padeniya TN, Rebuli N, Gray RT, Wood JG, Donovan B, Duan Q, Guy R, Hocking JS, Lahra MM, Lewis DA, Whiley DM, Regan DG, Seib KL. 2022. A Gonococcal Vaccine Has the Potential to Rapidly Reduce the Incidence of Neisseria gonorrhoeae Infection Among Urban Men Who Have Sex With Men. J Infect Dis 225:983-993.

VITAE

Sandhya Padmanabhan was born on 13th of February in 1992 in Chennai, India. She attended National Hill View Public School in Bangalore, India, where she majored in science and mathematics. She graduated with a Bachelor and Master of Technology in Industrial Biotechnology from SASTRA University, Thanjavur, India in 2015. During her Master's program at SASTRA, Sandhya was selected to enroll in a semester abroad program at Brigham and Women's Hospital in association with Harvard Medical School in Boston MA, where she completed a research project for her master's thesis. She worked in the Renal Cell Cancer Lab of Dr. Joseph Bonventre under the direction of Dr. Venkata Sabbisetti, at Harvard Medical School where she worked as a Research Trainee for a year post graduation in 2016. She matriculated into the Microbiology and Immunology Ph.D program at Virginia Commonwealth University in Richmond, VA, in 2017, under the direction of Dr. Cynthia Nau Cornelissen. She then moved with Dr. Cornelissen to the Institute for Biomedical Science at Georgia State University in 2019 where she continued her doctoral dissertation work. Sandhya completed her Ph.D in the Spring of 2024 and is in the process of securing a role as a postdoctoral research scientist at the University of Michigan. Her upcoming future publications are listed below.

- **Padmanabhan**, **S**., Stoudenmire, J., Mundre, S., Noinaj, N., Cornelissen, C.N. **Characterization of the mechanism of dual regulation by iron and zinc on the zinc import gene *tdfJ* of *Neisseria gonorrhoeae***- mBIO, Manuscript in progress 2024
- **Padmanabhan**, **S**., Branch, A.H., Stoudenmire, J., Criss, A.K., Cornelissen, C.N. **The zinc-dependent Zur regulon of *Neisseria gonorrhoeae* comprises of 26 genes** - Manuscript in progress 2024